Determination of Hydraulic Conductivities through Grain-Size Analysis

Author: Fernando Jose Alvarado Blohm

Boston College

Masters Thesis

Determination of Hydraulic Conductivities through Grain-Size Analysis

Author:
Fernando Jose Alvarado Blohm

Supervisor:
Dr. Alfredo Urzúa
Dr. John Ebel
Dr. Alan Kafka

A thesis submitted in fulfilment of the requirements for the degree of Master of Science in Geophysics

June 2016

BOSTON COLLEGE

Dr. Alfredo Urzúa, Dr. John Ebel, Dr. Alan Kafka
Department of Earth and Environmental Sciences

Master of Science in Geophysics

Determination of Hydraulic Conductivities through Grain-Size Analysis

by Fernando Jose ALVARADO BLOHM

Abstract

Nine empirical equations that estimate saturated hydraulic conductivity as a function of grain size in well-graded sands with gravels having large uniformity coefficients ($U > 50$) are evaluated by comparing their accuracy when predicting observed conductivities in constant head permeability tests. According to the findings of this thesis, in decreasing order of accuracy these equations are: USBR (Vukovic and Soro, 1992; USBR, 1978), Hazen (Hazen, 1892), Slichter (Slichter, 1898), Kozeny-Carman (Carrier, 2003), Fair and Hatch (Fair and Hatch, 1933), Terzaghi (Vukovic and Soro, 1992), Beyer (Beyer, 1966), Kruger (Vukovic and Soro, 1992), and Zunker (Zunker, 1932). These results are based on multiple constant head permeability tests on two samples of granular material corresponding to well-graded sands with gravels. Using the USBR equation saturated hydraulic conductivities for a statistical population of 874 samples of well-graded sands with gravels forming 29 loads from a heap leaching mine in northern Chile are calculated. Results indicate that, using the USBR equation, on average the hydraulic conductivity of the leaching heaps has a two standard deviation range between 0.18 and 0.15 cm/s. Permeability tests on the actual material used in the heaps provided by the mine shows that the results presented in this thesis are consistent with actual observations and represent saturated conductivities in heaps up to 3 m high under a pressures of up to 62 Kpa. In future work hydraulic conductivities can be combined with water retention curves, discharge rates, irrigation rates, porosities, and consolidation so as to evaluate the relationship between copper yields and the hydraulic conductivities of the heap.

Acknowledgements

I would like to thank Mr. Claudio Nicolas V., representing la Superintendencia de Geologia: Gerencia de Recursos Mineros y Desarrollo de Division Gabriela Mistral from Codelco Chile for his contribution to the development of this work through the delivery of data that facilitated the analysis presented in this document.

I would also like to thank my family for their continuous support through the hard times. I am eternally grateful for all the sacrifices you made towards my education. My sincere thanks.

To Boston College for offering the chance to prove myself as a geoscientist in grad school. I would also like to thank Weston Observatory for providing funding during the summers to graduate students to work on their research and the Linehan fund for financing the Humboldt permeameter used in this research. My fellow grad students Shaina and Caleb who offered transportation to buy and carry the material to craft the samples as well as my colleagues John, Aakash, and Vanessa for their friendship.

To DGI consultants for their disposition to help and for the donation of the Ottawa sands used to calibrate lab experiments.

To my fellow students of GE -167 Environmental Geoscience course where I assisted Prof. Suanna Crowley during Spring 2014. Thanks for allowing me to involve BC undergraduates in the making of over 40 constant head permeability test conducted in this thesis.

To John Ebel and Alfredo Urzúa, who I regard as friends and colleagues. Thank you for all those good advices, thank you for listening, thank you for the harsh comments, but most of all thank you for believing in me.

And last but not least, I thank God for the journey thus far.

Contents

List of Figures

List of Tables

Abbreviations, Physical Constants, and Symbols

GSD	Grain-Size Distribution	
SF	Shape Factor	
CI	Confidence Level	
UCL	Upper Confidence Level	
LCL	Lower Confidence Level	
g	Acceleration due to gravity	9.8 m/s^2
U	Uniformity coefficient	unitless
k	Permeability	Darcy
K	Hydraulic conductivity	length/time
d_x	The x^{th} percentile in the GSD	mm
h	Hydraulic Head	m
n	Porosity	unitless
T	Temperature	Celcius
t	Time	seconds
ν	Kinematic viscosity	cm^2/s
ρ	Density	Kg/cm^3
μ	Viscosity	$Pa \times s$

Chapter 1

Introduction

Hydraulic conductivity (K) is defined as the ease by which a fluid flows through a granular medium and is a function of both the material and the permeating fluid (Strobel, 2005). This parameter plays an important role in many disciplines within the earth sciences as it serves to help quantify the amount of fluid that can flow through rocks and soils. As an example, estimations of K serve to characterize the amount of fluid injection possible in oil reservoirs, the movement of lixiviants in heap leaching mines, and the ease of groundwater flow in underground aquifers. Direct estimations of K are often laborious and expensive because they require personnel for collecting samples and conducting laboratory experiments and equipment for small or large-scale in situ tests (Salarashayeri and Siosemarde, 2012; Petalas and Pilakas, 2011), which is why empirical methodologies that indirectly estimate conductivities through the maeterial parameters, such as grain-size, are attractive to project managers (Vukovic and Soro, 1992). In this thesis project, nine methods that estimate hydraulic conductivities as a function of grain-size are studied and evaluated in laboratory experiments and then applied to 874 samples of well-graded sands with gravels from a heap leaching mine. Afterwards, a statistical analysis of the resulting hydraulic conductivity was conducted to estimate the average range of conductivities in the leaching heaps composed of sediments within a certain grain-size distribution range.

This introduction contains four sections that aid the reader to understand the investigation presented in this thesis. First, the section entitled *Parameters Affecting Hydraulic Conductivities* explains a list of factors that affect estimations of K with emphasis on grain-size while also explaining the difference between hydraulic conductivity and permeability and its implication for this research. The second section, *Heap Leaching: Research and Objective*, offers a summarized explanation of heap leaching, introduces key concepts, and defines the scope and reach of this investigation. The third section, *Empirical Equations*, introduces the nine empirical equations that were used in this research. The fourth and last section of this introduction, *Previous Research*, presents the most relevant work of others who have also investigated this subject.

1.1 Parameters Affecting Hydraulic Conductivity

Since hydraulic conductivity is defined as the ease by which a fluid flows within a granular medium, one can separate the factors that affect its estimation into those pertaining to the fluid and those pertaining to the granular medium. Properties of the fluid such as its density (ρ), dynamic viscosity (ν), temperature (T), and chemical composition define the velocity and level of turbulence of the fluid as it reacts to certain conditions of pressure and temperature (Lambe and Whitman, 1969; Dullien, 1979; Binkhorst and Robbins, 1994). For this research, the fluid is assumed to be water at $10°C$ for the lab experiments and at $20°C$ for the mine's GSDs. In both cases the water's density is invariant at 1,000 Kg/m^3 and values for dynamic viscosity are assumed to be 0.0013 $Pa \cdot s$ at $10°C$ for lab experiments and 0.0010 $Pa \cdot s$ at $20°C$ for the mine (Vukovic and Soro, 1992). These fluid parameters, of course, can be changed so as to represent different conditions.

Some other properties of the granular medium (such as suffusion, compaction, consolidation, and crystallization) also play a significant role when calculating hydraulic conductivities in hard rocks and unconsolidated sediments (Dullien, 1979). Suffusion is the reduction in permeability that occurs when finer material resulting from the internal erosion of bigger grains clogs the pores in unconsolidated sediments (Ahlinhan, 2012). Compaction results from the rearrangement of soil particles from the expulsion of air within pores (McCarthy, 2001). Consolidation differs from compaction in that pores are saturated with liquids, and hence under the presence of loads liquids and gasses are expelled, leading to a rearrangement of particles (McCarthy, 2001). Crystallization reduces porosity and permeability in rocks because minerals precipitate within pores. However, such factors are not considered in this research due to budget, material, and instrumentation constraints. A summary of factors that affect the calculations of K is illustrated in Figure 1.1.

Hydraulic conductivity and permeability are two different concepts that are closely related. Permeability is an *intrinsic* parameter of any material that quantifies the potential ability of a fluid to enter that material's voids (Zimmerman and Gudmundur, 1996), whereas *hydraulic conductivity*, as previously discussed, relates more to the ease of flow of a certain fluid within that porous medium (Strobel, 2005). The main distinction between these two parameters is that permeability describes only the permeating potential

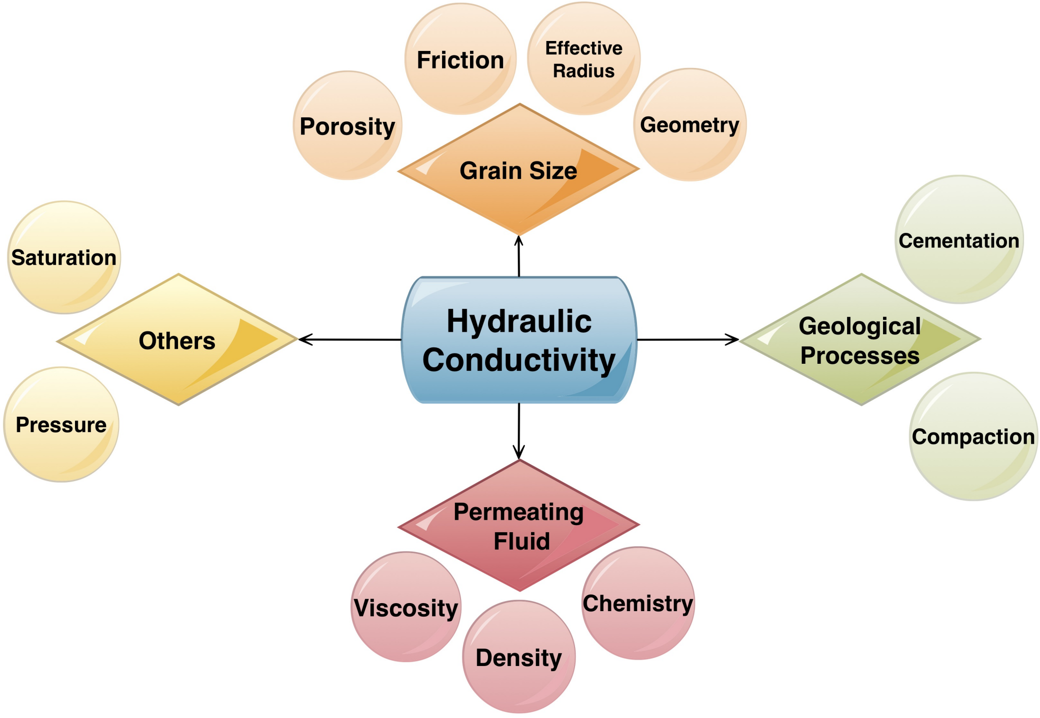

FIGURE 1.1: Some of the factors that affect estimations of K. In this research we focused solely on grain-size and other factors such as those pertaining to geological processes and the permeating fluid were omitted.

of a material and is measured in units of length squared or Darcy. In contrast, hydraulic conductivity is both a function of the material and the permeating fluid and is measured in units of velocity. However, since typically there are large uncertainties in the estimations of either of these parameters (Vukovic and Soro, 1992; Carrier, 2003; Petalas and Pilakas, 2011) and they both aim to represent the movement of liquids through soils, sediments, or hard rocks, in this thesis research the words hydraulic conductivity and permeability are often used as synonyms and both parameters are referred to using the letter K. Furthermore, by knowing properties of the permeating fluid such as its density and viscosity one can calculate hydraulic conductivity from permeability and vice-versa through the following relation:

$$k = K \frac{\mu}{\rho \cdot g} \tag{1.1}$$

where k is permeability (m^2), K is hydraulic conductivity (m/s), μ is dynamic viscosity ($Pa \cdot s$), ρ is density (Kg/m^3), and g is the acceleration due to gravity (m/s^2). This special consideration allows the use of the extensive literature on both topics and makes it applicable to the case of study defined in the next section of this introduction.

1.2 Heap Leaching: Research and Objective

The objective of this investigation is to suggest a way to optimize the recovery of metals in open-pit heap-leaching mines by demonstrating the accuracy of certain equations in the prediction of permeabilities solely as a function of grain-size. An accurate prediction of permeabilities can potentially allow mine operators and geoscientists to identify the optimum configuration of grains to form the leaching heap while making efficient decisions regarding rate of irrigation, comminution, agglomeration, and saturation. Heap leaching is a common mining practice consisting of five stages of ore processing (Cassiday, 2012; Breitenbach, 2000). First, ores are crushed into small particles in a process called *comminution*. Second, these particles are sieved, wetted, gradated, pelletized, and transported on conveyor belts from the grinding mill to the leaching heaps in a process called *agglomeration*. Third, the heaps are *irrigated* through pipes or sprinklers with an acidic solution called *lixiviant* that permeates the unconsolidated sediments and dissolves the metals from the ores. Fourth, the heaps are left inclined at some angle called the *angle of repose* and, after some time (30-120 days), a *pregnant solution or leachate* containing the metals drains and accumulates at the base of the heap via gravity drainage (Bleiwas, 1994). Lastly, in the fifth step, the pregnant solution is recovered through a pipe system and is later chemically processed to obtain the metals from the liquid solution (Figure 1.2). In general, heap leaching is part of a discipline called hydrometallurgy, and although the metals that are recovered through this technique are copper, silver, and gold, this thesis focuses on copper hydrometallurgy. Silver and gold leaching differs from copper leaching in the lixiviants that are used (cyanide for silver and gold and sulfuric acid for copper) and the amount of time that the heap is left in repose (longer periods for silver and gold).

The amount of recoverable metals in leaching heaps directly depends on the amount of lixiviants that percolate through the grains and the extent to which these acids saturate the porous medium (Mishra and Grayson, 1987). Furthermore, in copper leaching, approximately 30% of the estimated quantity is lost during leaching, mostly due to problems related to inaccuracies in the estimations of hydraulic conductivity of the unconsolidated sediments that form the leaching heaps (Mishra and Grayson, 1987). Therefore, there is a direct economical incentive to optimize the estimation of conductivities in copper hydrometallurgy, since a better representation of the movement of lixiviants within heaps will enable mine operators to better predict the amount of copper that can be recovered after leaching. The scheme of this investigation is summarized in Figure 1.3 and to better illustrate the motivation for this thesis here is an example: A mine working with an ore that for every 1,000 Kg (1 ton) of rock has on average 2.5 Kg of copper is said to mine an ore with a Cu concentration of 2,500 ppm (parts per millionth gram) corresponding to a grade of 0.25% (USA Congress, 1988). The average grade for copper ores in economically productive mines around the world is about 0.6% and, assuming a price of \$2.5/lb (\$5.5/kg), the ore in this hypothetical example with a grade of 0.25% results in 250 tons (\$1,375,000) of copper for every 100,000 tons (about one heap) of ore. However, 30% of this Cu will be lost after leaching (Mishra and Grayson, 1987), mostly due to problems related to the irrigation of the heaps and uncertainties in the estimation of permeabilities. This means that from the 250 tons of copper, 175 tons (or \$962,500) will, at most, be recovered during leaching. By identifying an empirical relation or a methodology that makes reliable estimations of hydraulic conductivities, those losses could be reduced by building the heaps with sediments of a certain grain-size distribution, agglomerating these grains with the right amount of solution, and irrigating at an optimum rate. With these simple changes, the surface area of grains exposed to the leachate increases and consequently more copper is recovered.

In a mathematical sense, this thesis research is an optimization problem because the goal is to enhance the amount of copper recovered (maximize profits) by detecting the right configuration of grains. A leaching heap formed by very fine sands, silts, and clays encompasses more surface area and hence more copper is exposed to leachates. Unfortunately, such grain-size distribution will also be less permeable than a sample with larger clasts (Dullien, 1979) and thus the leachate will not flow through the entire heap or it will take longer times to move through the heap. In the previously discussed example, improving the predictability of K just so that one can recover 1% more of the estimated reserves will increase profits by \$12,425 per 100,000 tons of ore. Hence, improving the estimation of conductivities as a function of grain-size is an attractive line of research.

1.2.1 Saturated Hydraulic Conductivities and Heap Leaching

Full saturation of lixiviants in the heap is difficult, uneconomical, and not recommendable as oxygen is necessary for the chemical reaction to dissolve the Cu from the ore. The degree of saturation in a heap can significantly impact the amount of Cu it yields because of decrepitation (loss of material and change in structural fabric as a result of the dissolution of metals from a lixiviant) and suffusion (internal erosion) (Williams, 2013). In the case of sulfide ores, which is the case in copper leaching, solution air needs to move freely through the heap for adequate agent-ore contact and hence to obtain optimum recovery (Milczarek, 2013). While heaps are commonly leached under unsaturated conditions, the saturated conductivities provide useful measures such as the maximum solution application rate (Lupo and Dolezal, 2010). According to the findings of Lupo and Dolezal (2010), the saturated hydraulic conductivity represents the maximum irrigation rate during leaching. If the heaps are irrigated at rates higher than the estimated saturated hydraulic conductivity, then the heap may become unstable due to high phreatic surface and large pore pressure within the heap. It is important to note that full saturation of the medium is a common assumption shared for all the empirical equations used in this research and described in detail later in Chapter 2. Even though this assumption does not hold in practice, these equations are studied in this research due to their simplicity because in unsaturated conditions unconsolidated materials significantly decrease their ability to conduct fluids (Lambe and Whitman, 1969). This is so due to the decrease in cross-sectional area of water flow, increment in tortuosity (or the difficulty in flow), increase of drag forces, and other factors that make up for a non-linear relationship between conductivity, hydraulic head, and degree of saturation (Hopmans, 2002). In summary, trying to represent heap leaching under non-saturated conditions will significantly increase the complexity of the problem. Whether this complexity enhances the accuracy in estimations of conductivity is still an open matter for discussion not addressed in this investigation, and thus for this thesis it will be assumed that the heap is fully saturated in order to make the empirical formulae applicable. For a more detailed discussion on the impact of saturated versus unsaturated flow conditions on hydraulic conductivity please refer to Hopmans (2002), Lambe and Whitman (1969), and Dullien (1979).

1.2.2 Irrigation Rates

Irrigation rates refer to the rate at which the lixiviants enters the heap during leaching. The industry standards according to several manufacturers of sprinklers ranges anywhere from 3 to 20 $Lt/m^2/h$ (permeabilitities 8x10-5 and 6x10-4 cm/s). For this research, it is important to clarify that in the data supplied by the mine there were no available metrics so as to make an educated guess on the irrigation rate or discharge rates in the heaps. This is a major barrier since without these metrics one cannot estimate the saturation of the heaps or correct the estimates of saturated hydraulic conductivity so as to represent the actual non saturated conditions. Without this understanding, one cannot explore the relationship between copper recovered, hydraulic conductivity, and grain size distributions with certainty.

1.3 Empirical Equations

In this thesis the accuracy of nine popularly used empirical equations that estimate K as a function of grain size was evaluated in the prediction of conductivities through constant head permeability tests in well-graded sands with gravels. These equations are:

- Hazen (Hazen, 1892).
- Kozeny-Carman (Carrier, 2003).
- Beyer (Beyer, 1966)
- Slichter (Slichter, 1898)
- Terzaghi (Vukovic and Soro, 1992; Salarashayeri and Siosemarde, 2012; Odong, 2007).
- USBR (Vukovic and Soro, 1992; USBR, 1978; Odong, 2007; Ishaku and Kaigama, 2011).
- Fair and Hatch (Fair and Hatch, 1933)
- Kruger (Vukovic and Soro, 1992)
- Zunker (Vukovic and Soro, 1992)

The mathematical equations, regions of applicability, general assumptions, and other important details concerning each of these relations can be found in Appendix A and will be further discussed in Chapter 2.

1.4 Previous Research

Many authors have conducted research closely related to this thesis where empirical equations that estimate K as a function of grain-size are compared to estimations from laboratory experiments or in-situ measurements. The main difference between this research and the earlier work of other scientists is the large number of samples that are being considered (Table 1.1). In this work I estimate permeabilities for almost 900 grain-size distribution (GSD) curves through nine empirical equations, and I validate these results with twenty two constant head permeability tests, which is approximately three times more than the number of samples used in Petalas and Pilakas (2011), the largest comparable research work investigated as background material for this thesis.

Table 1.1: **Comparison Among Selected Publications**

Paper	**GSD**	**Lab/M.**[1]	**Methods**	**Notes**
This Thesis	874	26	9	
(Salarashayeri and Siosemarde, 2012)	25	25	-	Statistical correlation of percentiles in the GSD
(Petalas and Pilakas, 2011)	212	1060	13	Five constant head permeability tests for every sample
(Ishaku and Kaigama, 2011)	15	1	6	Laboratory experiments referenced in previous work
(Odong, 2007)	4	-	7	The study does not reference lab tests or field observations
(Detner, 1995)	100	100	5	In situ measurements using an air permeameter
(Alyamani and Mahmoud, 1993)	22	-	-	Multiple regression analysis against different percentiles of the GSD
(Shepherd, 1989)	397	-	-	Samples taken from published literature and correlated against median grain size

[1] Laboratory tests or in situ measurements.

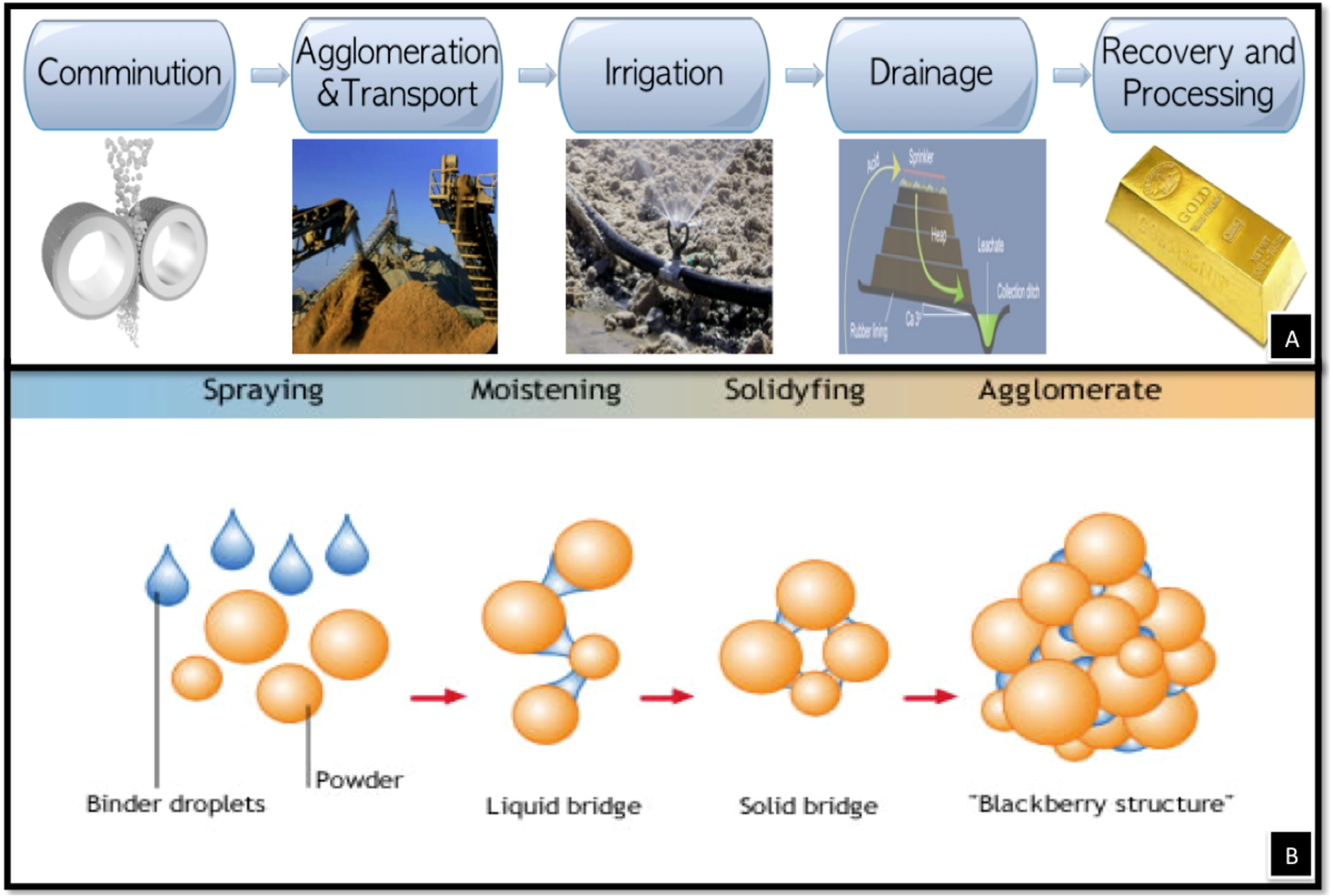

FIGURE 1.2: (A) Scheme of steps in heap leaching. (B) Representation of the agglomeration process. Figure modified from www.ipc-dresden.de and www.infomine.com.

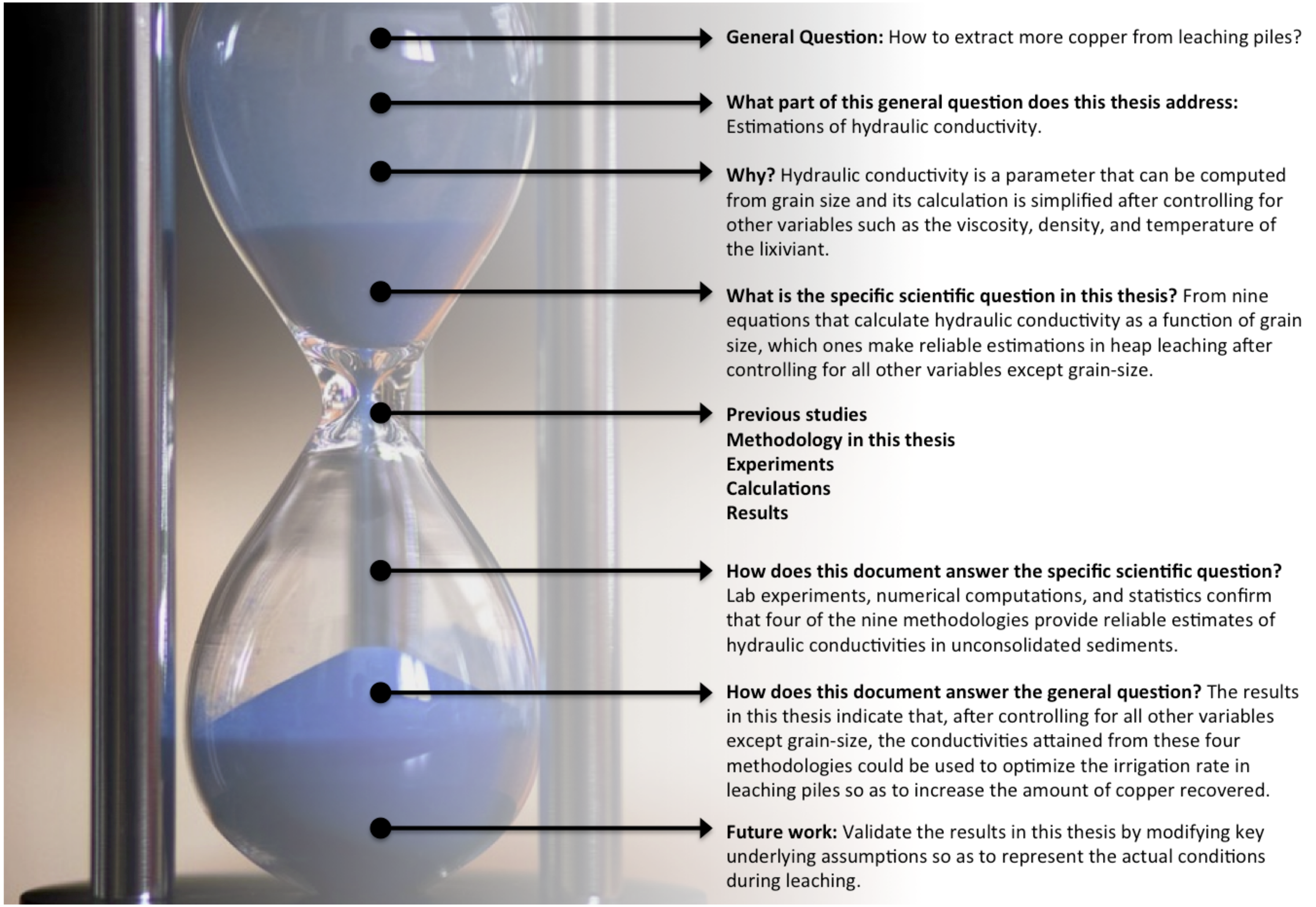

FIGURE 1.3: Scheme showing the scope and objectives for this thesis.

Chapter 2

Background and Literature Review

This chapter starts by explaining sieve analysis, grain-size distribution (GSD) curves, and d_x percentiles. Then in the second section the general form of all the equations used in this research as described by Vukovic and Soro (1992) is explained with a discussion of the parameters directly related to grain size that affect the estimations of K (porosity, effective porosity, and specific yield, void ratio, grain-size, surface area, uniformity coefficient, and shape factor). In the third section of this chapter there is a thorough discussion of all the empirical equations summarized in Appendix A. Lastly, in the fourth section of this chapter the reader will find a summary of key statistics concepts necessary to understand the analysis presented in this thesis research.

2.1 Sieve Analysis and Grain-Size Distributions (GSDs)

A sieve analysis is a set of procedures done so as to detect the proportion of grains corresponding to different grain sizes that form a soil or any granular material. Sieve analyses in this thesis were done according to the American Society for Testing and Materials (ASTM) D6913 and summarized as follows: First, a small amount (approximately 40 gr) of air-dried sample from a granular material is taken from the source. Then, sieves of different sizes are vertically stacked in decreasing order (Figure 3A) and the sample is poured into the top, largest, sieve. The stack is then moved in a circular motion with a vertical tapping impulse for a given time. Afterwards, the stack of sieves is set apart and the amount of material trapped in each sieve is weighed. These weights are divided by the total weight of the sample so as to calculate the percentage of grains corresponding to different sizes. This procedure is referred to as a sieve analysis, and the percentages of grains forming the sample and corresponding to different sizes (Figure 2.9B) form a grain-size distribution (GSD) of the initial sample. Adding the cumulative percentages of grains finer than a certain size and plotting these percentages against a range of grain-sizes form a *GSD curve* (Lambe and Whitman, 1969; McCarthy, 2001). These curves are a simple way to graphically determine the size of the GSD percentiles (d_x percentiles). For example, in Figure 2.9 to estimate the size of the grains corresponding to the finer 10% of the GSD (d_{10}), one finds the X-axis intercept of the 10% line on the granulometric curve, which corresponds to approximately 700 μm in Figure 2.9C. In industrial mining, instead of a stack of sieves a wide array of tools can be used such as vibrating conveyor belts[1] built with ASTM meshes.

2.2 General Form of Empirical Formulae

The general form of the equations that estimate hydraulic conductivities as a function of grain size used in this thesis is generalized in the following expression (Vukovic and Soro, 1992):

$$K = C \times \beta \times \theta(n) \times d_x \tag{2.1}$$

where d_x is defined in the previous section and the other parameters are defined in the following subsections.

2.2.1 Constants (C)

Most of the equations studied in this thesis have embedded assumptions regarding unit conversions and properties of the permeating fluid that are simplified by the use of a constant factor C. Some equations (Hazen, Kozeny-Carman, Beyer) include unit conversion factors in their constants so that grain-sizes are entered in millimeters and the resulting conductivities have units of meters per day, whereas the constant C in other equations (such as the USBR method) yields conductivities in centimeters per second with the same inputs. Furthermore, there are important considerations regarding properties of the permeating fluid intrinsic in each one of these equations that were not clearly stated by the authors of these empirical equations (Vukovic and Soro, 1992) (e.g. temperature, density, viscosity, etc.). Even so, some of these formulas (e.g., Hazen) are widely used in the earth sciences without revision (Carrier, 2003). For this research,

[1]As referenced by FAM manufacturer of mining equipment.

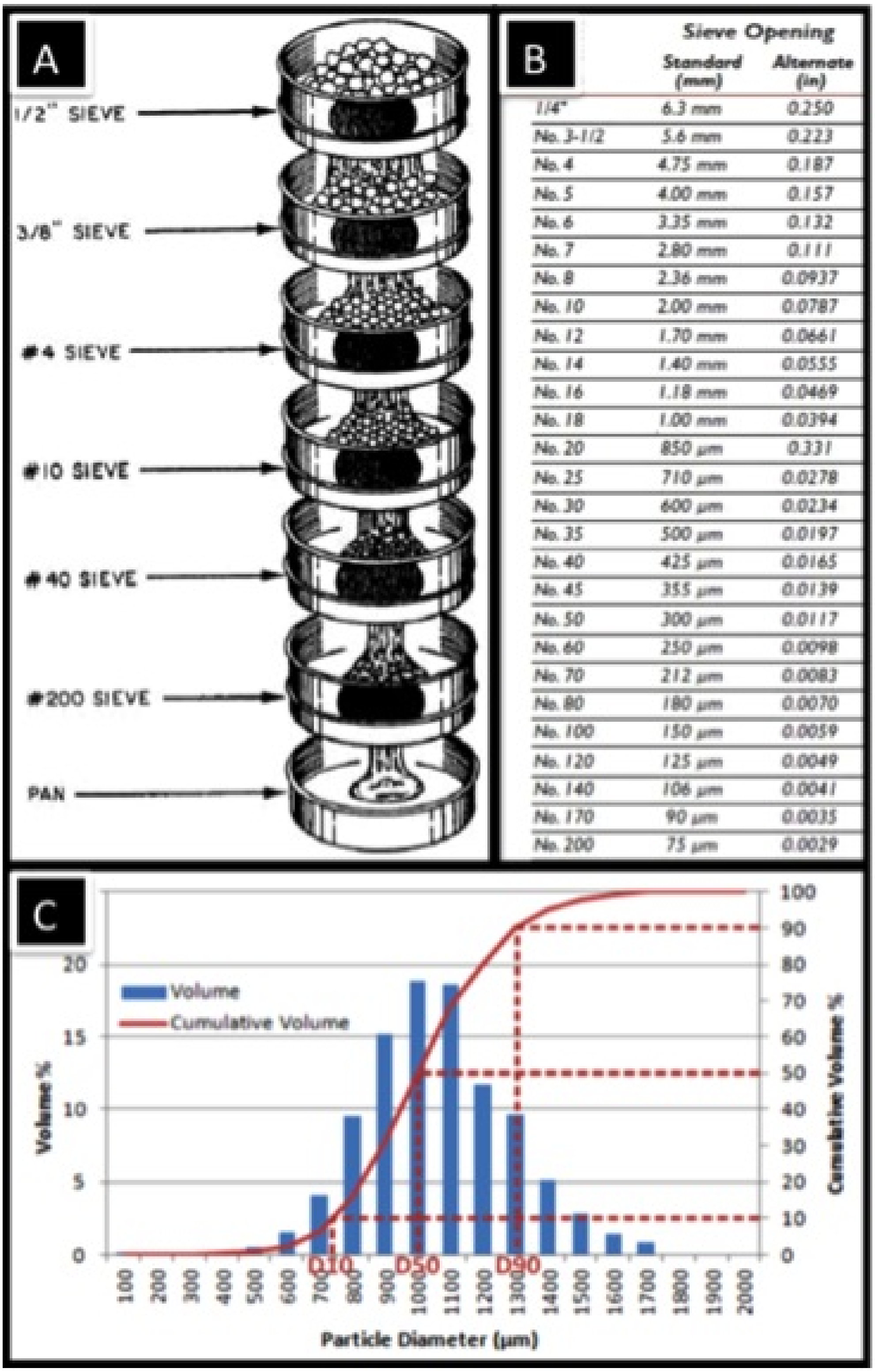

	Sieve Opening Standard (mm)	Sieve Opening Alternate (in)
1/4"	6.3 mm	0.250
No. 3-1/2	5.6 mm	0.223
No. 4	4.75 mm	0.187
No. 5	4.00 mm	0.157
No. 6	3.35 mm	0.132
No. 7	2.80 mm	0.111
No. 8	2.36 mm	0.0937
No. 10	2.00 mm	0.0787
No. 12	1.70 mm	0.0661
No. 14	1.40 mm	0.0555
No. 16	1.18 mm	0.0469
No. 18	1.00 mm	0.0394
No. 20	850 µm	0.331
No. 25	710 µm	0.0278
No. 30	600 µm	0.0234
No. 35	500 µm	0.0197
No. 40	425 µm	0.0165
No. 45	355 µm	0.0139
No. 50	300 µm	0.0117
No. 60	250 µm	0.0098
No. 70	212 µm	0.0083
No. 80	180 µm	0.0070
No. 100	150 µm	0.0059
No. 120	125 µm	0.0049
No. 140	106 µm	0.0041
No. 170	90 µm	0.0035
No. 200	75 µm	0.0029

FIGURE 2.1: A) Sketch showing the stack of sieves (decreasing size) used in mechanical sieving. B) Standard sieve notation by ASTM standards. C) An example of a GSD (blue histogram, left axis) and a GSD curve or granulometric curve (red, right Y axis) attained by plotting cumulative percentages against grain size (X axis).

I adopt the constants proposed by Vukovic and Soro (1992), Cheng and Chen (2007), Odong (2007), Carrier (2003) and summarized in Appendix A.

2.2.2 Effective Radius (β)

The effective radius represents the seepage of fluids through the entire porous medium as if it were a single conduit, and is a function that is mathematically defined differently across equations. Hazen, USBR, Beyer, Terzaghi, and Slichter's equations simply make use of the GSD percentiles following the commonly shared assumption that seepage is controlled by the size of the smaller particles forming the porous medium (Hazen, 1892). However, other equations define an effective radius through more elaborate mathematical formulas. For example, Kruger's equation uses weighted geometrical averages in logarithmic scales so as to weight the effects of big and small particles on fluid seepage. In contrast with the Hazen, Beyer, Slichter, Terzaghi, and USBR equations where the lower percentiles of the GSD are directly taken as the effective radius, the Kozeny-Carman (Carrier, 2003), Kruger, and Zunker's equations represent the effective radius using the fraction of particles Δg_i trapped in the larger and smaller sieves of sizes d_l and d_s, respectively (Table 2.1). Some authors (Carrier, 2003) hypothesized that by including the entire GSD curve in the estimations of the effective radius theoretically-derived values of K could be more accurate for estimating conductivities in empirical observations.

TABLE 2.1: **Effective Radius and Porosity Functions**

Methodology	Effective Radius	Porosity Function
Hazen	d_{10}^2	-
Kozeny-Carman	$\left[\frac{100\%}{\sum \frac{\Delta g_i}{d_l^{0.404} \times d_s^{0.595}}}\right]^2$	$\frac{n^3}{(1-n)^2}$
Beyer	d_{10}^2	-
Slichter	d_{10}^2	$n^3.287$
Terzaghi	d_{10}^2	$\left(\frac{n-0.13}{\sqrt[3]{1-n}}\right)^2$
Fair and Hatch	$\left(\sum \frac{d_i}{\Delta g_i}\right)^2$	$\frac{n^3}{(1-n)^2}$
Kruger	$\left[\sum \Delta g_i \left(\frac{2}{d_l - d_s}\right)\right]^{-1}$	$\frac{n}{(1-n)^2}$
Zunker	$\left[\sum \Delta g_i \frac{d_l - d_s}{d_l d_s \log \frac{d_i}{d_s}}\right]^{-2}$	$\frac{n}{(1-n)}$
USBR	$d_{20}^{2.3}$	-

2.2.3 Porosity Function ($\theta(n)$) and GSD percentiles (d_i)

Similar to the effective radius, the porosity function is also a mathematical expression that helps quantify the void space within the granular medium. The effective radius quantifies the mechanical composition of the sample (grain diameter) whereas the porosity function defines the voids within (Lambe and Whitman, 1969). Conceptually, the porosity function depends on the shape, size, structure, composition, and surface area of the grains that make up the sample along with other properties of the overall material such as its uniformity, compactness, consolidation, etc. Porosity functions were empirically estimated by the authors of the equations studied in this thesis presented in Table 2.1 and Appendix A.

The smaller d_x percentiles and the porosity function are the most important variables across methodologies affecting the estimations of K. A sensitivity analysis for porosities (n) from 25% to 45% corresponding to sands and gravels (McCarthy, 2001) shows the net effect that different values of n has on porosity functions (Figure 2.2). As seen in Figure 2.2, differences of up to three orders of magnitude in estimations of K among different equations can be attributed to the mathematical representations of porosity. Kruger's method provides the largest values of porosity functions while Terzaghi's yields the lowest values, together spanning about two orders of magnitude. The Hazen and USBR equations do not include porosity in their methodologies as they simplify their calculations by approximating the conduits in the porous medium to a pipe of a certain diameter (Vukovic and Soro, 1992). The expression for Kozeny-Carman modified by Carrier (2003) produces the same porosity function as that of Fair and Hatch, which recreates the case of interconnected granular beds (Fair and Hatch, 1933).

In general, the nine equations studied in this research have different formulas for effective radius and porosity function. Both of these factors are the most significant source of variation for conductivities among the equations. Quantification of the net impact that different grain-sizes have on fluid seepage through effective radius calculations is much more complex than with porosity functions. In effective radius calculations one has x number of variables in the formula (d_x percentiles) compared to just porosity (n) in porosity functions (Table 2.1). By looking at the mathematical representation of these two concepts across the different equations it is clear that the equations follow the widely accepted fact that smaller particles (those trapped on smaller sieves) cause the largest variations in K (Vukovic and Soro, 1992; Hazen, 1892; Carrier, 2003; Lambe and Whitman, 1969; Dullien, 1979; Odong, 2007; Alyamani and Mahmoud, 1993).

It is important to mention that since neither void space calculations nor permeability experiments were provided with the mine GSDs, porosities (n) for those samples

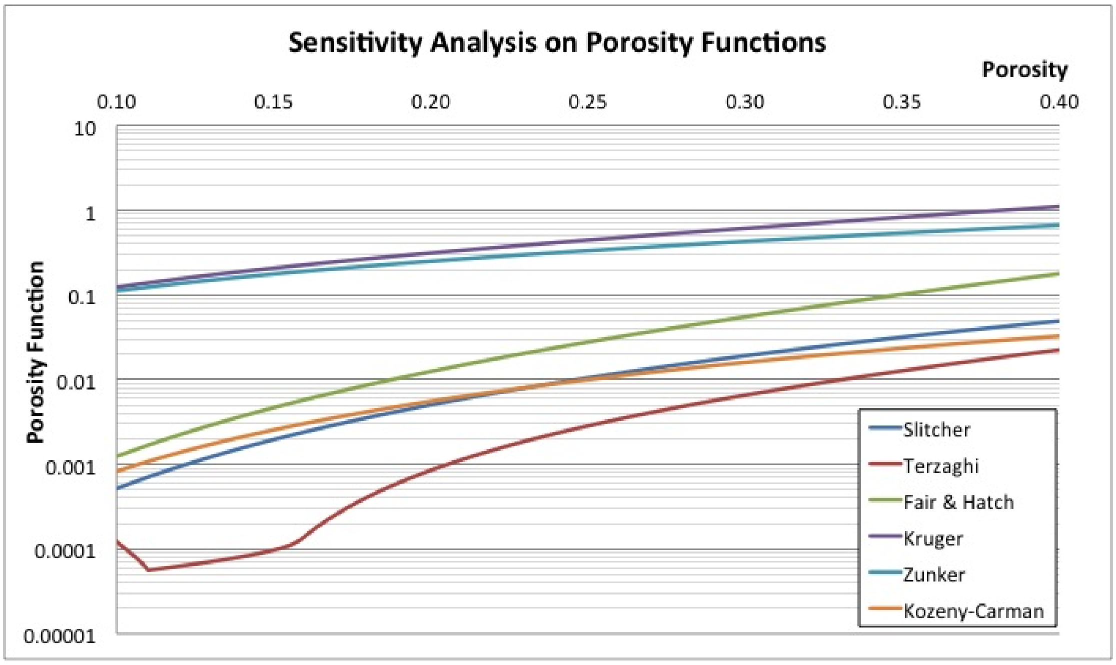

FIGURE 2.2: Sensitivity analysis of different porosity functions at different values of porosity starting from 0.10 to 0.40. The Kruger and Zunker equations can yield values up to two orders of magnitude higher than the others.

were estimated using the uniformity coefficient U (defined in the next subsection) as proposed by Istomina (1957):

$$n = 0.255(1 + 0.83^U) \tag{2.2}$$

this equation resulted from an empirical trend (Figure 2.3) found after extensive analysis on sandy sediments and has proven to be accurate for well-graded sands and gravels with little clay content (Istomina, 1957). Other researchers have also studied this relationship (Dimkic, 2008), revealing that it works well when estimating porosities in sandy sediments where low uniformity coefficients yield high porosities. However, it is evident that this empirical relation converges to a value of 0.255 as the uniformity coefficient U becomes large. In the mine GSDs the average U for the 874 samples is 50, so using this equation provides porosities very close to 0.255.

2.2.4 Uniformity Coefficient (U) and Shape Factor (SF)

Two other factors that are included in most of the equations for K are the uniformity coefficient and the shape factor. The uniformity coefficient (defined as C_U in soil mechanics (Lambe and Whitman, 1969)) assesses the gradation of grain sizes in the samples and is mathematically calculated through the following expression:

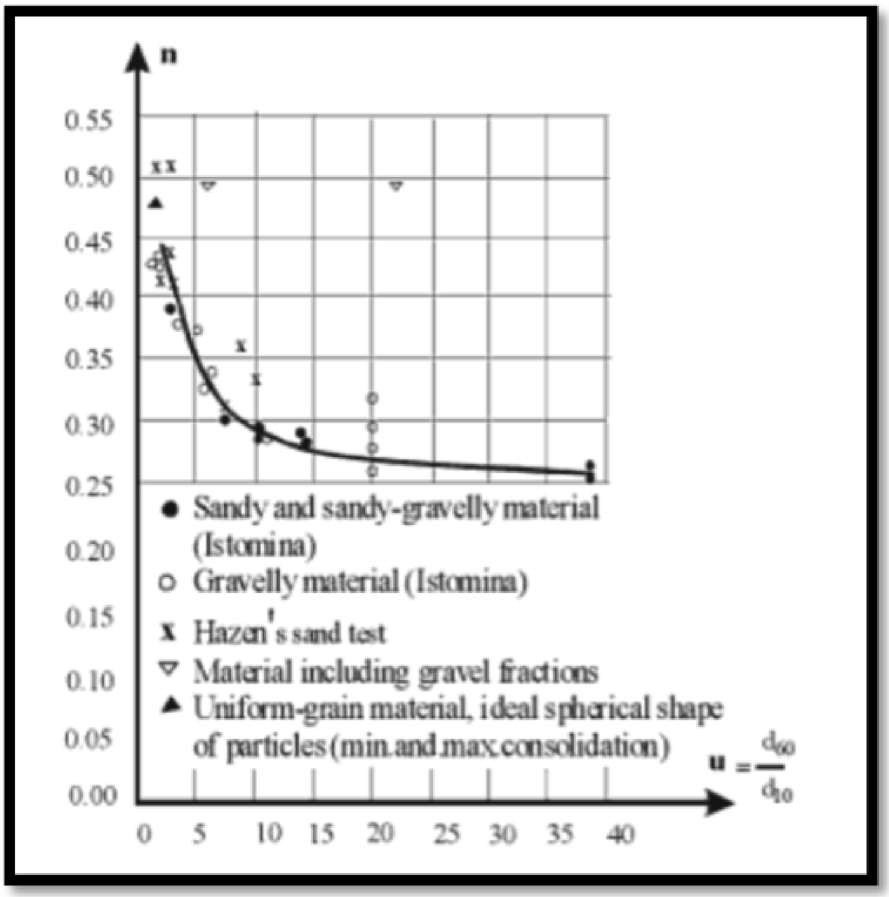

FIGURE 2.3: Estimates of porosity plotted as a function of the uniformity coefficient for different granular materials. Summary of results of Istomina (1957).

$$U = \frac{d_{60}}{d_{10}} \tag{2.3}$$

The shape factor (SF) takes into consideration the angularity and sphericity of the grains through surface area concepts and is calculated as the surface area of a grain divided by its volume (Carrier, 2003). All calculations of conductivities in my research assume grains with shapes resembling worn angular sand grains for a value of SF = 6.4 as stated by Fair and Hatch (1933).

2.3 Background Statistics

In this section definitions of key statistics concepts used throughout this thesis are presented. The first part titled *Statistical Distributions* provides a short summary on random variables, lognormal distributions, point estimators, z-distributions, confidence intervals, and least squares errors. The second part titled *Absolute Error Propagation* explains the calculations by which the uncertainty in the lab experiments is quantified.

2.3.1 Statistical Distributions

A *variable* is defined as a characteristic that changes over time for different individuals or objects. Similarly, a *random variable* is the numerical value of a variable obtained after the random outcome of an experiment or observation (Mendenhall, 2009). The total number of possible experiments or observations define what is referred to as the *statistical population* or simply *population*. The probability for each of the potential realizations of the random variables over the whole statistical population forms the *probability distribution* or simply the *distribution* of a random variable. This distribution could have many different shapes, but for this thesis research only lognormal distributions are discussed. When the number of observations is large enough, the distribution for the population becomes a smooth bell-shaped curve centered at a certain value $\overline{\mu}$ and with a standard deviation of σ. This is what is referred to as a *normal distribution*. When the random variable is normally distributed across orders of magnitude then the population presents a *lognormal distribution* (Figure 2.4). In this thesis research the random variable that is being studied is hydraulic conductivity (K), which is known to be lognormally distributed (Kieber, 1966).

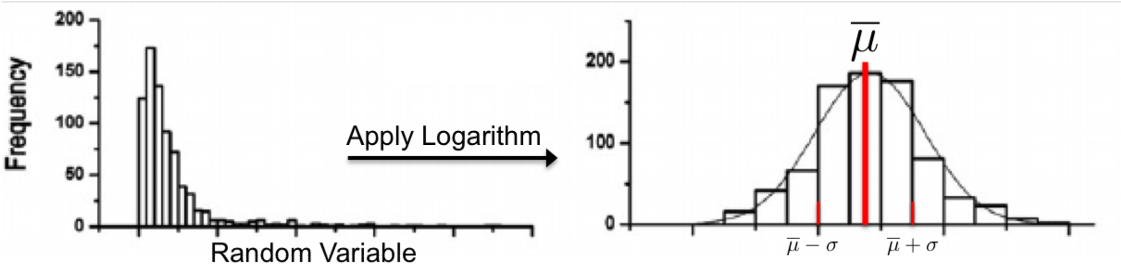

FIGURE 2.4: Illustration of lognormal distributions. A random variable normally distributed across orders of magnitude looks like the skewed curve on the left, but after applying logarithms this skewed curve becomes normally distributed across a mean $\overline{\mu}$ and standard deviation σ.

The mean ($\overline{\mu}$) and standard deviation (σ) that characterize lognormal distributions are rarely known, yet these parameters are estimated via *point estimators*. For example, suppose a statistician is interested in knowing the average income for families across the US. $\overline{\mu}$ represents the actual average income for all the families residing in the US, and hence one will never truly know $\overline{\mu}$ as this would mean going door by door to every household in the US asking for their income. However, one can estimate this mean by using a point estimator. There are many types of point estimators used to assess the mean of statistical distributions given a set of samples or observations. For example, the naive estimator approximates $\overline{\mu}$ as the simple average of the observed values and the maximum likelihood estimator uses likelihood functions and probabilities to estimate $\overline{\mu}$ (Mendenhall, 2009). For simplicity and consistency, in this thesis research the true mean $\overline{\mu}$ for the distributions of conductivities is approximated via the naive estimator calculated as the simple average of the observations.

When a normal distribution is standardized by centering values across zero and normalizing by the standard deviation, then a *z-distribution* results (Mendenhall, 2009). z distributions are important because they represent populations in terms of standard deviations and probabilities (i.e., a z-distribution shows the probability that a certain value for a variable is x standard deviations away from its mean). However, when the statistical population is small and standard deviation is large, z-distributions tend to overestimate probabilities and hence t-distributions are used in this scenario. Depending on the situation, either z or t distributions are used to derive $z_{\alpha/2}$ or $t_{\alpha/2}$ critical values (Mendenhall, 2009) through which confidence intervals are estimated. α is referred to as the *significance level* and represents the proportion of values within the tails of the normal distribution, and the critical values $z_{\alpha/2}$ or $t_{\alpha/2}$ represent the probability that the random variable obtains a value in the lower or upper tail of a normal distribution (Figure 2.6). Critical values for t and z distributions are well-studied for many significance levels and appear in tables in the vast majority of statistics books. Mathematically, confidence intervals (CIs) are estimated via the following formula:

$$CI = parameter \pm z_{\alpha/2}\frac{\sigma}{\sqrt{n}} \tag{2.4}$$

where $t_{\alpha/2}$ can replace $z_{\alpha/2}$ and n represents the number of observations or experiments. The subtraction in (2.4) represents the *lower confidence interval* (LCL) for the parameter and the addition represents the *upper confidence interval* (UCL). To better illustrate these concepts here is an example. To estimate the 95% confidence interval for a mean point estimator $\mu = 2$ with $\sigma = 1$ derived after $n = 25$ observations one would use (2.4) and find a LCL=1.608 ($2 - 1.96/\sqrt{25}$) and a UCL =2.392 ($2 + 1.96/\sqrt{25}$). This means that the point estimator $\mu = 2$ for the 25 observations having a $\sigma = 1$ could approximately be between 1.6 and 2.4 95% of the time. The number 1.96 is the critical value for the z-distribution found after looking up the $z_{\alpha/2} = z_{0.025}$ critical value in a z-table in a statistics book.

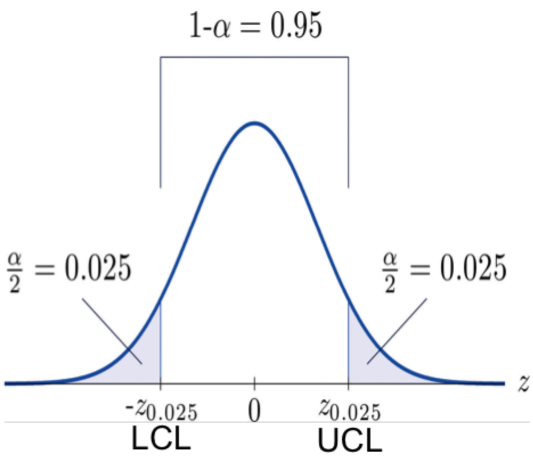

FIGURE 2.5: Confidence intervals are estimated after the critical values $z_{\alpha/2}$.

2.3.2 Normal Probability Plots

Normal probability plots (NPP) are used to assess if a sample of n observations comes from a much larger population that follows a normal distribution. Mendenhall (2009) defines NPPs as graphs that plot the values for each of the n observations against the expected value of those observations had they come from a normal distribution. In NPPs the cumulative probability of observe a certain value is plotted on the y axis and the value for each of the n observations on the x axis (Figure 2.6). A straight line in these plots marks a perfectly normal distribution and the points around this line represent the observed data. Normal probability plots test the normality assumption for a certain set of observations.

2.3.3 Absolute Error Propagation

Using the equations cited on Appendix A, the observed values for the lab samples' permeabilities (K_{obs}) were compared to permeabilities derived from the nine equations using the parameters that describe the GSD as called for by each empirical equation. For each of the nine values of conductivities, confidence intervals (CIs) were estimated through the absolute error propagation approach. In standard lab experiments, an absolute error propagation approach consists of taking the total derivative of the equation estimating the metric the experimenter is interested in with respect to the control variables (Harvard Instructional Physics Lab, 2008). For example, in a physics lab if one is measuring the kinetic energy of a certain object one will measure the object's mass (m) and its velocity (v) to use the formula $E_k = \frac{1}{2}m \times v^2$. The error associated with this point estimator will be $\Delta E_k = \frac{1}{2}[\Delta m \times v^2 + 2m \times v\Delta v]$ where the quantities Δm and Δv correspond to the instrument precision of the balance used to measure the object's

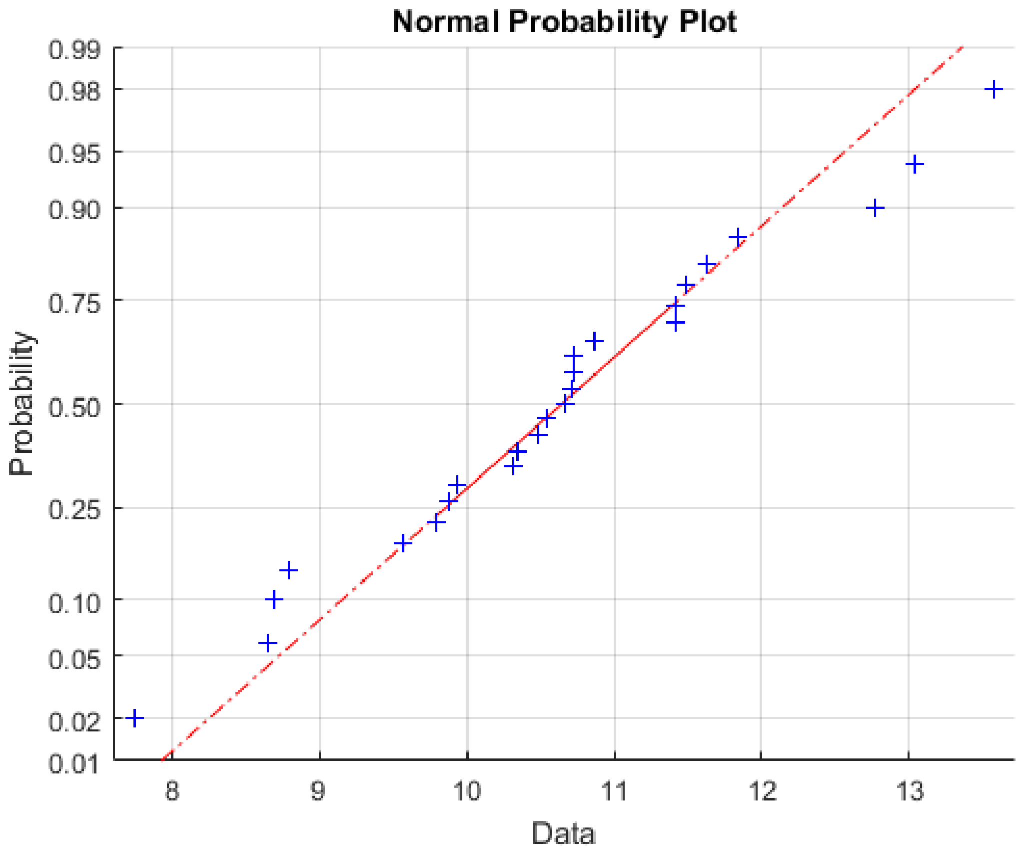

FIGURE 2.6: An example of a normal probability plot taken from Matlab 2015 help browser for the "normplot" function. The plus blue signs mark the observations and the red line represents the expected value of these observations had they come from a normal distribution. Observed values close to the straight line permits assuming a normal distribution for the population of interest.

mass and whatever artifact is used to measured its velocity. Since hydraulic conductivities are lognormally distributed (Kieber, 1966), the equations in Appendix A were first log transformed prior to taking the derivative with respect to the d_x percentiles. These derivatives used to quantify uncertainties in the estimations of conductivities in lab samples can be found in Appendix B. As an example of how this procedure was carried out, using the log transformed USBR equation ($\log \Delta K_{USBR} = \log(0.36 \times d_{20}^{2.3})$) we will estimate the error corresponding to this estimate by calculating the total derivative of this expression in terms of the factors we control for, which is d_{20} in this example ($\log \Delta K_{USBR} = 1/(0.36 d_{20}^{2.3}) \times 0.36(2.3 d_{20}^{1.23} \Delta d_{20}) = 0.36(2.3 d_{20}^{1.23} \Delta d_{20})/K_{USBR}$). Having a confidence interval for each of the nine conductivities permits evaluating how well do each of these equations represent observed values in a controlled setup. However, many assumptions were made in the quantification of the error in the measured quantities during lab experiments to acknowledge experimental and time limitations. The following *assumptions* are based on the judgment of the author of this thesis:

1. Δd_x: The error associated with the d_x percentiles in the GSD. This value is taken as a fixed constant of 0.01 mm corresponding to coarse silt (Chester, 1922). An example illustrates this parameter. When mechanical sieve analysis takes place at large scales in a mine, it is possible that not all particles trapped on, for example, sieve #100 are exactly 0.149 mm. It is possible that these particles will be a little larger or smaller than this value. I am representing this variability in the sizes of the d_x percentiles that make up the GSD curve as a fixed value of 0.01 mm that represents small particles (fine silt) adhered to larger grains. The logic behind this assumption is that if the air-dried samples were to contain some moisture, then very small particles (such as coarse silt) could have been adhered to larger grains and thus affect the GSD of the sample and introduce a bias in the discharge rate observations at large scales.

2. ΔP_i and Δf_i: The error associated with the cumulative percent of material trapped at the i^{th} sieve (ΔP_i) and the net fraction of material in the i^{th} sieve (Δf_i) were arbitrarily estimated as 5% of P_i and f_i. To make these estimates robust, several sieve analyses would have to be made on the same, well-known, amount of granular material and after several iterations it will be possible to estimate the error associated with ΔP_i and Δf_i for the instrument.

3. Δn: The error associated with porosity calculations. This parameter was estimated considering that 50 ml of water, corresponding to the instrument precision, could affect the discharge observations. If so, this error of 50 ml in specific yield calculations represents a constant value of 0.011 or 1.1% error in porosity estimates.[2]

4. Δh and ΔL: The error associated with hydraulic head (Δh) and length (ΔL) was 0.1 cm, corresponding to the instrument precision of the ruler used to measure these parameters.

all other parameters that may be present in the equations and not mentioned before were regarded as constants for error calculations.

2.4 Description of the Mine Samples

The samples from the mine used in this thesis research consists of 874 grain-size distribution (GSD) samples collected over a period of six years in a copper mine in northern Chile. These samples were taken from porphyritic rocks that provide chalcopyrite

[2] From the specific yield equation we have that $n = \frac{Vol_{water}}{4{,}355cc} = \frac{50}{4{,}355} = 0.011$

ores with an average Cu grade of 0.62% and sieved with 1" [25.4 mm], 3/4" [19 mm], 1/2" [12.7 mm], 1/4" [6.35 mm], #10 [2 mm], #50 [0.297 mm], #100 [0.149 mm], #200 [0.07 mm] sieves. These 874 samples came from 16 loads (LOAD 2 through LOAD 17) and these loads were further segregated into two modules (A and B) with the exception of LOAD 2 and LOAD 15 (only B module) and LOAD 17 (only A module). A load is simply the movement of the conveyor belt from point to point across the mine (Figure 2.7) and a module is a way to identify the side where the conveyor belt is depositing the heap (e.g. east/west, left/right, or in this case A/B, Figure 2.7). A sample is referred to as a portion of the material that makes up the overall heap (Figure 2.8). Such segregation of material into loads, modules, and samples is done so as to track mining operations through time. In Table 2.2 the loads, modules, and number of samples within each leaching heap researched in this thesis are summarized. The same table also contains information about the average weight and the average percentage (net of weight) of Cu estimated in each sample as well as the percentages of Cu recovered and lost after leaching. On average, the heaps encompassed an area of 8,225 m^2 and were 7.5 m high. It is advantageous to construct heaps that are shorter than they are wide, as this geometry diminishes compaction, increases aeration, and thus makes the granular medium more permeable for leachates (Yao et al., 2013). It took approximately one day of sieving via conveyor belts to transport and deposit each sample into its leaching heap.

The GSDs for all 874 samples plotted together can be seen in Figure 2.9. The average U for the 874 GSDs is 50 and the average d_{10} is 0.2 mm corresponding to well-graded fine sands with gravels (Lambe and Whitman, 1969). Summary statistics depicting averages, minimums, maximums, medians, and standard deviations of the d_x percentiles of the 874 GSDs along with the weights of each of these mine samples in Figure 2.10.

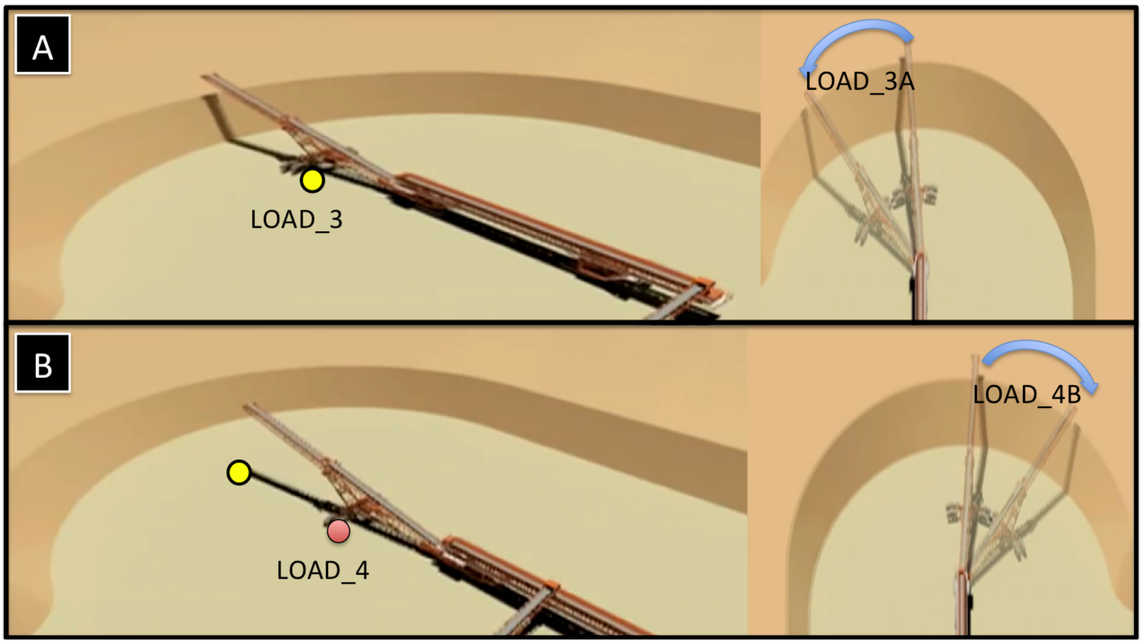

FIGURE 2.7: (A) This figure illustrates a conveyor belt depositing LOAD 3A. (B) After enough samples have been deposited into LOAD 3A, the conveyor moves to location 4 and starts depositing samples to its right (LOAD 4B). NOTE: The leaching heaps in our case are discreet mounds of material. (images from superior industries, manufacturer of mining equipment `www.youtube.com/user/superiorind1972/about`).

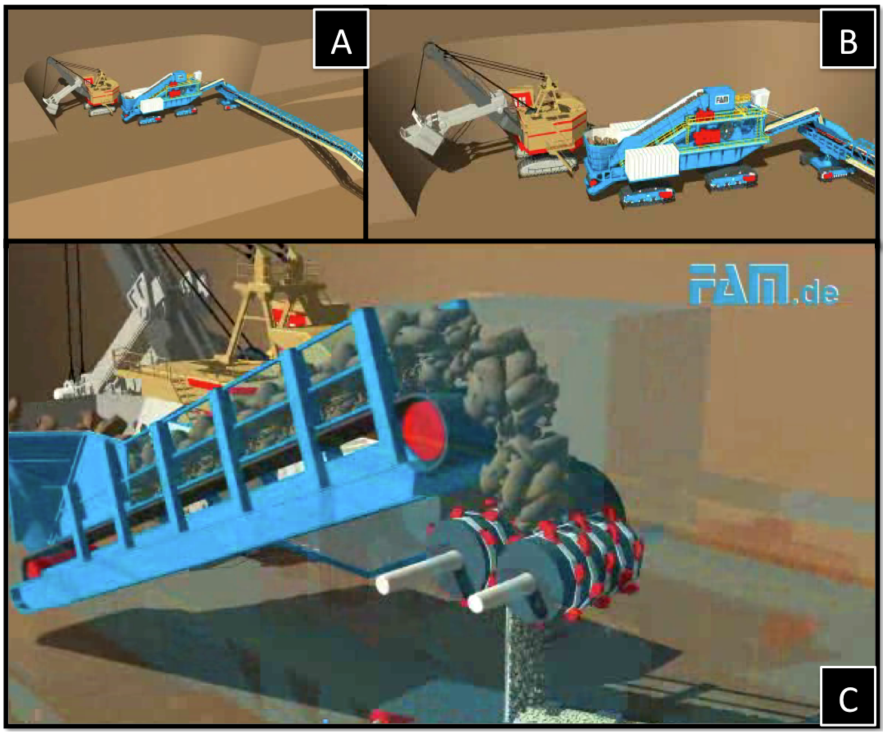

FIGURE 2.8: (A) A loader truck takes a certain amount of material X from the mineral deposit and (B) places it into the grinder. (C) The grinder crushes the material and the sands, gravels, and silts, constituting a sample, are transported to form the heaps. (images from FAM, manufacturer of mining equipment `www.FAM.de`).

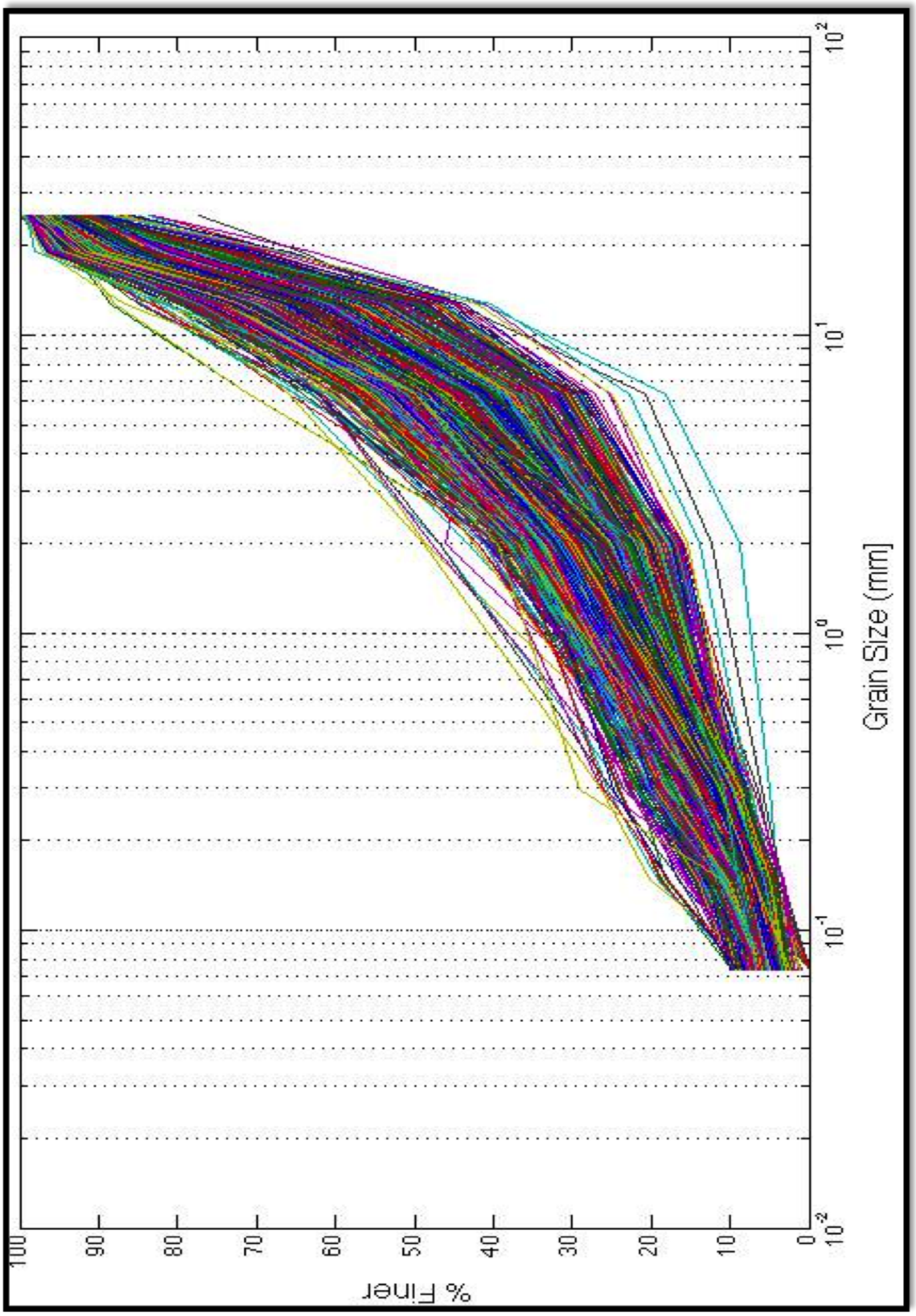

FIGURE 2.9: GSD of 874 mine samples plotted together.

Table 2.2: **Data Segregation**

heap	**Name**	**N**	**Avg Weight [T]**	**Avg %Cu Estimated**	**Avg %Cu Lost**	**Avg %Cu Recovered**
1	LOAD_2B	8	102,780	0.74	0.19	0.55
2	LOAD_3A	9	107,310	0.63	0.18	0.45
3	LOAD_3B	9	103,510	0.71	0.15	0.56
4	LOAD_4A	7	87,540	0.81	0.14	0.67
5	LOAD_4B	27	100,362	0.88	0.15	0.73
6	LOAD_5A	25	110,640	0.71	0.15	0.56
7	LOAD_5B	31	105,110	0.71	0.1	0.61
8	LOAD_6A	25	109,410	0.89	0.09	0.8
9	LOAD_6B	14	97,807	0.73	0.4	0.33
10	LOAD_7A	14	107,580	0.98	0.27	0.71
11	LOAD_7B	11	95,140	0.89	0.27	0.62
12	LOAD_8A	18	103,340	0.92	0.22	0.7
13	LOAD_8B	12	96,181	0.71	0.19	0.52
14	LOAD_9A	32	91,138	0.69	0.18	0.51
15	LOAD_9B	45	77,321	0.71	0.19	0.52
16	LOAD_10A	37	74,240	0.61	0.18	0.43
17	LOAD_10B	52	81,180	0.57	0.14	0.43
18	LOAD_11A	41	82,783	0.54	0.13	0.41
19	LOAD_11B	32	79,332	0.53	0.15	0.38
20	LOAD_12A	41	96,219	0.55	0.13	0.42
21	LOAD_12B	40	80,593	0.65	0.22	0.43
22	LOAD_13A	51	98,669	0.62	0.18	0.44
23	LOAD_13B	48	96,843	0.58	0.15	0.43
24	LOAD_14A	48	91,379	0.58	0.14	0.44
25	LOAD_14B	55	96,150	0.53	0.16	0.37
26	LOAD_15B	26	93,739	0.52	0.16	0.36
27	LOAD_16A	44	105,540	0.58	0.11	0.47
28	LOAD_16B	49	97,955	0.62	0.13	0.49
29	LOAD_17A	22	106,780	0.57	0.14	0.43

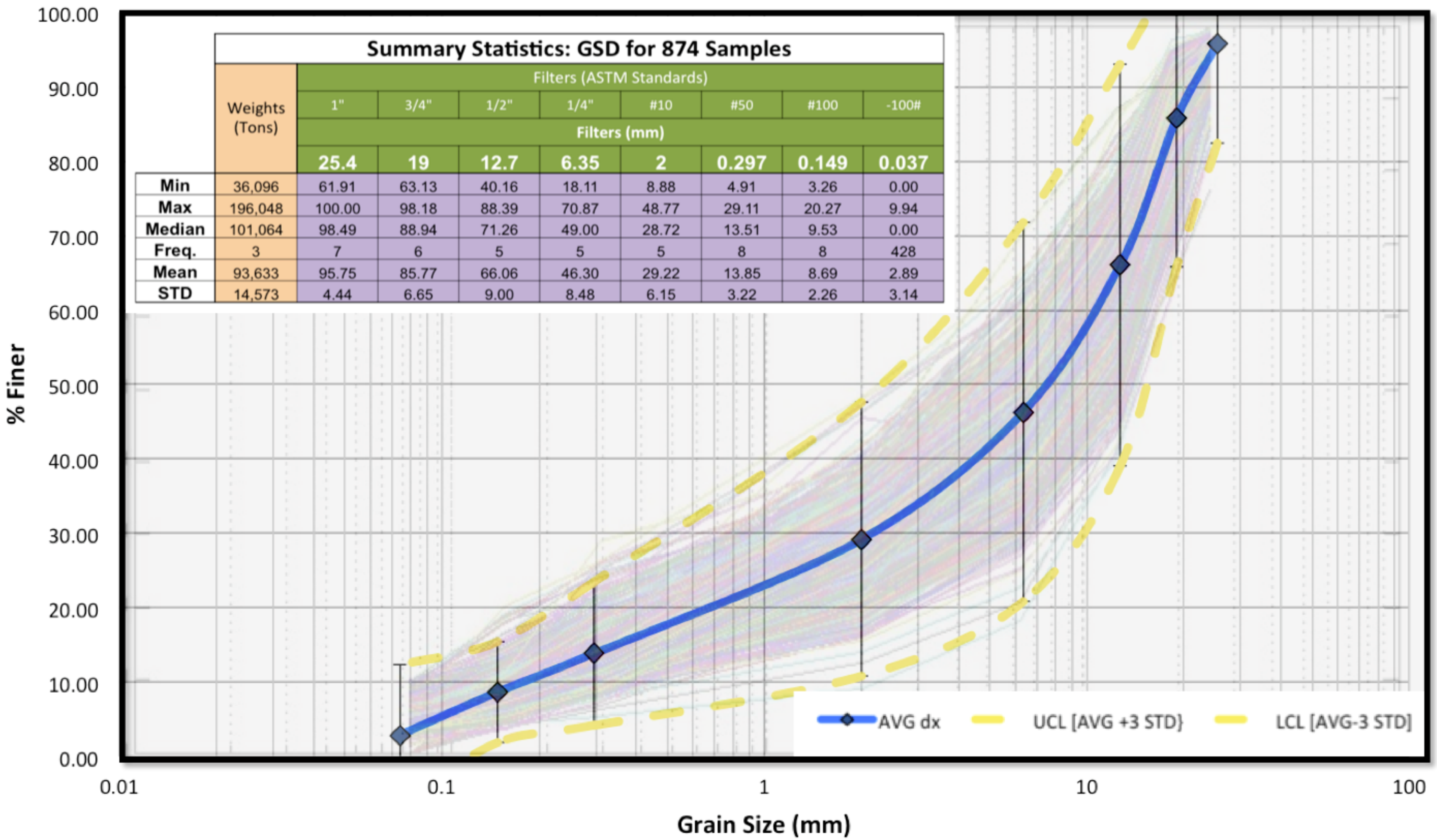

Summary Statistics: GSD for 874 Samples

	Weights (Tons)	Filters (ASTM Standards)							
		1"	3/4"	1/2"	1/4"	#10	#50	#100	-100#
		Filters (mm)							
		25.4	19	12.7	6.35	2	0.297	0.149	0.037
Min	36,096	61.91	63.13	40.16	18.11	8.88	4.91	3.26	0.00
Max	196,048	100.00	98.18	88.39	70.87	48.77	29.11	20.27	9.94
Median	101,064	98.49	88.94	71.26	49.00	28.72	13.51	9.53	0.00
Freq.	3	7	6	5	5	5	8	8	428
Mean	93,633	95.75	85.77	66.06	46.30	29.22	13.85	8.69	2.89
STD	14,573	4.44	6.65	9.00	8.48	6.15	3.22	2.26	3.14

FIGURE 2.10: A graphical representation of the GSDs from the mine and summary statistics. In the table, the green region represents the sieve sizes both in ASTM standards and in millimeters. The purple region contains the summary statistics for the dx percentiles of the GSDs and in orange the summary statistics for the samples weights. In the chart, the blue solid line represents the average dx corresponding to the cumulative material trapped in each sieve. The yellow lines represents the upper confidence level (UCL) and lower confidence level (LCL) taken as a 99.% confidence (average dx plus (UCL) or minus (LCL) three times its standard deviation).

2.5 Description of the Nine Equations

Before discussing the details of each of the nine equations being analyzed in this thesis, it is important to know that these equations were either empirically calculated from lab experiments or mathematically derived under various assumptions. The authors of these equations showed that each of these formulas provide accurate estimates under what is referred to in this thesis as a *region of validity*, which is a series of restrictions placed on certain parameters of the granular medium such as grain size or uniformity coefficient. The region of validity for each equation is described in the section below summarized in Table 2.3 and Appendix A. As previously discussed, all these equations describe saturated hydraulic conductivities.

Hazen (1892) identifies hydraulic conductivity as the velocity of water in his experiments and concluded that hydraulic conductivity is a function of temperature (T), effective grain-size (d_{10}), head loss (H), and sediment thickness (L). Hazen (1892) made the observation that "[hydraulic conductivity] probably varies also somewhat with the uniformity coefficient, but no satisfactory data are at hand upon that point," and he limited the scope of his experiments to sands with a uniformity coefficient $U < 5$ and an effective radius d_{10} within the range of 0.1 - 3.0mm. According to Hazen (1892), this simplification of his formula offers the "maximum rate" of fluid flow since his equation is based on the most ideal circumstances of a fully saturated medium with water at $10°C$ undergoing a gradient of one (loss of head equal to the sediment thickness). However, Carrier (2003) shows that correcting Hazen's equation for water at $16°C$ yields permeabilities at least 18% larger than at $10°C$. Carrier (2003) also showed that Hazen's method relies heavily on its empirical assumptions and yields values of K that can differ up to several orders of magnitude from lab experiments. Yet, Hazen's equation continues to be the standard in the geosciences due to its simplicity.

The formula for hydraulic conductivity of Kozeny-Carman as explained in Carrier (2003) was originally developed by Kozeny for a series of capillary tubes in sands with $d_{10} \leq 3mm$ and later modified by Carman so as to include the notion of hydraulic radius and the pore diameter of an equivalent capillary (Chapuis and Aubertin, 2003). Therefore, Kozeny-Carman equation makes use of sediments' GSDs to estimate an effective radius. According to Carrier (2003) many authors often interpret this effective radius in different ways; some say it corresponds to d_{10} while others express it as an arithmetic expression including the entire GSD (Carrier, 2003). In this work I adopt the latter.

Beyer's method (Beyer, 1966) was empirically derived so as to assess the movement of pollutants through geological beds. This method also approximates the movement of liquids as if passing through a pipe and thus porosity takes on the value of one. Beyer's

TABLE 2.3: **Region of validity for empirical equations**

Equation	Uniformity Coefficient	Grain Size	Notes
Hazen	U<5	0.1mm≤ d_{10} ≤3mm	No porosity
Kozeny-Carman	-	d_{10} ≤3mm	Not applicable in clayey sediments
Beyer	U<20	0.06mm≤ d_{10} ≤0.6mm	Porosity of one
Slichter	-	0.01mm≤ d_{10} ≤5mm	No uniformity coefficient
Terzaghi	-	0.25mm≤ d_{10} ≤2mm	Shape and gradation of grains included in the empirical coefficient C_t
Fair & Hatch	-	0.1mm≤ d_{10} ≤2mm	Derived for unstratified sand beds Includes a shape factor between 7.7 and 6.0
Kruger	U>5	0.25mm≤ d_{10} ≤2mm	Shape factor included in empirical coefficient β_k
Zunker	-	-	Shape and gradation of grains included in the empirical coefficient β_z
USBR	U<5	.06mm≤ d_{10} ≤2mm	Suitable for sands

method is believed to be mostly useful for heterogeneous, poorly sorted, samples with effective grain sizes between 0.06 and 5 mm and $U < 20$ (Odong, 2007). Slichter's formula (Slichter, 1898) uses potential theory in groundwater flow to quantitatively describe the steady-state flow field in response to a discharging well, and according to the USGS, it could be the first quantitative analysis of groundwater. The equation is derived after Slichter's multiple laboratory experiments of water moving through porous soils or rock under different pressures. As originally published in Slichter (1898), the formula makes use of an average grain-size, does not takes into consideration the shape of the grains, and is simplified for water at $10°C$. Several researchers (Vukovic and Soro, 1992; Odong, 2007; Cheng and Chen, 2007) tested this formula with different materials, and their findings indicate that it is most reliable in sand samples with grain sizes between 0.01 and 5mm with no restrictions on the uniformity coefficient of the granular media.

The Fair and Hatch method (Fair and Hatch, 1933) calculates the head lost for expanding, unstratified, and stratified filter beds. In this thesis I will only consider their model for unstratified filter sand beds with d_{10} between 0.1 and 2mm describing grain sizes in the interval of very fine to coarse sands (Chester, 1922) as it most resembles the physical configuration of grains in heap leaching heaps. Fair and Hatch (1933) reworked the results of Poiseuille in the 1840s (Sutera, 1993) and Darcy in the 1850s (Darcy, 1856) so as to factor in the length of the path followed by the water and the diameter and shape of the particles constituting the granular medium. Fair and Hatch's equation is based on experimental data and takes into consideration the viscosity (μ) and density (ρ) of the permeating fluid. This equation also makes use of a pipe constant (κ) which represents the porous medium conduits as a pipe of constant diameter. Fair and Hatch (1933) assume this value to be 32 and hence this thesis makes this same assumption. A noticeable distinction of this method is that it directly includes the entire GSD curve in its calculations and defines a shape factor (SF) for the grains calculated as the ratio of surface area to volume between 7.7 for angular grains and 6.0 for well-rounded grains.

As summarized in Vukovic and Soro (1992), the United States Bureau of Reclamation (USBR) in collaboration with several scientists developed a formula for the hydraulic conductivity of soils comprising medium-grain sands with average grain sizes between 0.06 and 2mm and uniformity coefficients less than five (USBR, 1978). Some studies indicate that the USBR tends to underestimate conductivities (Salarashayeri and Siosemarde, 2012; Odong, 2007; Ishaku and Kaigama, 2011). The USBR developed this formula specifically to aid irrigation in agriculture as "excess water and salt must be removed from soils for irrigation to be permanently successful" (USBR, 1978). When simplified for water at $10°C$, converting inches per hour to centimeters per second, and using grain-sizes corresponding to uniform sand grains, the expression can be simplified to the one appearing in Appendix A (Vukovic and Soro, 1992).

Terzaghi's equation is based on a one-dimensional consolidation equation representing the visco-elastic behavior of soils as they react to applied loads in civil engineering (Di Francesco, 2013). Even though Terzaghi's equation is intended for civil-engineering consolidation problems, several authors have applied it to groundwater flow situations and obtained hydraulic conductivities close to observed values (Vukovic and Soro, 1992; Odong, 2007; Cheng and Chen, 2007). In this work, I adopt the Vukovic and Soro (1992) simplification of Terzaghi's equation as Vukovic and Soro (1992) stated that Terzaghi's equation yields results matching empirical observations for coarse sands with average grain sizes between 0.25 and 5mm. Terzaghi's equation includes the shape of the grains and gradation of the sediments through an empirical constant C_t, which takes a value of 0.0061 for coarser sands and 0.107 for smooth grains (Vukovic and Soro, 1992).

The last two methods for calculating hydraulic conductivities based on grain-size distributions that are used in this thesis research are Kruger's (Vukovic and Soro, 1992) and Zunker's (Zunker, 1932) formulas. Vukovic and Soro (1992) analyzed Kruger's formula and determined that it yields best results when applied to medium-grain sands with average grain size between 0.25 and 2mm and uniformity coefficients larger than five. Zunker's equation also makes use of an empirical coefficient β_z that describes the gradation and angularity of the grains. β_z has a value of 0.0024 for uniform sand with smooth rounded grains, a value of 0.0014 for a uniform composition of coarse grains, 0.0012 for non-uniform grains, and 0.007 for clayey grains of irregular shape. Kruger's method includes a large portion of the grain-size distribution curve and represents water moving through sand at $0°C$. Therefore, after eliminating some simplifications appearing in Vukovic and Soro (1992) and using values of viscosity corresponding to water at ten degrees Celsius, the modified version of Kruger's method appearing in Appendix A is obtained. Zunker's formula (Zunker, 1932) is derived for agriculture and fertilization and contains an empirical coefficient (β_k) that is a function of grain-size and the uniformity coefficient. For this thesis, $\beta_k = 0.00435$ representing homogeneous well rounded sands is used (Vukovic and Soro, 1992). Zunker's formula has been found to yield values of conductivities that, on average, are two orders of magnitude higher than observed values (Vukovic and Soro, 1992; Petalas and Pilakas, 2011) and hence is ignored for practical applications in science and engineering.

In application to this research, the average grain size d_{10} for the sediments in the leaching heaps is 0.2mm and the average uniformity coefficient U is 50. This means that the well-graded fine sands with gravels used in leaching are different from the homogeneous sands under which these nine equations have proved to estimate observed conductivities (Vukovic and Soro, 1992). In the next chapter of this thesis these nine equations will be used to test how well they predict the observed conductivities in sediments with a GSD similar to the ones used in leaching in controlled lab experiments.

Chapter 3

Determinations of Hydraulic Conductivity in Lab Experiments

As discussed at the end of the previous chapter, the well-graded fine sands with gravels used in leaching differ from the homogeneous sands where the nine equations have proven to represent observed conductivities. In this Chapter we will use the nine empirical equations to compute values of conductivities in sediments resembling those used in leaching and compare these empirical values to actual observations.

This Chapter is divided into three main sections. The first section titled *Constant Head Permeability Tests* describes the procedure followed, equipment used, constructed samples, assumptions made, and calculations done so as to compute the observed conductivities that constitute the best estimates of conductivities for each sample. The second section, *Results*, shows and explains the results of the constant head permeability tests that indicate that the USBR equation provides the most accurate estimate of hydraulic conductivity for leaching heaps. The third section, *Discussion of Results*, provides some detail about the equations and the impact of changing some of the assumptions made for the lab experiments.

3.1 Constant Head Permeability Tests

3.1.1 Equipment and Lab Samples

Constant head permeability tests were conducted in accordance with the ASTM D-2434 standards for granular sediments, as summarized in this section. A Humboldt HM-3894 permeameter (Figure 3.1) with a cylindrical chamber measuring 15.2 cm diameter by 24 cm height was used for testing. Four different lab samples (OTT, HBB, MOTG, and MBBG) were constructed using Ottawa sands donated by GEI consultants, unconsolidated granular material collected from the St. Mary's renovation site on the Boston College campus, and Quickrete gravels and sands bought in a local hardware store. It is important to make the distinction that lab samples refer to the samples of sands and gravels formed at Boston College, which is different from the samples of granular material of metal ore that the leaching heaps were formed with.

In theory, every granular medium has a certain hydraulic conductivity X that can be observed in constant head permeability tests, and the equations that I am researching approximate that X through a mathematical relationship based on different parameters derived from GSDs. Samples HBB and OTT have uniformity coefficients of 4.7 and 3.0 respectively and a d_{10} of 0.17 and 0.30 mm, respectively. Therefore, these samples are within the region of validity of all nine equations researched in this thesis. Comparing the observed conductivities from the constant head permeability tests in these samples to the conductivities obtained through the nine equations highlights the equations that best predict the observed conductivities.

The OTT and HBB samples were constituted solely from the Ottawa and Quickrete uniform sands, respectively, and their purpose was two fold. First, the Ottawa sands have been extensively studied and their hydraulic conductivity estimated as $K = 0.05\ cm/s$ (Lambe and Whitman, 1969), which is the same result I obtained from my constant head experiments, indicating no bias in my hydraulic conductivity measurements. Second, experimenting solely with the Quickrete sediments formed by medium to fine sands allows the evaluation of the underlying assumptions and region of validity implied by each of the nine equations. GSDs for the OTT and HBB samples appear in Tables 3.1 and 3.2, respectively. In these tables the last sieve, called *base*, refers to the solid receptacle at the bottom of the stack. Particles on this sieve were assumed to have a size of 0.02 mm, corresponding to medium to fine silt.

The other two samples (MOTG and MBBG) were formed by carefully mixing proportions of sediments so as to recreate, as closely as possible, the well-graded sands with gravels falling in the range of GSDs of the mine samples (Figure 2.9 and 2.10). To form

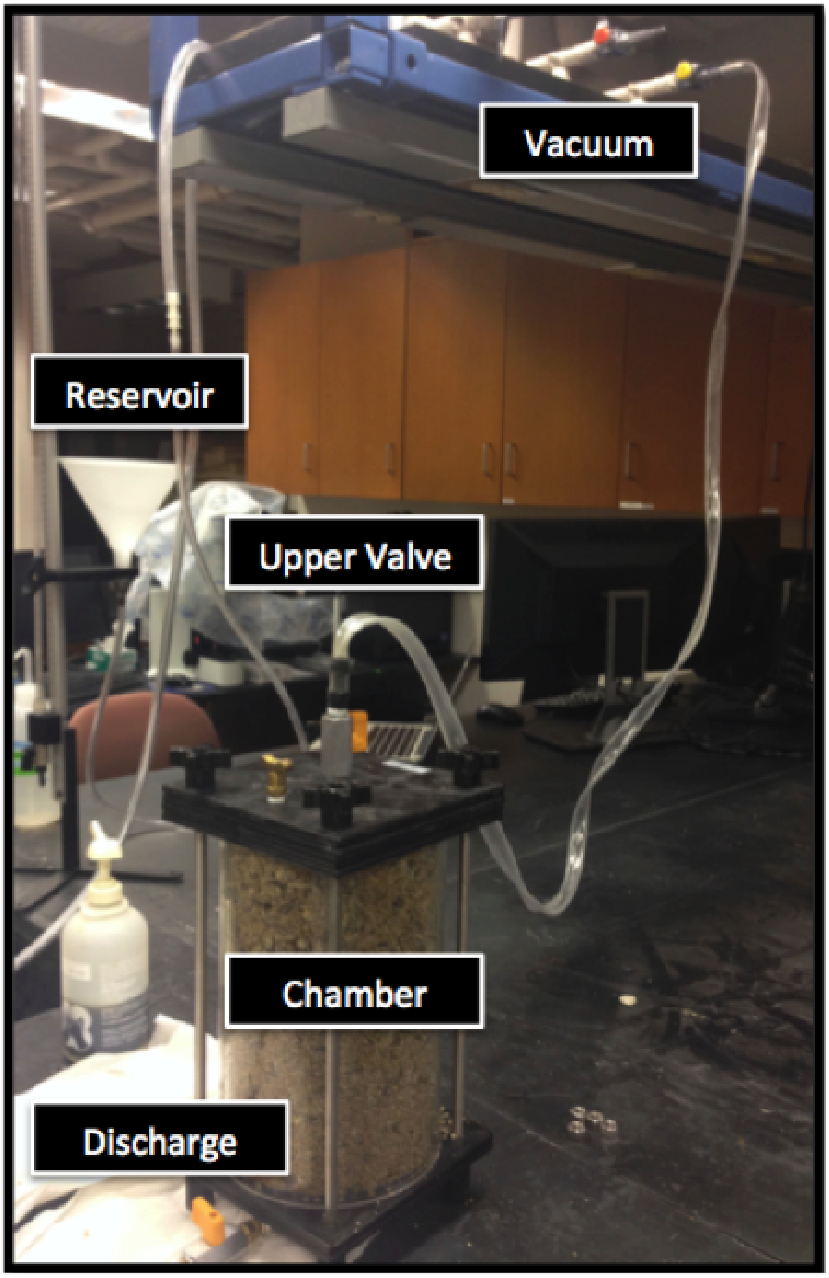

FIGURE 3.1: Assembled Humboldt permeameter, important parts referenced in the text are identified in black boxes.

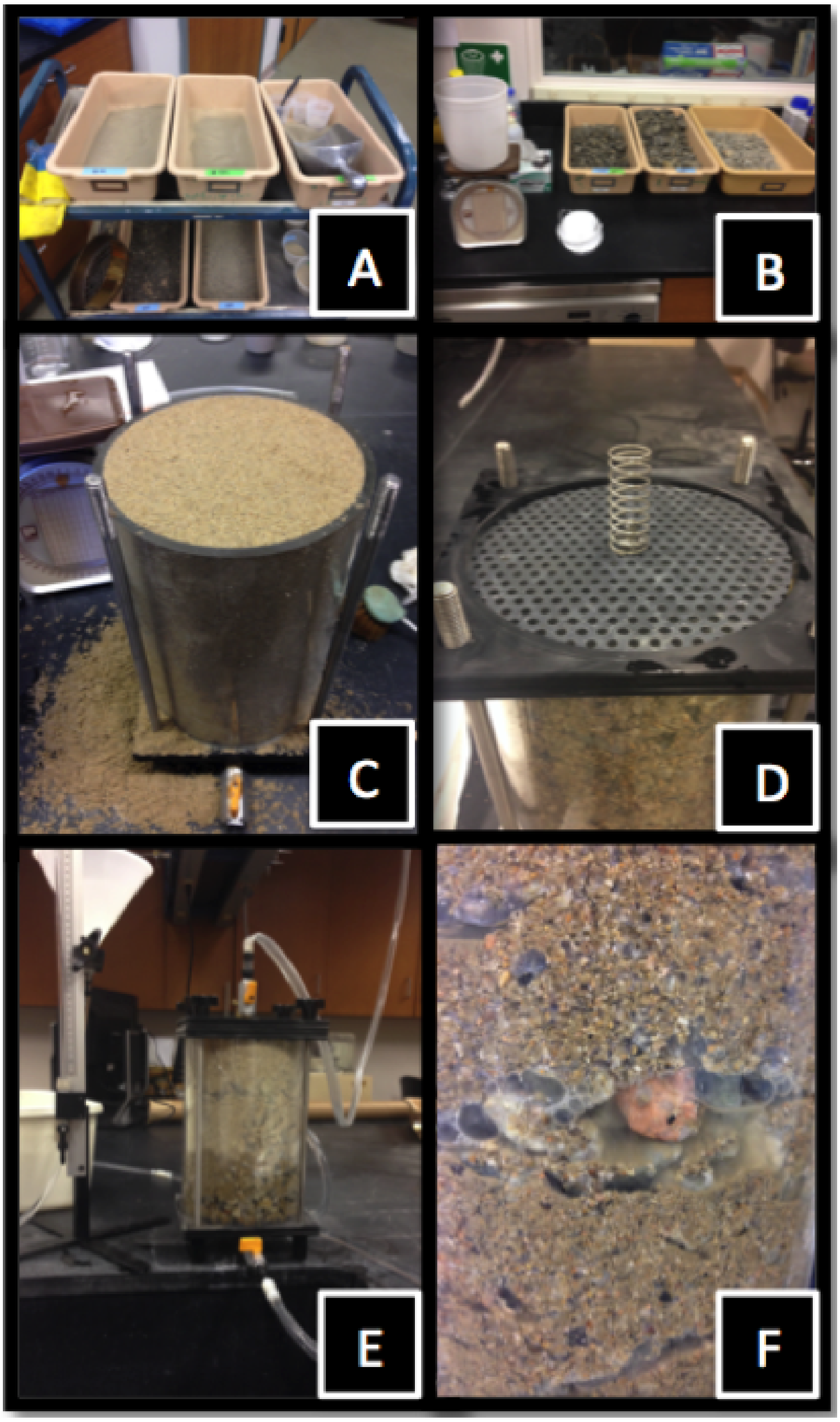

FIGURE 3.2: Sample setup.

the MOTG and MBBG samples approximately 8 Kg of sieved unconsolidated sediments of different sizes (Figure 3.2A) were weighed out (3.2B). These sediments were then thoroughly mixed by hand in a circular fashion with water at 20°C so as to simulate the agglomeration process and to have finer particles adhere to larger ones (forming pellet-like structures, Figure 1.2). Once the sediments were agglomerated and mixed in the desired proportions the sample was ready for permeability tests. The GSD for the MOTG sample appears in Table 3.3 and for MBBG in Table 3.4.

Once the samples were crafted they were placed in the chamber of the permeameter with the lower valve (or discharge in Figure 3.1) closed and were manually compacted with a closed fist after each additional four to six centimeters of additional material was added to the chamber. After the chamber was filled (Figure 3.2C), the top was leveled and a porous stone was held on top along with a net to prevent material escaping the chamber while allowing water to drip through. A spring (Figure 3.2D) that applied a pressure of 1.2-2.4 KPa was placed between the porous stone and the upper cap so as to prevent density changes and to preserve the mechanical stability of the sample during testing. After the spring was placed and the top cap closed, the chamber was finally secured with four knobs, and a vacuum of 15 mmHg (1.8 KPa) was placed through the upper valve for approximately five minutes so as to get most of the air out of the chamber. While the vacuum was being held in the chamber, the reservoir was connected to the bottom valve which was gradually opened until small drops of water started infiltrating the chamber. This part of the process is called *saturation under vacuum* and it was done so as to ensure full saturation (Figure 3.2 E-F).

TABLE 3.1: **OTT GSD**

OTT GSD						
Sieve			Weights (241.2 gr Total)			
			Retained		Finer	
#	mm	log10	[gr]	%	[gr]	%
10	2	0.30	0	0%	241.2	100%
40	0.425	-0.37	185	77%	56.2	23%
60	0.25	-0.60	42	17%	14.2	6%
100	0.149	-0.83	11.4	5%	2.8	1%
Base	0.02	-1.70	2.8	1%	0	0%

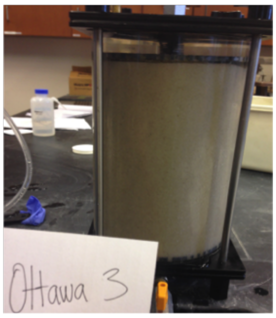

Ottawa monocrystaline fracking sands.

After the chamber was fully saturated, the vacuum was disconnected and the reservoir was placed at the upper valve. The next step was to open the bottom valve so that a continuous flow of water was allowed to pass through the sample via the upper valve at a certain, constant, hydraulic head (which in this case equals the elevation of the reservoir above the bottom of the chamber). After the rate of discharge was observed

TABLE 3.2: **HBB GSD**

HBB GSD						
Sieve			Weight (646.4 gr Total)			
			Retained		Finer	
#	mm	log10	[gr]	%	[gr]	%
10	2	0.30	43.4	7%	603	93%
40	0.425	-0.37	368.7	57%	234.3	36%
60	0.25	-0.60	100.8	16%	133.5	21%
100	0.149	-0.83	83.6	13%	49.9	8%
200	0.074	-1.13	22.2	3%	27.7	4%
230	0.063	-1.20	19.2	3%	8.5	1%
Base	0.02	-1.70	8.5	1%	0	0%

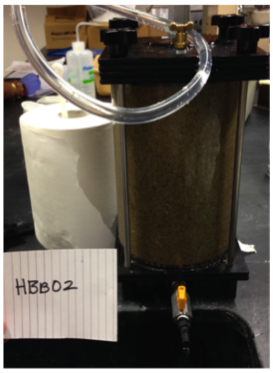

Homogeneous Quickrete brown bag sands.

TABLE 3.3: **MOTG GSD**

MOTG GSD						
Sieve			Weights [8.55 gr Total]			
			Retained		Finer	
#	mm	log10	[gr]	%	[gr]	%
1"	25.4	1.40	0.081	1%	8.47	99%
3/4"	19	1.28	3.3615	39%	5.11	60%
1/2"	12.7	1.10	0.6075	7%	4.50	53%
10	2	0.30	0.00	0%	4.50	53%
40	0.425	-0.37	3.45	40%	1.05	12%
60	0.25	-0.60	0.78	9%	0.26	3%
100	0.149	-0.83	0.21	2%	0.05	1%
Base	0.02	-1.70	0.05	1%	0.00	0%

Mixed ottawa and gravels.

TABLE 3.4: **MBBG GSD**

MBBG GSD						
Sieve			Weights (6.75 gr Total)			
			Retained		Finer	
#	mm	log10	[gr]	%	[gr]	%
1"	25.4	1.40	0.063	1%	6.69	99%
3/4"	19	1.28	2.6145	39%	4.07	60%
1/2"	12.7	1.10	0.4725	7%	3.60	53%
10	2	0.30	0.24	4%	3.36	50%
40	0.425	-0.37	2.05	30%	1.30	19%
60	0.25	-0.60	0.56	8%	0.74	11%
100	0.149	-0.83	0.47	7%	0.28	4%
200	0.074	-1.13	0.12	2%	0.15	2%
230	0.063	-1.20	0.11	2%	0.05	1%
Base	0.02	-1.70	0.05	1%	0.00	0%

Mixed Quickrete sands with gravels.

to remain constant for at least 30 seconds, the sample was interpreted to have reached steady state and a graduated cylinder with an instrument precision of 10 ml was placed at the discharge and 10 volumes of water were recorded for 5, 10, 15,..., 50 seconds. These ten measurements are referred to here as *observations* of discharge rate. With these ten observations, ten hydraulic conductivities were calculated through the following equation based on Darcy's law. This equation assumes full saturation of a Newtonian fluid in mechanically stable samples with constant density:

$$K = \frac{Q \times L}{A \times H} \tag{3.1}$$

where Q is the discharge [cc/s], L is the length of the sample [24 cm], A is the cross-sectional area of the cylindrical chamber (181 cm^2), and H is the elevation head [cm]. In reality, the aforementioned assumptions about a fully saturated medium and a mechanically stable sample are rarely met in heap leaching. Leaching heaps are not exactly mechanically stable as decrepitation and suffusion are intrinsic consequences of the leaching process itself (Williams, 2013). Furthermore, oxygen is required for the chemical reaction to dissolve the metals. Thus, as stated in Chapter 1, full saturation of lixiviants, besides being difficult and uneconomical, is not recommendable even when the equations that I am using assume full saturation.

3.1.2 Porosity

After the measurements for discharge rate were completed, the specific yield was calculated by closing the lower valve, disconnecting the reservoir, placing a graduated cylinder with a 50 ml precision directly below the lower valve, and opening this lower valve so as to let the water flow out of the chamber and into the cylinder. The volume of water drained divided by the total volume of the chamber is the specific yield, which is used to give an estimate of the sample porosity in the lab experiments of this thesis. This same procedure was repeated for each sample in a total of 22 experiments (6 experiments for the OTT sample, 4 HBB, 5 MBBG, and 7 MOTG). Mathematically, this calculation was done as follows:

$$n = \frac{Vol_{water\_drained}}{Vol_{chamber}} = \frac{Vol_{water\_drained}}{4,355cc}$$

3.1.3 Shape Factor

Some of the equations studied in this research make use of a shape factor (SF), which was estimated by inspection of the sediments forming the samples through a microscope (Figure 3.3). According to the findings of Fair and Hatch (1933) summarized in Figure 3.3, a SF of 6.4 corresponding to worn sand grains was chosen for the calculations of hydraulic conductivity as this value bests describes the grains that constitute the samples. Fair and Hatch (1933) derived the values that appear in Figure 3.3C by looking through the microscope at several soil samples with different angularity and sphericity and estimating a ratio of surface area over volume. Photographs of the grains constituting the samples from the mine (shown in the next Chapter) show rounded and angular grains that can also be represented with the SF of 6.4 used in the lab experiments.

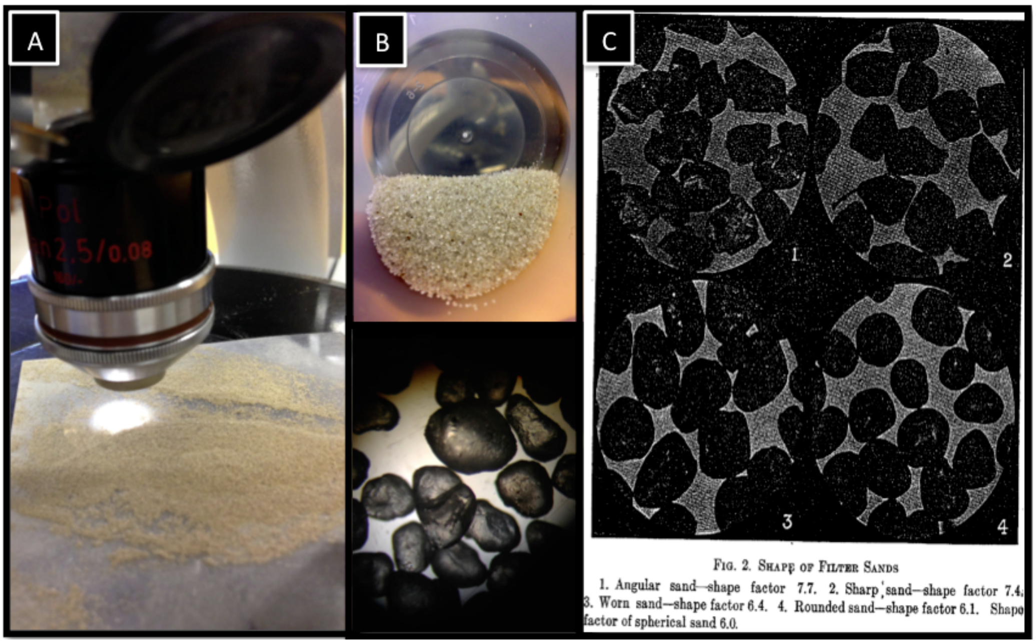

Figure 3.3: A SF of 6.4 as studied in Fair and Hatch (1933) and summarized in Panel C was chosen for the lab samples and assumed for samples coming from the mine.

3.1.4 Observed Permeabilities

The best estimate of observed permeability was calculated for each sample by carrying out the following five steps. First, a number of experiments were conducted on each sample (6 for the OTT sample, 4 for HBB, 5 for MBBG, and 7 for MOTG), and during each experiment a total of ten discharge observations were made (Figure 3.4A-B). Second, for each of these discharge observations a permeability was calculated using (3.1). Third, the logarithm of each of these permeabilities was taken (Figure 3.4C). Fourth, the average and standard deviation of the 10 log transformed permeabilities were calculated. This average is regarded as the observed permeability of a certain sample in the following chapters. Fifth, a 95% confidence interval was then calculated for the observed conductivities as shown in Figure 3.4D using the mean and standard deviation among all observations. The logarithmic transformation is a necessary step because hydraulic conductivities are lognormally distributed (Kieber, 1966). After the UCL and LCL were estimated for the observed permeabilities in log scale for each sample, these values were transformed back to permeabilities using base ten exponentials. As an example, 7 experiments were conducted on the MOTG sample (Figure 3.4) where a total of 70 values of permeability (10 for each experiment) result from the discharge observations. These 70 permeabilities were then log transformed and their average and standard deviation calculated and used to construct a 95% confidence interval for the observed permeability of the MOTG sample.

3.1.5 Confidence Intervals for Empirical Equations

The main goal of these lab experiments is to compare the conductivities from the empirical equations to the ones observed in the experiments and detect which of the nine equation offers the best estimate of conductivity. To calculate confidence intervals (CI_i) that take into account the range of uncertainties for the calculated permeabilities the following approach was implemented:

1. Nine permeabilities (K_i) were calculated for each lab sample using the equations in Appendix A and log transformed afterwards ($\log K_i$).
2. Uncertainties ($\Delta \log K_i$) were calculated for each $\log K_i$ using the equations in Appendix B.
3. Confidence intervals (CIs) for each of the nine $\log K_i$ were calculated using the following modified version of the naive estimator for means in log normal distributions proposed by Olsson (2007) and McCarthy (2001), treating $\log \Delta K_i$ as an estimator for σ:

$$CI_i = 10^{(\log K_i \pm 1.96 \times \Delta \log K_i)} \tag{3.2}$$

To better illustrate this procedure here is an example. The observed conductivity estimated from all 70 observations on the MOTG sample was 0.033cm/s with a standard deviation of 0.004cm/s. The USBR equation provided a value of $\log K = -1.36$ for this same sample, and through the absolute error propagation approach an uncertainty of $\Delta \log K = 0.31$ was found. The confidence interval of the conductivity

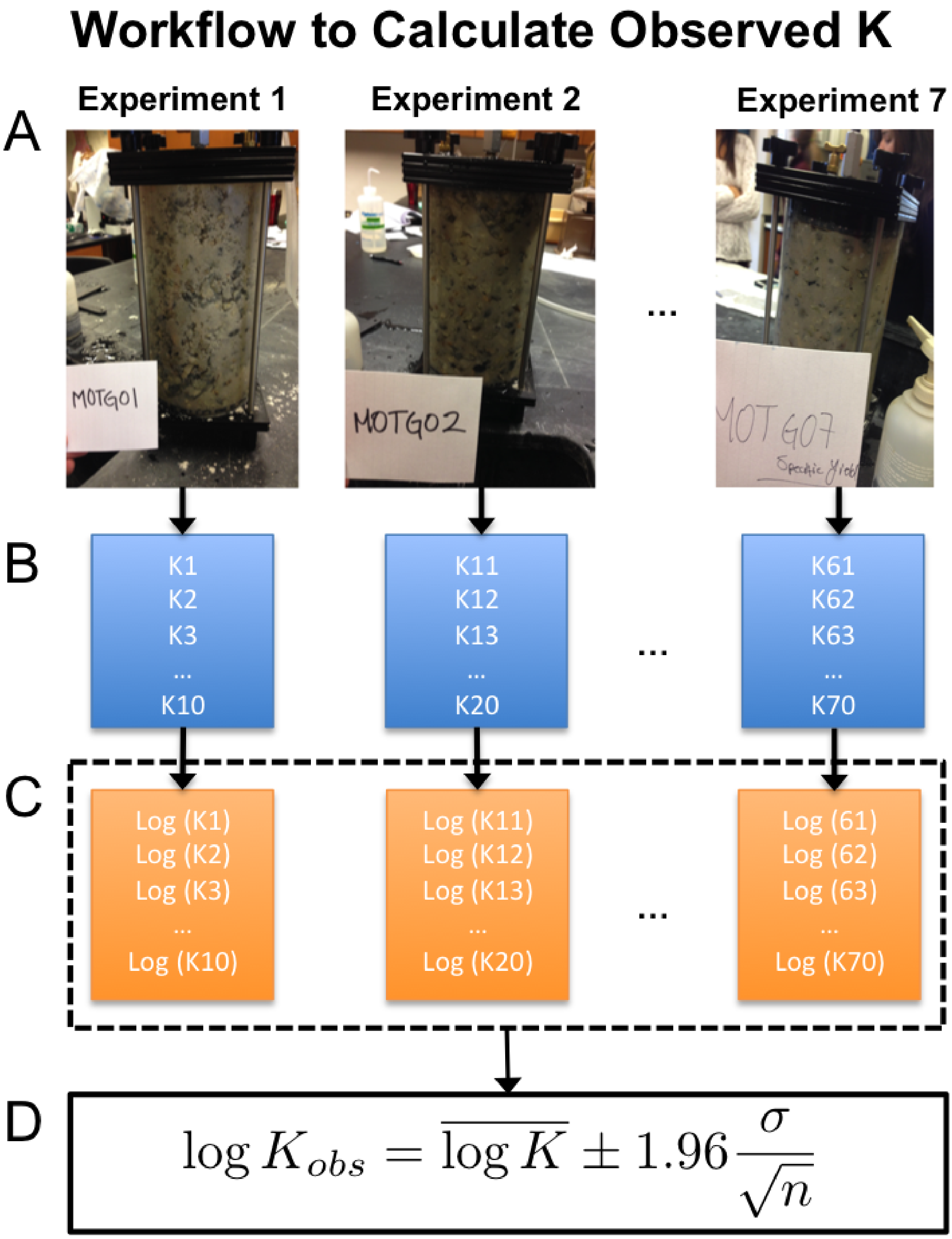

FIGURE 3.4: Workflow diagram illustrating the procedure to calculate a sample's observed hydraulic conductivity. (A) A number of experiments conducted on the same granular material. (B) 10 permeabilities were calculated from 10 discharge observations in each experiment. (C) All observations from all experiments on the same sample (n) were log transformed and the mean $\log \overline{K_i}$ and standard deviation σ calculated. (D) 95% confidence intervals for the observed permeabilities were calculated.

estimated using the USBR equation for the MOTG sample was then calculated as $CI = 10^{(-1.36\pm1.96\times0.31)}$ for a UCL of 0.18 and a LCL of 0.01cm/s.

3.1.6 Ranking and Least Squares Errors

In statistics least squares errors refer to squared differences between actual observations and the predicted values resulting from a model (Mendenhall, 2009). In this thesis research, least squares errors are the parameters used to rank the nine equations. The observed values were the conductivities observed during lab experiments and the predicted values the conductivities resulting from the nine equations. The squared difference between these two conductivities in logarithmic space was used to rank the nine equations in terms of best fit using the following equation:

$$E_i = (\log K_i - \log K_{obs})^2 \tag{3.3}$$

where K_i are conductivities from empirical equations and K_{obs} the observed conductivity in lab experiments.

3.2 Results

The results of the lab experiments are summarized in Figures 3.5, 3.6, 3.7, and 3.8. Table 3.5 shows the accuracy and ranking of the nine equations using the least squares errors calculated using 3.3. According to these results, the USBR equation provides values of conductivities that most closely represent lab observations for these two samples.

Figure 3.9 shows the GSDs of all lab samples compared to the range of GSDs from the mine. Specifically, this figure shows the GSDs from samples MBBG and MOTG falling within the range of the GSD of the mine. Using (3.1) the observed conductivities were $K = 0.033\pm0.003$ cm/s for sample MBBG (Figure 3.7) and $K = 0.033\pm0.001$ cm/s for sample MOTG (Figure 3.8), and for both samples the equation that best estimated the observed conductivity was the USBR.

TABLE 3.5: **Ranking of Equations By Least Squares Errors (E)**

	MOTG	MBBG	Avg. E	Ranking
USBR	0.015	0.015	0.015	1
Hazen	0.064	0.063	0.064	2
Slitcher	0.042	0.342	0.192	3
KC	0.000	0.623	0.311	4
F&H	1.527	0.184	0.856	5
Terzaghi	0.600	0.830	0.715	6
Beyer	2.220	1.075	1.648	7
Kruger	3.465	0.608	2.036	8
Zunker	4.825	2.778	3.801	9

Ranking was done in increasing order of the average error for samples MOTG and MBBG.

3.3 Discussion of Results

3.3.1 Least Squares Errors

When focusing on samples MOTG and MBBG (samples that were most representative of the GSDs from the mine) the USBR equation offered the most reliable estimates of saturated conductivities as shown by the lowest average least square errors (Table 3.5). For samples OTT and MBBG the Hazen equation yielded the second best estimates after USBR. For sample MOTG, Kozeny-Carman equation had a least squares error very close to zero and the USBR equation offered the second best estimate (Figure 3.8B). Lastly, for sample HBB, the Slichter equation had the lowest least squares error, and once again the USBR equation offered the second best estimate (Figure 3.6B). These results point out that from the nine equations studied in this thesis, the USBR, Hazen, Slichter, and Kozen-Carman offered the most reliable estimations of saturated hydraulic conductivity. However, among these four equations the USBR is the most reliable when estimating saturated conductivities in sediments similar to the ones used in leaching.

3.3.2 Evaluation of Uncertainties Estimated by The Absolute Error Propagation Approach

The estimated uncertainty for the Hazen equation as calculated through the absolute error propagation approach is, on average, lower than the uncertainty estimated for other equations as seen on the short error bars on Figures 3.5C, 3.6C, 3.8C, and 3.7C.

This is so because the Hazen's equation only makes use of the d_{10} percentile in K calculations, and hence the uncertainty estimated through the absolute error propagation approach only depends on the error associated with the size of the lowest 10th percentile of the samples GSD (Δd_{10}). As presented in Chapter 2 section 2.4.3, in this thesis it was assumed a fixed value for all Δd_x of 0.01 mm corresponding to coarse silt particles due to the inability to measure Δd_x accurately.

3.3.3 Grain Sizes and Uniformity Coefficients

In this subsection the impact that different grain-sizes (d_x percentiles) and uniformity coefficients (U) have on the most accurate equations (USBR, Hazen, Slichter and Kozeny-Carman) is discussed. The d_{10} percentiles and U for the lab samples were (in increasing d_{10} order): $d_{10} = 0.18$ mm and $U = 4$ for HBB, $d_{10} = 0.25$ mm and $U = 80$ for MBBG, $d_{10} = 0.3$ mm and $U = 3$ for OTT, and $d_{10} = 0.4$ mm and $U = 48$ for MOTG. All d_{10} are within the same order of magnitude of medium to fine sand in the Wentworth grain size scale (Chester, 1922) and, as seen on Figure 3.9, samples MOTG and MBBG have large uniformity coefficients simulating the well-graded materials used in leaching.

According to Vukovic and Soro (1992), the USBR and Hazen's equations closely describe observed values of conductivities in sediments with $U < 5$ and a d_{10} between 0.1 to 3 mm, which is the case for samples OTT ($d_{10} = 0.3$ mm, $U = 3$) and HBB ($d_{10} = 0.18$ mm, $U = 4$) but not for MOTG ($d_{10} = 0.4$ mm, $U = 48$) and MBBG ($d_{10} = 0.25$ mm, $U = 80$). However, the fact that Hazen and USBR equations closely predicted the observed conductivities in all samples having small variations in d_{10} but very distinct U supports the Vukovic and Soro (1992) hypothesis that the size of the smaller grains is the primary factor affecting K calculations more so than U.

Slichter's equation had a low least square error for OTT, HBB, and MOTG. As previously stated in Chapter 2, Slichter's equation has been demonstrated to describe lab observations for samples with effective grain sizes (d_{10}) between 0.01 and 5 mm, which makes the Slichter equation applicable to all samples. However, the USBR equation provides more accurate estimates with fewer inputs.

Comparing samples MBBG and MOTG the biggest difference between them is the rounding of the grains. Sample MOTG was crafted with a mixture of smooth, well rounded, Ottawa sands and angular gravels (Table 3.3). Looking at Figure 3.8, it is clear that Kozeny-Carman was the most accurate equation predicting the observed conductivity in MOTG as shown by a least squares error of almost zero. As explained by Carrier (2003) and Chapuis and Aubertin (2003), Kozeny-Carman represents a pore diameter of an equivalent capillarity through an effective radius, and in the presence of well-rounded grains it is difficult for isolated pores to exist (Lambe and Whitman, 1969). Therefore, the results of this thesis point out that Kozeny-Carman's representation of effective radius confirms observed permeabilities in well-rounded sediments. However, since there are no data characterizing the grains used to construct the leaching heaps, then the Kozeny-Carman equation is considered a poor choice when estimating the conductivities of the mine samples in the following chapter of this thesis.

Summarizing the findings of this chapter, under the limited diversity in grain size of granular material available for testing, the accuracy of the nine equations was tested in only two samples representative of the range of GSDs from the mine. Based on the least square error between the observed and calculated conductivities on these two samples, the USBR equation was shown to provide accurate estimates of conductivity in well-graded sands with gravels. Looking at Table 3.5, even when the USBR had the lowest least square error other equations such as Hazen, Slichter, and Kozeny-Carman also provided estimates of conductivities close to the observed values. Therefore, to make the conclusion that the USBR is the best method for predicting the conductivity in well-graded sands with gravels more robust, more samples of granular material with a GSD mimicking those used in the heap should be included in this analysis.

A

	OTT n = 60				
	log K	log σ	K	UCL	LCL
Observed	-1.336	0.066	0.0461	0.048	0.044

	log K	Δlog K	K	UCL	LCL
Hazen	-1.575	0.165	0.027	0.057	0.012
KC	-1.634	0.535	0.023	0.273	0.002
Beyer	0.160	0.396	1.446	8.941	0.234
Slitcher	-1.130	0.693	0.074	1.800	0.003
Terzaghi	-0.010	0.471	0.977	8.557	0.112
USBR	-1.359	0.307	0.044	0.180	0.011
F&H	-2.558	0.977	0.003	0.249	0.000
Kruger	0.040	0.169	1.096	2.384	0.504
Zunker	-0.352	0.775	0.445	15.816	0.013

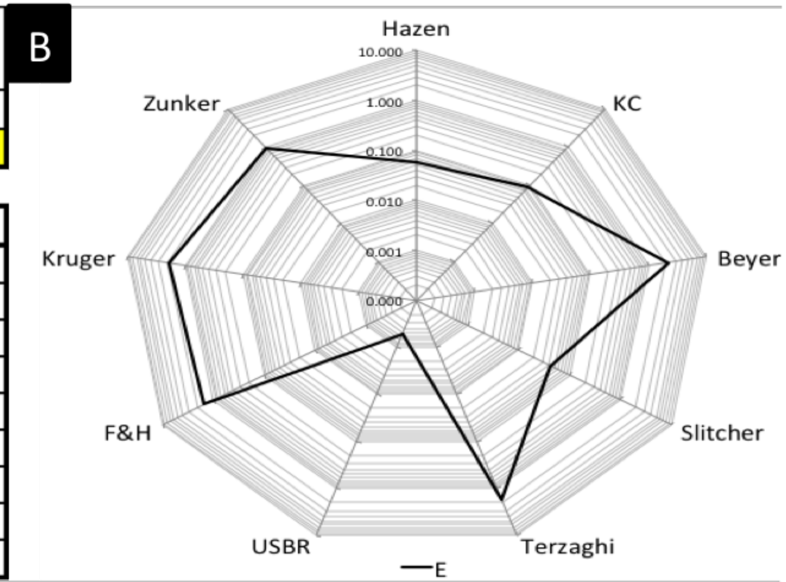

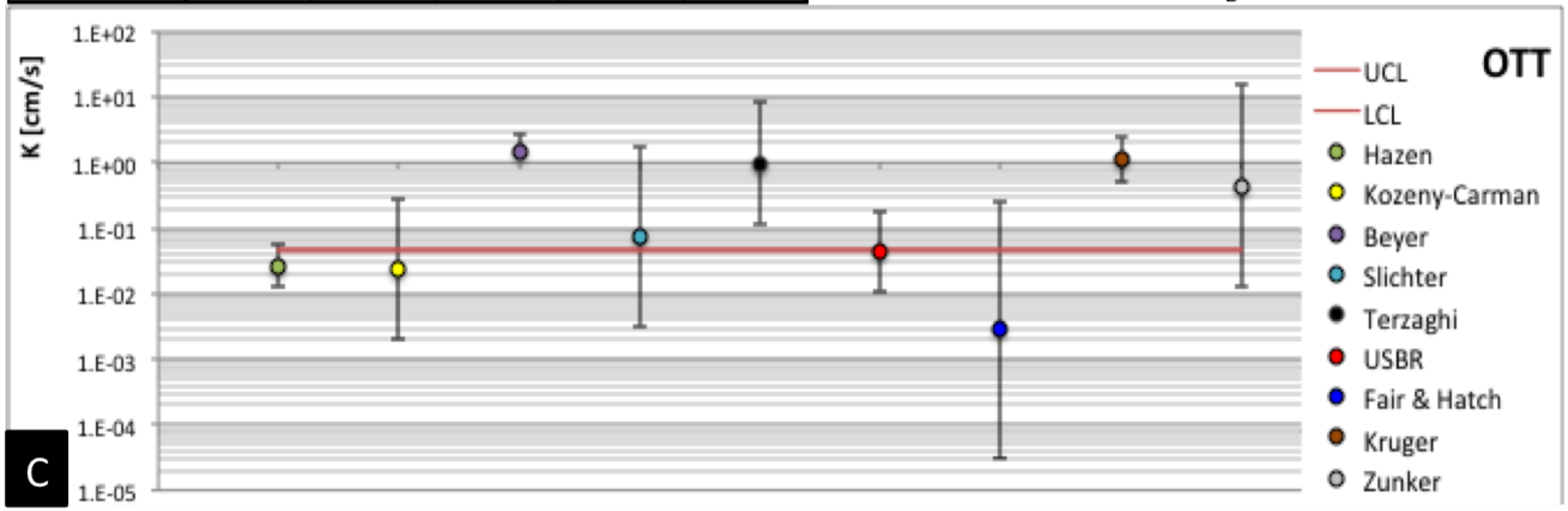

FIGURE 3.5: Results from the OTT sample. A) observed (yellow) and calculated conductivities in cm/s. B) least squares errors in different equations calculated using (3.3) (the closer the line to the center of the graph the lower the error). C) confidence intervals for the observed conductivities calculated using (2.4). Note that the UCL and LCL for the observed conductivities (red lines) are almost indistinguishable.

A

	HBB n = 40				
	log K	log σ	K	UCL	LCL
Observed	-1.413	0.0927	0.0386	0.041	0.037

	log K	Δlog K	K	UCL	LCL
Hazen	-1.9419	0.182	0.011	0.026	0.005
KC	-2.4228	0.607	0.004	0.062	0.000
Beyer	-0.3183	0.521	0.481	5.287	0.044
Slitcher	-1.1304	0.124	0.074	0.131	0.042
Terzaghi	-1.4395	0.681	0.036	0.838	0.002
USBR	-1.8284	0.507	0.015	0.153	0.001
F&H	-1.1262	0.187	0.075	0.177	0.032
Kruger	0.0398	0.017	1.096	1.187	1.012
Zunker	-0.2086	0.763	0.619	20.795	0.018

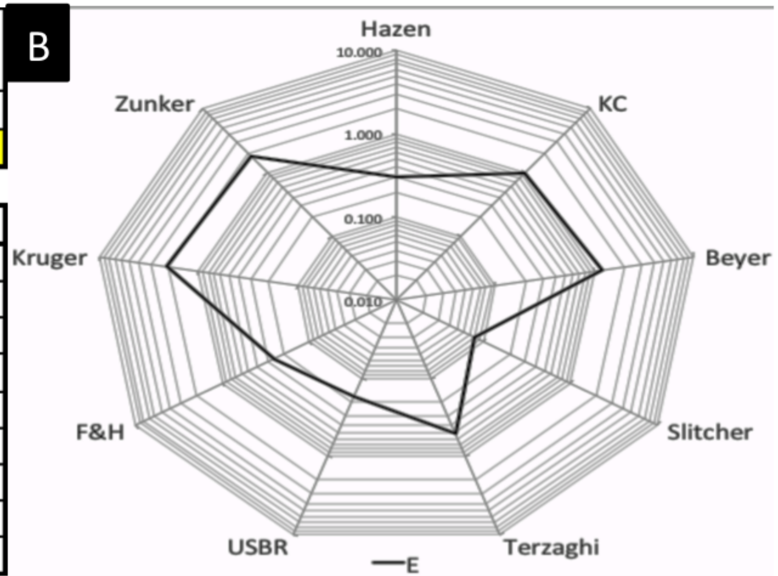

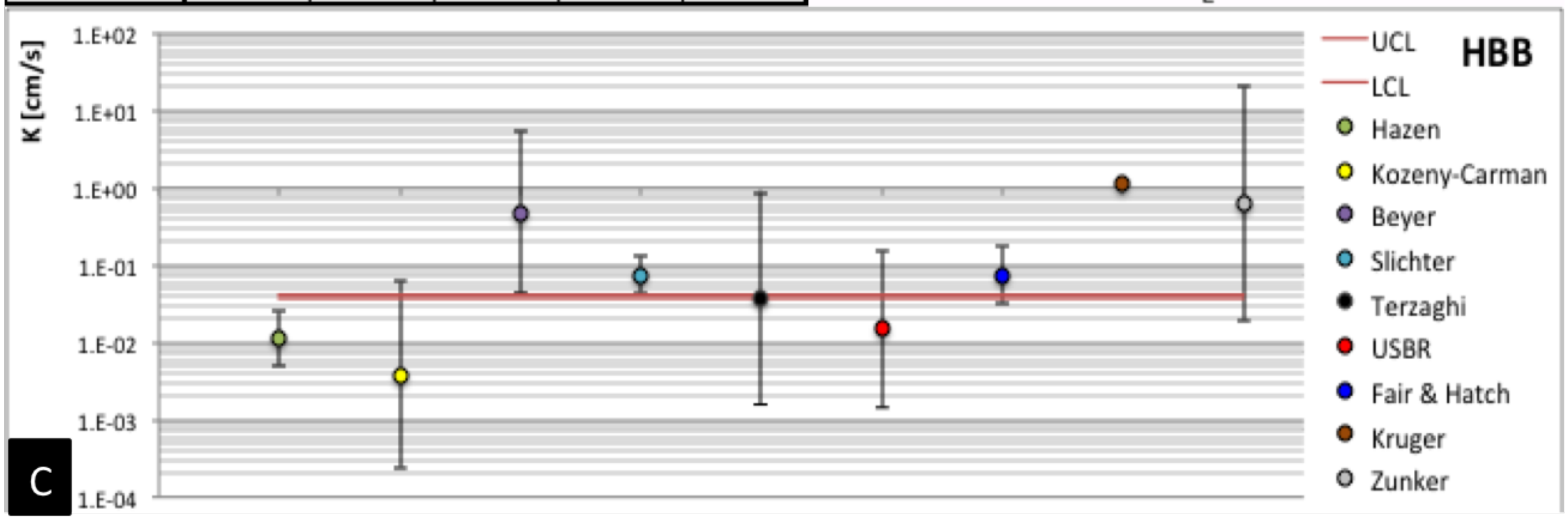

Figure 3.6: Results from the HBB sample. A) observed (yellow) and calculated conductivities in cm/s. B) least squares errors in different equations calculated using (3.3) (the closer the line to the center of the graph the lower the error). C) confidence intervals for the observed conductivities calculated using (2.4). Note that the UCL and LCL for the observed conductivities (red lines) are almost indistinguishable.

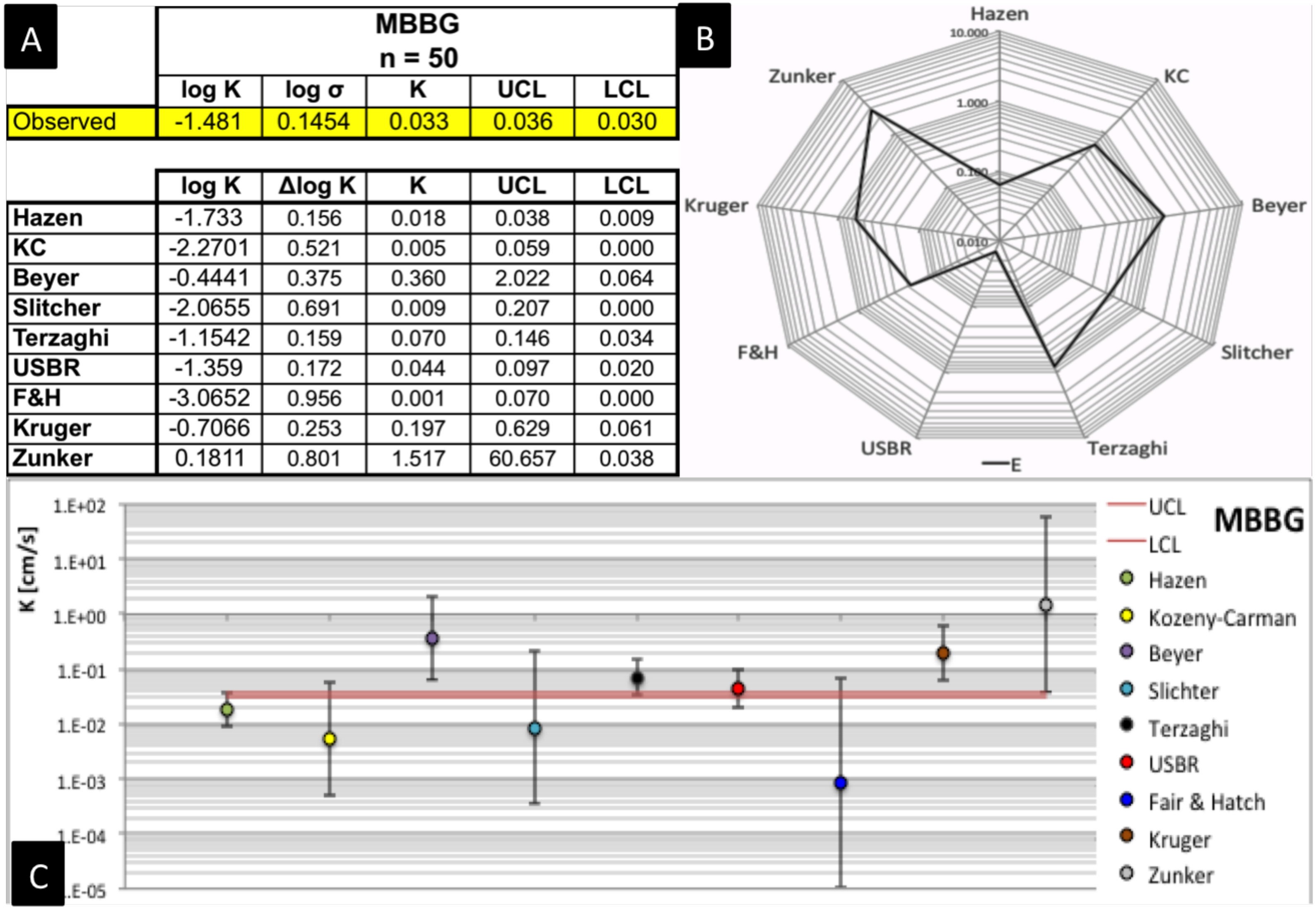

	MBBG n = 50				
	log K	log σ	K	UCL	LCL
Observed	-1.481	0.1454	0.033	0.036	0.030

	log K	Δlog K	K	UCL	LCL
Hazen	-1.733	0.156	0.018	0.038	0.009
KC	-2.2701	0.521	0.005	0.059	0.000
Beyer	-0.4441	0.375	0.360	2.022	0.064
Slitcher	-2.0655	0.691	0.009	0.207	0.000
Terzaghi	-1.1542	0.159	0.070	0.146	0.034
USBR	-1.359	0.172	0.044	0.097	0.020
F&H	-3.0652	0.956	0.001	0.070	0.000
Kruger	-0.7066	0.253	0.197	0.629	0.061
Zunker	0.1811	0.801	1.517	60.657	0.038

Figure 3.7: Results from the MBBG sample. A) observed (yellow) and calculated conductivities in cm/s. B) least squares errors in different equations calculated using (3.3) (the closer the line to the center of the graph the lower the error). C) confidence intervals for the observed conductivities calculated using (2.4). Note that the UCL and LCL for the observed conductivities (red lines) are almost indistinguishable.

A

	MOTG n = 70				
	log K	log σ	K	UCL	LCL
Observed	-1.481	0.0734	0.033	0.034	0.032

	log K	Δlog K	K	UCL	LCL
Hazen	-1.228	0.074	0.059	0.083	0.042
KC	-1.469	0.257	0.034	0.111	0.010
Beyer	0.009	0.247	1.021	3.180	0.328
Slitcher	-1.277	0.479	0.053	0.480	0.006
Terzaghi	-0.707	0.782	0.196	7.215	0.005
USBR	-1.359	0.307	0.044	0.180	0.011
F&H	-2.245	1.480	0.006	5.177	0.000
Kruger	0.381	0.223	2.402	6.698	0.861
Zunker	0.716	0.214	5.196	13.904	1.942

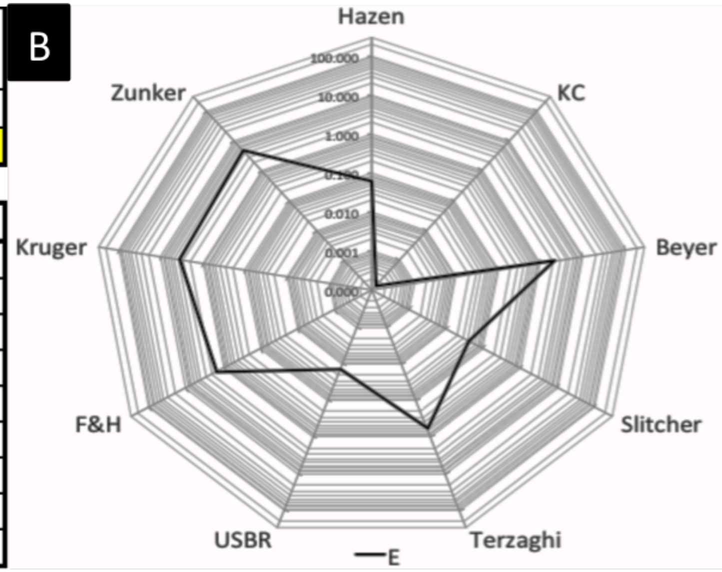

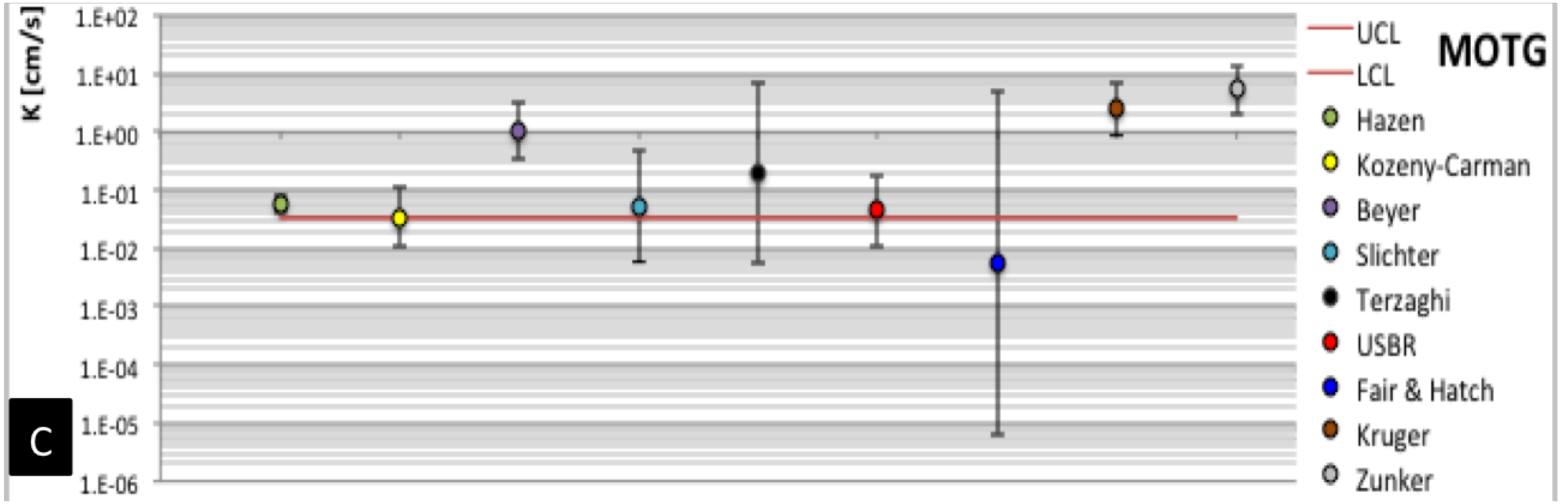

FIGURE 3.8: Results from the MOTG sample. A) observed (yellow) and calculated conductivities in cm/s. B) least squares errors in different equations calculated using (3.3) (the closer the line to the center of the graph the lower the error). C) confidence intervals for the observed conductivities calculated using (2.4). Note that the UCL and LCL for the observed conductivities (red lines) are almost indistinguishable.

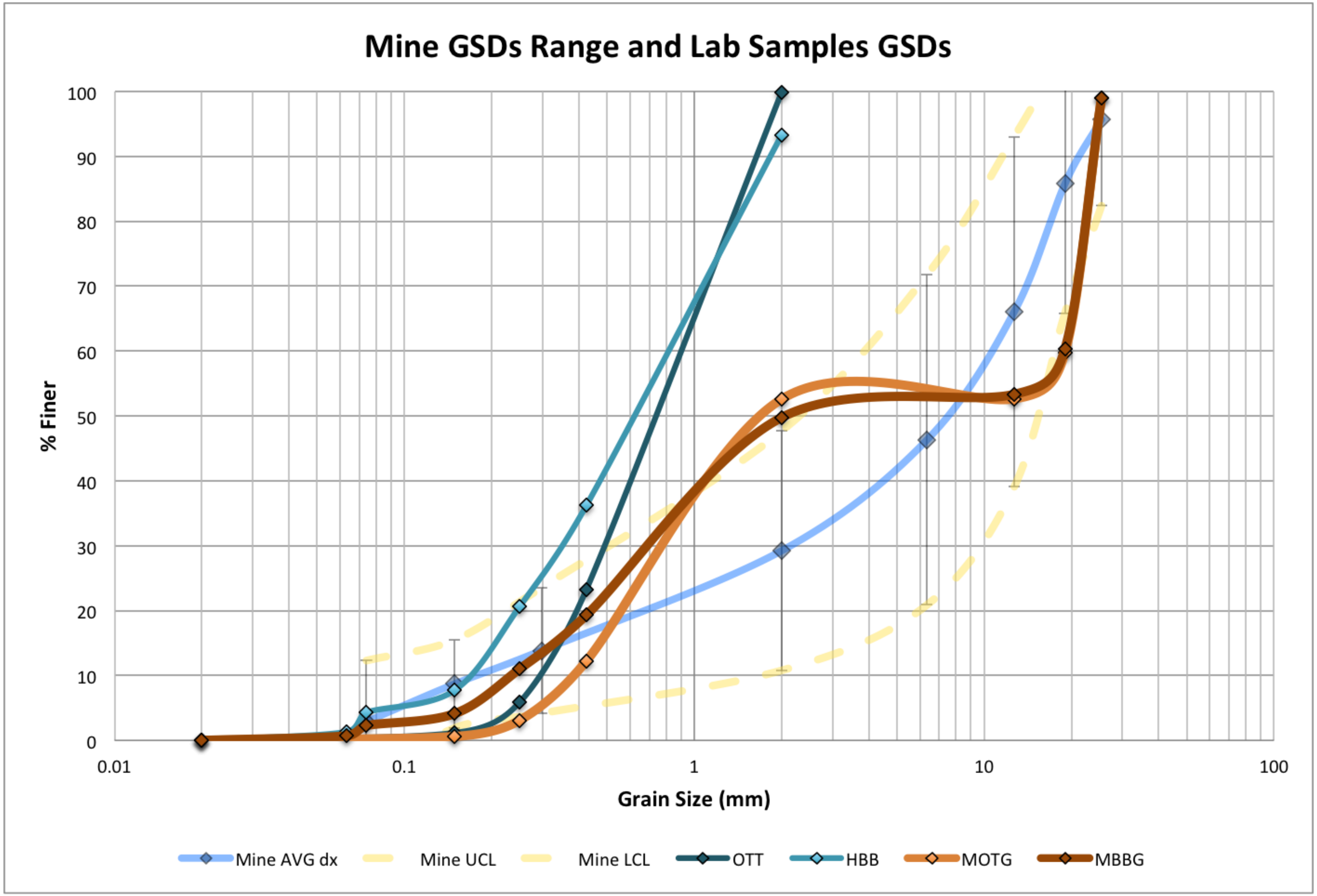

FIGURE 3.9: GSD of the lab samples compared to the range of GSDs from the mine samples. Samples MOTG and MBBG are approximately within three standard deviations of the mean d_x percentiles from the mine GSDs.

Chapter 4

Estimating The Hydraulic Conductivities in Leaching heaps

In this Chapter hydraulic conductivities for the mine samples are estimated using the nine empirical equations but emphasizing conductivities obtained through the USBR equation. This is so because, as shown in the previous chapter, the USBR equation provided accurate estimations of conductivities in controlled constant head permeability tests for the MOTG and MBBG samples both having a similar GSD to that of the leaching heaps. In the first section of this Chapter the empirical relationship proposed by Istomina (1957) to estimate porosity from uniformity coefficient is analyzed considering the results from lab experiments. In the second section, the reader is presented the assumptions under which the 95% confidence interval for the hydraulic conductivity of the heaps is calculated. In the third section, the steps followed in the calculations of hydraulic conductivity are explained. And in the last section the average hydraulic conductivities with their standard deviations for the GSDs as calculated by the nine empirical equations are shown. Focusing on the conductivities estimated by the USBR equation, the average hydraulic conductivity of the heaps constructed by this mine operator is between 0.14 and 0.18 cm/s at two standard deviation precision.

4.1 Evaluating Istomina (1957) Porosity Calculations

In the absence of porosity or specific yield estimates for the mine samples, Istomina (1957) relation was used to estimate hydraulic conductivities. However, these porosity values are likely to introduce a positive bias in the conductivity estimates. This is so because in the previous chapter the specific yield (S_p) experiments provided porosities of 0.17 and 0.13 for samples MOTG and MBBG, respectively. Sample MOTG had a uniformity coefficient U= 46 and sample MBBG U=80 which using equation 2.2, means that these uniformity coefficients yield to porosity values of approximately 0.25 for both samples. As shown by Dimkic (2008), the Istomina (1957) relationship works well when estimating porosities in homogeneous sandy sediments where low uniformity coefficients yield high porosities, but for well-graded sands with gravels with high uniformity coefficients this relationship seems to overestimate conductivities. As discussed in Chapter 2.2.3 where a sensitivity analysis is presented on the porosity functions for Slichter, Terzaghi, Fair & Hatch, Kruger, Zunker, and Kozeny-Carman, changes in porosity could bring changes of up to half an order of magnitude in porosity functions ultimately biasing the estimations of hydraulic conductivity.

Table 4.1: **Quantification of the Bias in Conductivities From Istomina (1957) Porosity Calculations**

	MOTG		MBBG	
	n=0.17	n=0.25	n=0.13	n=0.25
USBR	0.040	0.040	0.040	0.040
Hazen	0.060	0.060	0.020	0.020
Slichter	0.050	0.170	0.008	0.050
KC	0.034	0.120	0.010	0.049
F&H	0.010	0.020	0.001	0.008
Terzaghi	0.200	1.500	0.070	0.650
Beyer	1.020	1.020	0.360	0.360
Kruger	2.400	4.160	0.197	0.500
Zunker	5.200	8.170	1.520	3.390
Observed	0.033		0.033	

In gray are the calculated conductivities using the observed porosities, and in yellow are the observed conductivities. As shown, some of the most accurate equations (USBR and Hazen) do not depend on porosity and hence are not affected by a potential porosity bias. Beyer also does not depend on porosity but provides less accurate estimates. For the other six equations conductivities are overestimated by up to an order of magnitude.

4.2 Assumptions

Due to incomplete information, the following are key assumptions made about the leaching heaps:

1. It is assumed that a porosity close to 0.25 is representative of the granular materials that make up the mine GSDs. As previously discussed, samples in the mine GSDs have large uniformity coefficients ($U \approx 50$), and therefore according to the findings of Istomina (1957) summarized in Figure 2.3 and in equation 2.2 the porosity for granular material with large uniformity coefficients converge to a value of 0.25.

2. A shape factor of SF = 6.4 is assumed for the mine samples and used in lab experiments as provided by Fair and Hatch (1933). This is consistent with the photographs of the granular material that form the mine samples provided by the mine (Figure 4.1).

3. The permeating fluid for the mine calculations is assumed to be water at $20°C$ with a kinematic viscosity of 0.001 $Pa \cdot s$.

With these assumptions the unknowns in the equations in Appendix A are reduced to three variables that permit testing the ceteris paribus effect of grain size on hydraulic conductivity: the d_x percentiles, the percentage of grains trapped in between sieves (fi), and the cumulative percentage of finer grains to a certain sieve (Pi).

4.3 Steps in the Calculations of Hydraulic Conductivities

A workflow diagram that illustrates the methodology to estimate the conductivities in the mine samples is described in this section and is summarized in Figure 4.2. MATLAB scripts for each of the nine equations in Appendix A and attached in Appendix C were designed so as to compute nine permeabilities for each of the 874 samples, but only the distribution of conductivities for the USBR equation is presented here as a main result of this thesis. The permeabilities estimated with the USBR method were log transformed and plotted in a histogram, which shows a lognormal distribution of conductivities for the leaching heaps formed by the mine operator through time. Histograms and probability density functions for the other eight equations can be found in Appendix D.

A 95% confidence interval for the hydraulic conductivity of the heaps is calculated using the following formula after McCarthy (2001) and Olsson (2007) for a lognormal distribution of values.

$$CI = 10^{\left(\overline{\mu} \pm 1.96 \frac{\sigma}{\sqrt{874}}\right)} \tag{4.1}$$

where $\overline{\mu}$ is the simple average of log transformed conductivities estimated in the same manner as in lab experiments and σ is the standard deviation of the log transformed distribution of conductivities. Mathematically, these parameters were calculated with the following formulas according to Olsson (2007) and Brown (2006):

$$\overline{\mu} = \frac{\sum_{i=1}^{n}(\log(K_i))}{n} \tag{4.2}$$

$$\sigma^2 = \frac{\sum_{i=1}^{n}(\log(K_i) - \overline{\mu})^2}{n} \tag{4.3}$$

were K_i is the ith hydraulic conductivity calculated by each method over n observations or GSD samples. Olsson (2007) evaluated how well several point estimators represent the mean and standard deviation in lognormal populations. According to his findings, defining point estimators $\overline{\mu}$ and σ in this way leads to accurate estimations of the confidence interval of any variable that follows a lognormal distribution.

4.4 Results

In this section the average conductivities for the mine samples according to the nine equations appears in Table 4.2 and the range of conductivities as estimated through the USBR equation is emphasized in the following figures. Statistically, the hydraulic conductivities for the leaching heaps constructed by the mine operator are lognormally distributed (Figure 4.3) and have average values between 0.18 and 0.15 cm/s with 95% confidence (Figure 4.4). This result does not indicate that conductivities for any given heap should be between 0.18 and 0.15 cm/s, but it indicates that for the period studied and with the current data the average conductivity of the heaps lays within this range (Mendenhall, 2009). In the population of estimated hydraulic conductivities, the maximum hydraulic conductivity is 22.185 cm/s and the minimum 0.012 cm/s with a mean of 0.49 cm/s and a standard deviation of 1.44 cm/s. Figure 4.5 illustrates a range of conductivities calculated by the USBR equation for some representative GSDs of the granular materials used in the leaching heaps.

Table 4.2: **Average hydraulic conductivities for the mine samples through the nine equations**

Equation	Avg K [cm/s]	Std Dev [cm/s]
USBR	0.165	3.852
Hazen	0.004	2.085
Slichter	0.044	2.104
KC	0.110	1.617
F&H	0.021	1.632
Terzaghi	0.390	2.108
Beyer	0.222	2.348
Kruger	3.435	1.743
Zunker	4.433	1.610

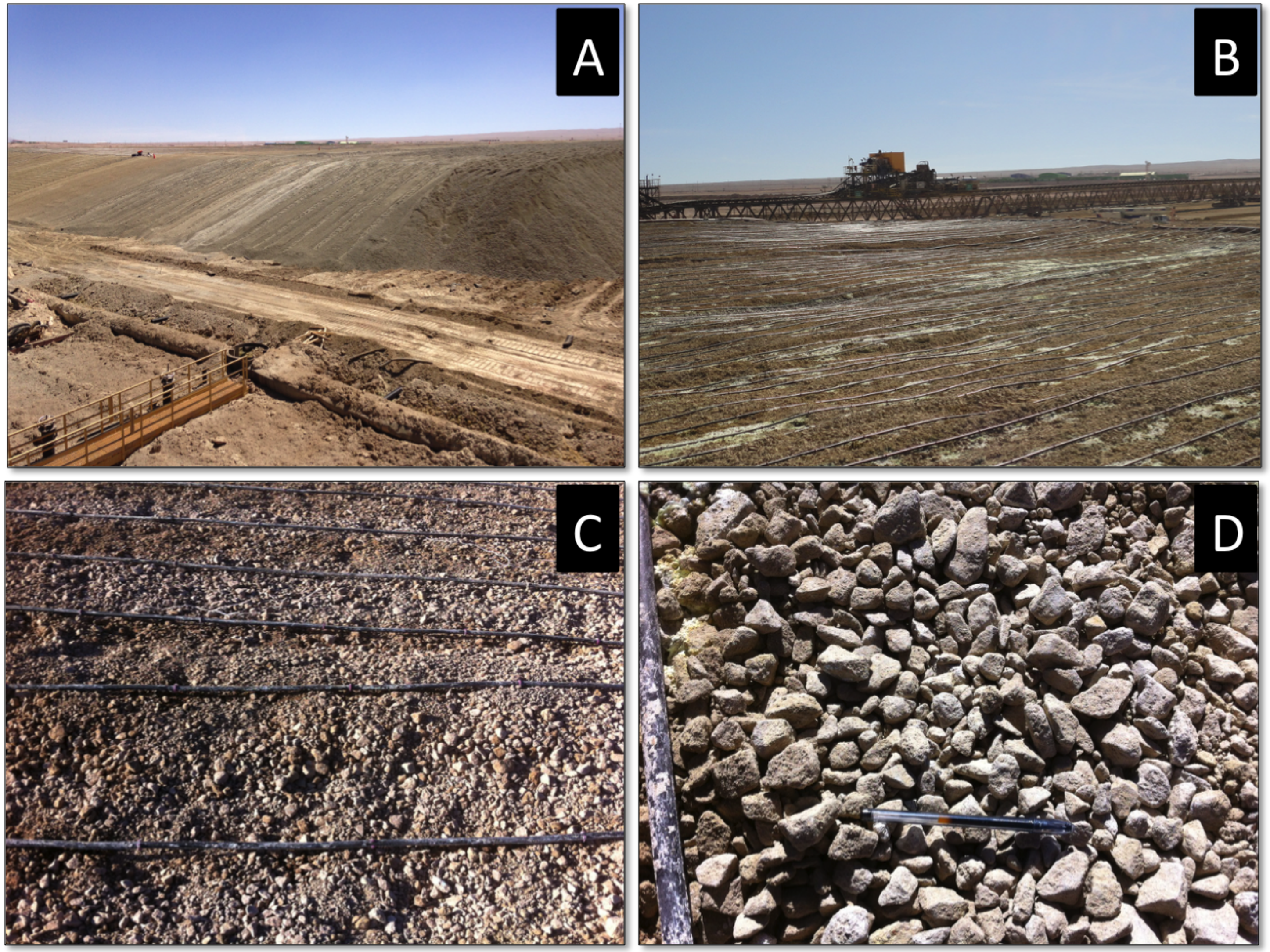

FIGURE 4.1: Pictures of the mine and the grains constituting the GSD samples. A) The heap shown in the background. B) The irrigation system and the green pods are showing the pregnant solution. C) The sprinklers distributing the lixiviant across the heap. D) The grains constituting the samples.

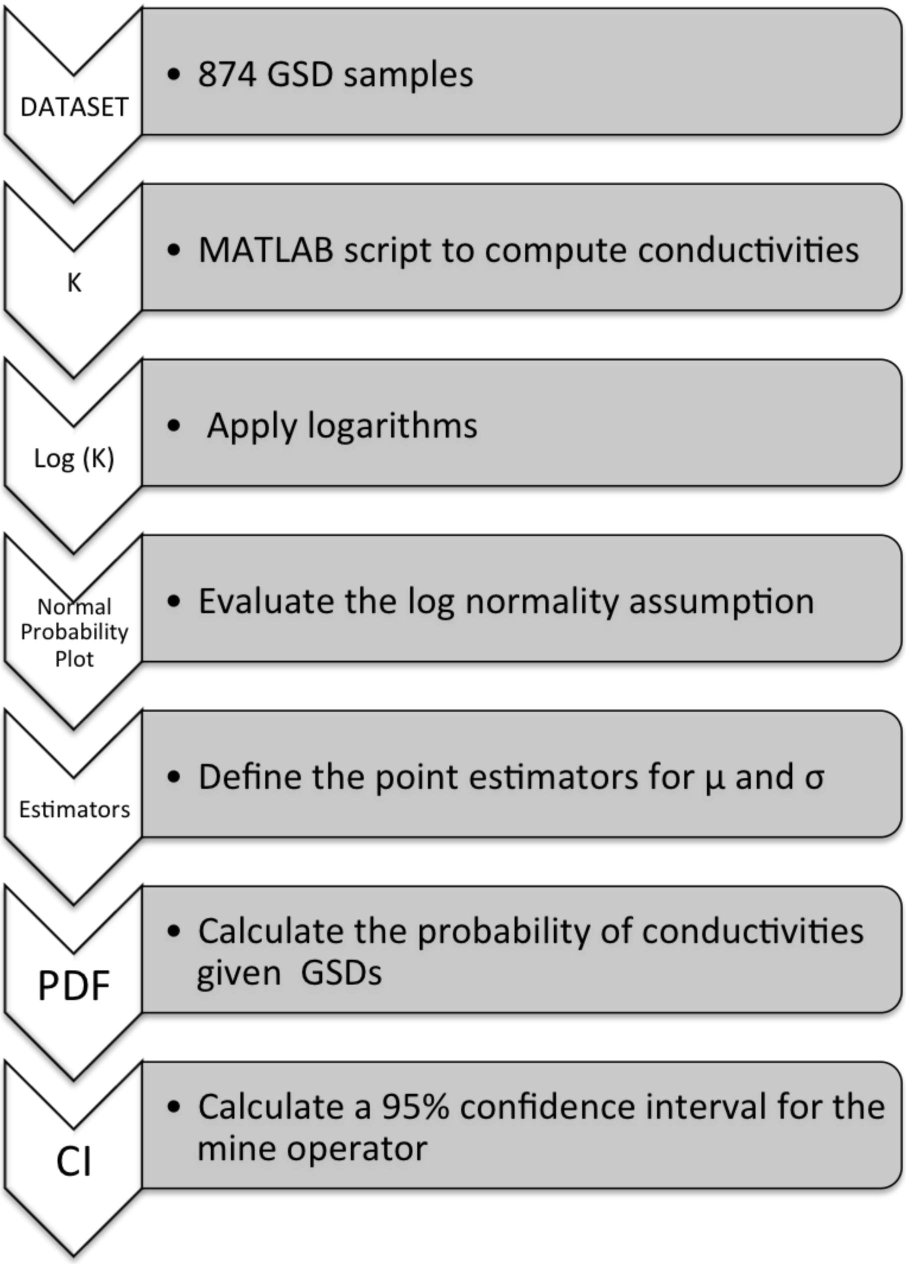

FIGURE 4.2: Workflow diagram illustrating the steps implemented to estimate confidence intervals among the distributions of permeabilities obtained through each of the nine equations.

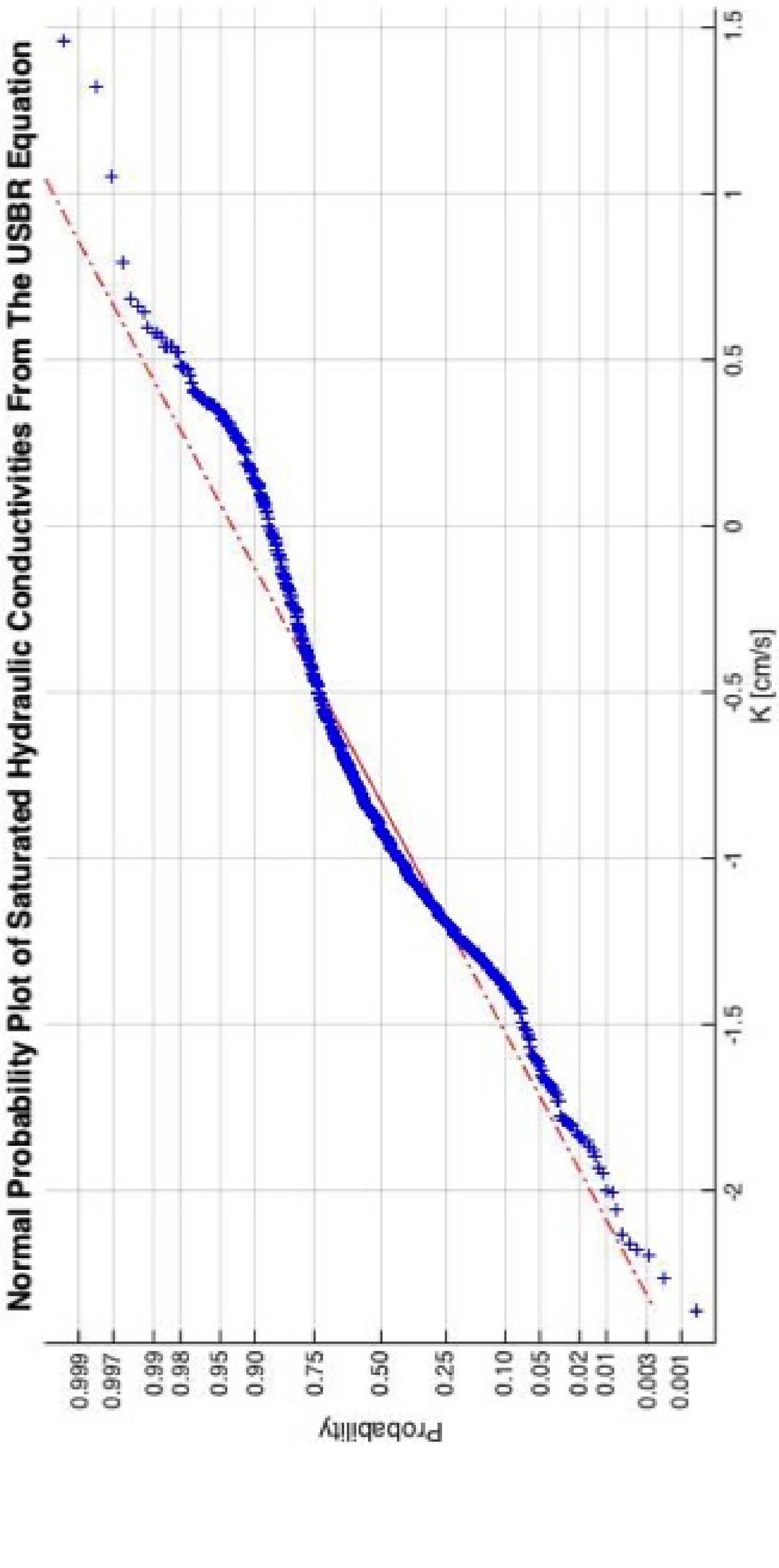

FIGURE 4.3: Cumulative probability plots of the hydraulic conductivities estimated by the USBR equation evidencing a lognormal distribution

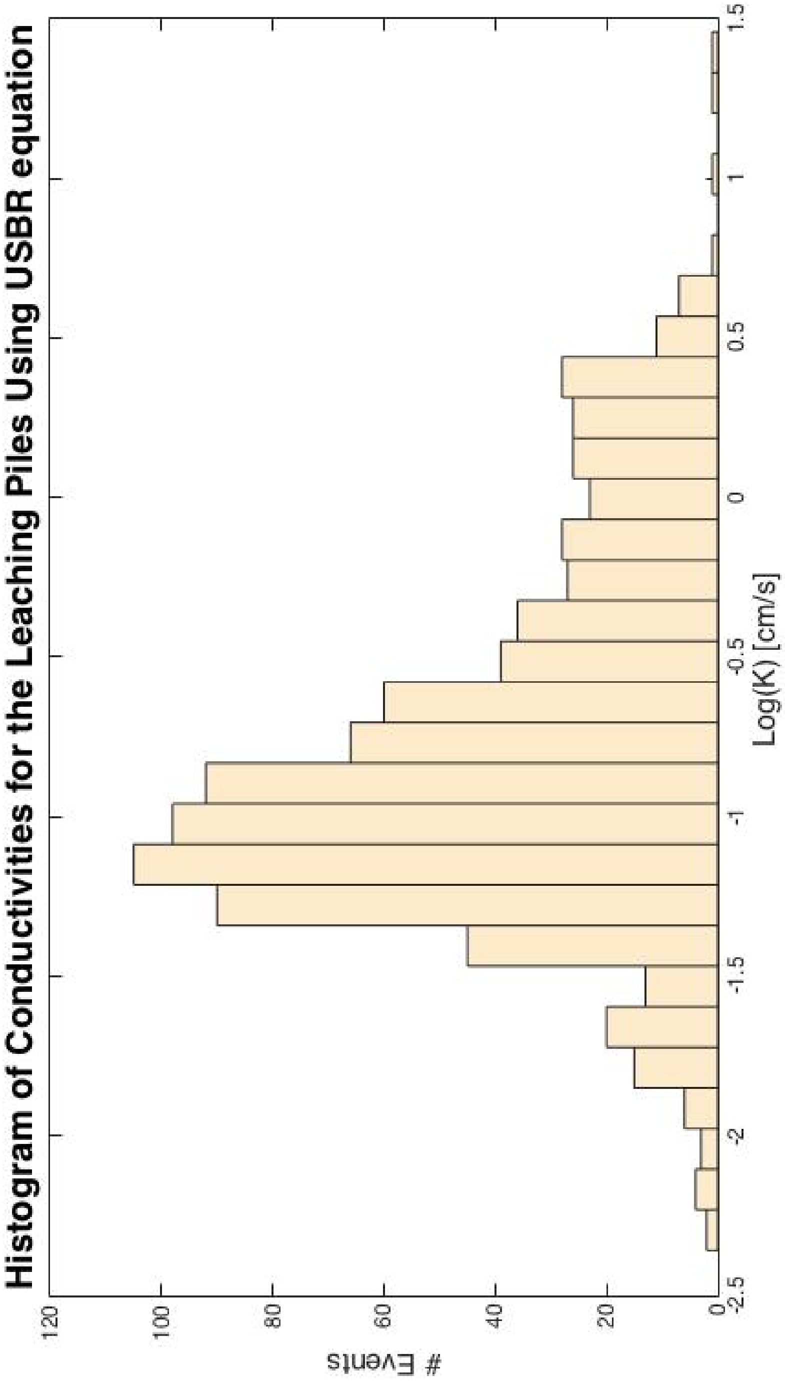

FIGURE 4.4: Results from USBR's equation on the 874 GSD samples. Histogram and PDF describing the distribution of conductivities.

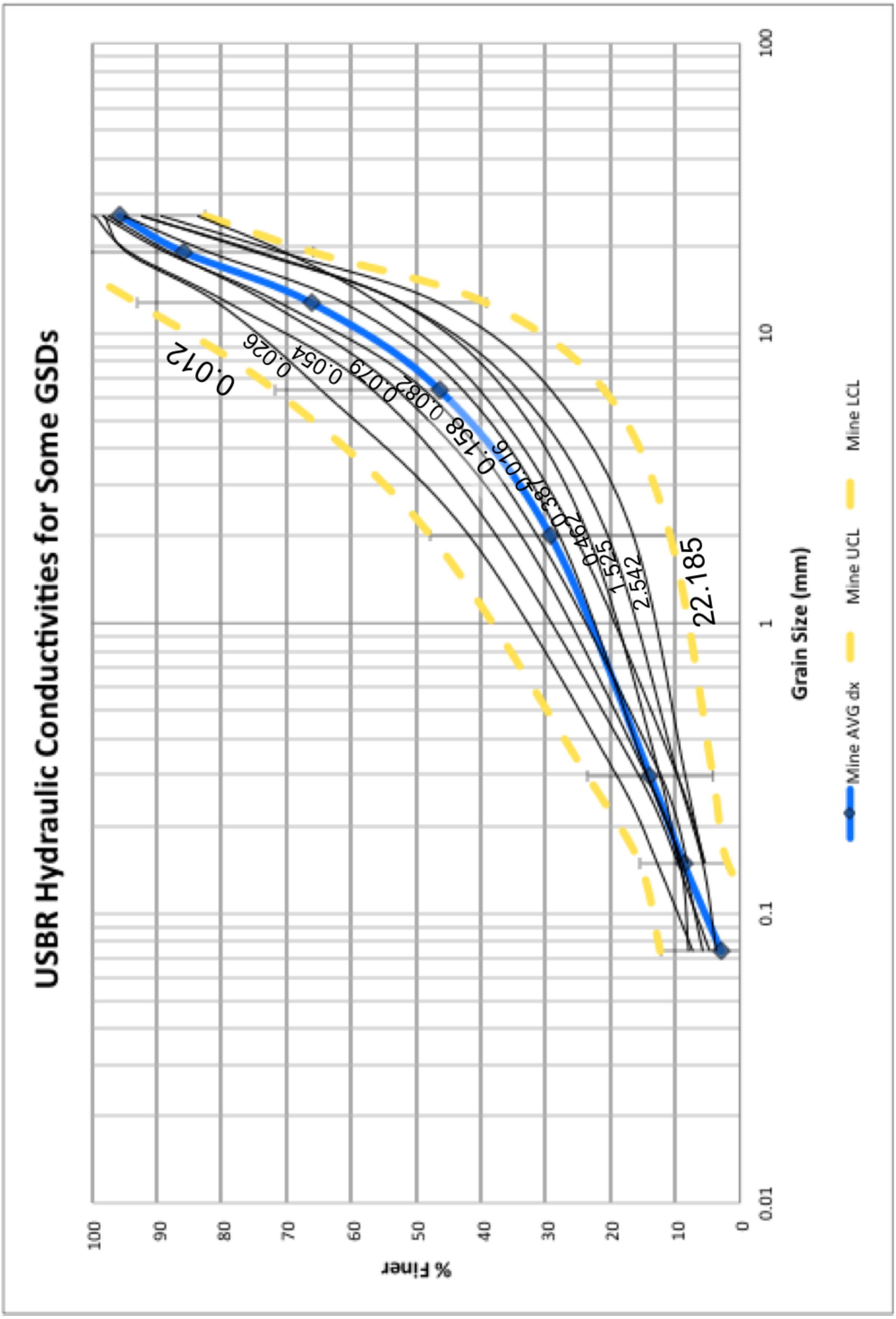

FIGURE 4.5: GSDs for the MOTG and MBBG lab samples plotted together with the range of GSDs from the mine and the hydraulic conductivities calculated through the USBR, Hazen, Slichter, and Kozeny-Carman abbreviated as KC. Notice that there are no observed conductivities for the mine samples.

Chapter 5

Conclusion

Nine different equations that calculate hydraulic conductivity from GSDs were analyzed in this thesis research. Results from lab experiments confirm the claims from some researchers that Fair and Hatch, Kozeny-Carman, Hazen, Slichter, and Terzaghi are methodologies that work well estimating observed hydraulic conductivities even when applied to granular materials with uniformity coefficients and effective grain sizes outside their region of validity (Carrier, 2003; Salarashayeri and Siosemarde, 2012; Petalas and Pilakas, 2011; Odong, 2007; Ishaku and Kaigama, 2011). However, in this thesis the USBR equation proved to be the most precise equation as shown by its low mean squared error when estimating conductivities in controlled constant head permeability tests. However, these results are based on a limited amount of samples and thus more data is needed to draw robust conclusions about the accuracy of this equation in predicting conductivities of well graded sands with gravels. Even though some studies have pointed out that the USBR tends to underestimate conductivities when applied to sediments within its region of validity of $U < 5$ (Salarashayeri and Siosemarde, 2012; Odong, 2007; Ishaku and Kaigama, 2011), such significant underestimations were not observed in my lab experiments. Furthermore, since observed hydraulic conductivities for the leaching heaps were not included in the mine GSDs it is not possible to determine if the USBR or any other equation offer estimations that underestimate or overestimate observed conductivities. Therefore, when applied to the mine GSDs the USBR equation estimates average hydraulic conductivities for the heaps constructed by the mine operator in the past five years with an average value between 0.18 and 0.15 cm/s.

Another conclusion drawn from this thesis is that the relationship proposed by Istomina (1957) for calculating porosity from uniformity coefficients overestimates observed porosities when applied to samples with large uniformity coefficients. This bias could bias estimates of conductivity by up to an order of magnitude, but the USBR equation is unaffected as this expressions is not a function of porosity.

The relationship between copper yields and hydraulic conductivities as a function of grain size in leaching heaps can be explored by including observations of discharge rates, irrigation rates, and porosities for all the heaps. With the discharge and irrigation rates one could estimate the degree of saturation of the heap and use it to correct the values of conductivity from the empirical equations since these assume full saturation. Given actual porosity measurements of the sediments forming the leaching heaps, the Istomina (1957) relationship is no longer necessary, which resolves the potential bias associated with using this mathematical approximation to porosity in six equations including Kozeny-Carman. Given more samples of granular material with GSDs similar to the range used in the heaps, the conclusions presented regarding the accuracy of the USBR equation could be made more robust as in this thesis this result relies on only two samples of well-graded sands with gravels. The relationship between copper yields and hydraulic conductivity can be then studied using multiple regressions. According to the data provided by the mine up to 7% of the variations in copper yields can be explained by changes in hydraulic conductivity, and after verifying that the USBR equation provides the best estimates of conductivity for the well-graded sands with gravels used in the heap, one could back solve the problem to detect the optimum GSD to build the heaps with so as to control conductivity and optimize the amount of copper recovered from leaching.

Comparing the results of this thesis with the ones in Yao (2011), the saturated conductivities estimated through the USBR method (solely as a function of grain size) correspond well to observations of saturated conductivities in heaps of up to 3 m high. Specifically, the sediments used in Yao (2011) are homogeneous fine sands with a d_{20} matching the MOTG and MBBG samples, therefore we can conclude that the results from the USBR equation are representative of hydraulic conductivities of heaps up to 3 m high with sediments under a pressure of up to 62 Kpa, With higher heaps we have higher pressures, more consolidation, and smaller permeabilities resulting from the mechanical rearrangement of particles that is not reflected in the USBR equation. In unsaturated conditions, the permeability from the USBR equation are from one to two order of magnitude less than the observed values according to the studies presented in Yao (2011). Future analysis could be conducted in the calibration of the USBR equation so as to represent saturated conductivities with a dynamic rearrangement of particles resulting from larger pressures. Under unsaturated conditions, it is more challenging to validate the estimates of conductivity from the USBR equation.

Appendix A

The Nine Methodologies

Method	Equation	Variables	Region of Validity/notes
Hazen	$K_H = C \times \frac{h}{l}(0.7 + 0.03T)d_{10}^2$	• *C is an empirical coefficient equal to 1000.* • *h is the change in head [length].* • *l is length* • *T is temperature (in ºC).* • *d_{10} is the lower 10th percentile of finer grains [in mm].*	$U \leq 5$ $0.1\text{mm} \leq d_{10} \leq 3\text{mm}$ K results in m/day
Kozeny-Carman	$K_{KC} = 1.99_{x10}{}^{4}\left(\frac{n^3}{(1-n)^2}\right)\left(\frac{1}{SF^2}\right)d_{carrier}{}^{2}$	• *SF is the shape factor taken from (Fair & Hatch, 1933)* $d_{carrier} = \frac{100\%}{\Sigma\left(\frac{f_i}{d_l{}^{0.404} \times d_s{}^{0.595}}\right)}$ where f_i is the fraction entrapped within a larger filter (d_l) and a smaller filter (d_s)	$d_{10} \leq 3\text{mm}$ Samples cannot come from clayey soils K results in m/d
Beyer	$K_B = \frac{g}{v} \times 6_{x10}^{-4} \times log\left(\frac{500}{U}\right)d_{10}^2$	$v = \frac{\mu}{\rho}$ $U = \left(\frac{d_{60}}{d_{10}}\right)$	The method doesn't consider porosity and is most useful in poorly sorted, heterogeneous, materials with: $1 \leq U \leq 20$ $0.06\text{mm} \leq d_{10} \leq 0.6\text{mm}$ K results in m/s
Slitcher	$K_S = \frac{g}{v} \times 1_{x10}^{-2}\, n^{3.287} d_{10}^2$	$n = 0.255(1 + 0.83^U)$ $v = \frac{\mu}{\rho}$	Best results when: $0.01\text{mm} \leq d_{10} \leq 5\text{mm}$
Terzaghi	$K_T = \frac{g}{v} \times C_t\left(\frac{n - 0.13}{\sqrt[3]{1-n}}\right)^2 d_{10}^2$	$n = 0.255(1 + 0.83^U)$ $v = \frac{\mu}{\rho}$ $0.0061 < C_t < 0.107$	Mostly applicable for large-grain sand C_t is an empirical coefficient, high end for smooth grains and low end for coarser grains with: $0.25\text{mm} \leq d_{10} \leq 2\text{mm}$ d_{10} must be plugged in cm K results in cm/s.

Fair & Hatch	$K_{FH} = \frac{h * g * \rho}{L * k * \mu} * \frac{n^3}{(1-n)^2} * \left[\frac{s}{100} \sum_i \frac{P_i}{d_i}\right]^{-2}$	• *h is the loss of head* • *L is the length of the bed* • *g is the gravity* • *k is a pipe flow constant of 32* • *ρ is the density of the permeating fluid* • *μ is the absolute viscosity of the permeating fluid* • *n is the porosity function* • *S is the area-volume shape factor. (Fair & Hatch, 1933) offers a table for S values* • *P_i and d_i refer to the % of grains (P_i) corresponding to a certain grain size (d_i)*	(Fair & Hatch, 1933) offers a detailed discussion on the region of validity for this method. Mostly useful for, but not limited to, sand beds where: $0.1mm \le d_{10} \le 2mm$
Kruger	$K_K = \frac{g}{v} \times \beta_k \times \left[\frac{n}{(1-n)^2}\right] \times d_e^{\ 2}$	• $\beta_k = 4.35_{x10}^{\ -3}$ • $\frac{1}{d_e} = \sum_{i=1}^{n} \Delta g_i \left[\frac{2}{d_i^g - d_i^d}\right]$ • *Δg_i is the fractional weight of the ith component of the sample* • *d_i^g is the maximum grain diameter* • *d_i^d is the minimum grain diameter*	Best results for medium grain-size sands with C>5 and $0.25mm \le d_{10} \le 2mm$ K results in m/day for water at 0°C.
Zunker	$K_Z = \frac{g}{v} \times \beta_z \left[\frac{n}{(1-n)}\right] \times d_e^{\ 2}$	β_z is an empirical coefficient that depeneds on the characteristics of the porous medium: • *For uniform sand with smooth, rounded grains is $2.4_{x10^{-3}}$* • *For uniform composition with coarse grains is $1.4_{x10^{-3}}$* • *For non-uniform composition is $1.2_{x10^{-3}}$* • *For non-uniform composition, clayey, with grains or irregular shape is $0.7_{x10^{-3}}$* $\frac{1}{d_e} = \sum_{i=1}^{n} \Delta g_i \times \frac{d_i^g - d_i^d}{(d_i^g)(d_i^d) Ln\left(\frac{d_i^g}{d_i^d}\right)}$	K results in (m/day).
USBR	$K_{US} = 0.36 \times d_{20}^{2.3}$		Most suitable for sands with U<5 and $0.06mm \le d_{10} \le 2mm$ (Cheng and Chen 2007) K results in cm/s

Appendix B

Absolute Derivatives with Respect to d_i

Method	Equation	Variables
Hazen	$\log \Delta K_H = \dfrac{2C\times\frac{h}{L}(0.7+0.03T)d_{10}\Delta d_{10}}{K_H}$	-
Kozeny-Carman	$\log \Delta K_{KC} = \dfrac{1.99_{x10}^{4}\times SF^2\left(\frac{\partial F_{(d_i)}}{\partial d_i}G(d_i)+\frac{\partial G_{(d_i)}}{\partial d_i}F_{(d_i)}\right)}{K_{KC}}$	• $F_{(d_i)} = \left[\dfrac{100\%}{\Sigma\left(\frac{f_i}{d_i^{0.404}\times d_s^{0.595}}\right)}\right]^{-2}$ • $\dfrac{\partial F_{(d_i)}}{\partial d_i} = 2\left[\dfrac{100\%}{\Sigma\left(\frac{f_i}{d_i^{0.404}\times d_s^{0.595}}\right)}\right]^{-3}\times\left[\Sigma\dfrac{\Delta F_i(d_i^{0.404}d_s^{0.595})-F_i\Delta d_i((d_id_s)^{0.595}+(d_id_s)^{0.404})}{(d_i^{0.404}d_s^{0.595})^2}\right]$ • $G_{(d_i)} = \left[\dfrac{e^3}{1+e}\right]$ • $\dfrac{\partial G_{(d_i)}}{\partial d_i} = \Delta e\times e^2\left(\dfrac{3+2e}{(1+e)^2}\right)$
Beyer	$\log \Delta K_B = \dfrac{\frac{g}{v}\times 6E^{-4}\times d_{10}\left\{2\Delta d_{10}\times\log\left(\frac{500}{U}\right)-\frac{d_{10}\Delta U}{500Ln(10)U}\right\}}{K_B}$	
Slitcher	$\log \Delta K_S = \dfrac{\frac{g}{v}\times 0.01\times d_{10}\left\{3.287n^{2.287}\times\Delta n\times d_{10}+2\times n^{3.287}\times\Delta d_{10}\right\}}{K_S}$	
Terzaghi	$\log \Delta K_T = \dfrac{A\{BC+D\}}{K_T}$	• $A=\frac{g}{v}\times C_t$ • $B=d_{10}^2\times 2\left(\frac{n-0.13}{\sqrt[3]{1-n}}\right)\times\Delta n$ • $C=\dfrac{\left(\sqrt[3]{1-n}+(n-0.13)\times\frac{1}{3}(1-n)^{-\frac{2}{3}}\right)}{(1-n)^{\frac{2}{3}}}$ • $D=2d_{10}\times\Delta d_{10}\times\left(\frac{n-0.13}{\sqrt[3]{1-n}}\right)^2$

Fair & Hatch	$\log \Delta K_{FH} = \dfrac{A\left[\dfrac{\partial B}{\partial d_i} CD + B\dfrac{\partial C}{\partial d_i} D + BC\dfrac{\partial D}{\partial d_i}\right]}{K_{FH}}$	• $A = \left(\dfrac{g \times \rho}{k \times \mu}\right)$ • $B = \dfrac{h}{L}$ • $\dfrac{\partial B}{\partial d_i} = \dfrac{L \times \Delta h - \Delta L \times h}{L^2}$ • $C = \left(\dfrac{n^3}{(1-n)^2}\right)$ • $\dfrac{\partial C}{\partial d_i} = 2\Delta n\left(\dfrac{n(1-n)+1}{(1-n)^3}\right)$ • $D = \left[S\sum\left(\dfrac{P_i}{d_i}\right)\right]^{-2}$ • $\dfrac{\partial D}{\partial d_i} = 2S^{-2}\left(\sum\dfrac{P_i}{d_i}\right)^{-3}\left[\sum\dfrac{\Delta P_i d_i - \Delta d_i P_i}{d_i^2}\right]$
Kruger	$\log \Delta K_K = \dfrac{A\left[\dfrac{\partial B}{\partial d_i} C + B\dfrac{\partial C}{\partial d_i}\right]}{K_K}$	• $A = \beta_k \dfrac{g}{\nu}$ • $B = \dfrac{n}{(1-n)^2}$ • $\dfrac{\partial B}{\partial d_i} = \Delta n\left(\dfrac{1+n}{(1-n)^3}\right)$ • $C = \left[2\sum\dfrac{\Delta g_i}{d_i^g - d_i^d}\right]^{-2}$ • $\dfrac{\partial C}{\partial d_i} = -\dfrac{1}{2}\left[\sum\dfrac{\Delta g_i}{d_i^g - d_i^d}\right]^{-3} \times \left[\sum\dfrac{(d_i^g - d_i^d)\Delta(\Delta g_i) - \Delta g_i(\Delta d_i^g - \Delta d_i^d)}{(d_i^g - d_i^d)^2}\right]$

Zunker	$\log \Delta K_Z = \dfrac{A\left[\dfrac{\partial B}{\partial d_i} C + B \dfrac{\partial C}{\partial d_i}\right]}{K_Z}$	• $A = \beta_k \dfrac{g}{\nu}$ • $B = \dfrac{n}{(1-n)}$ • $\dfrac{\partial B}{\partial d_i} = \dfrac{\Delta n}{(1-n)^2}$ • $C = \left[\sum \dfrac{\Delta g_i \left(d_i^g - d_i^d\right)}{d_i^g d_i \ln\left(\dfrac{d_i^g}{d_i^d}\right)}\right]^{-2}$ • $\dfrac{\partial C}{\partial d_i} = -2\left[\sum \dfrac{\Delta g_i \left(d_i^g - d_i^d\right)}{d_i^g d_i^d \ln\left(\dfrac{d_i^g}{d_i^d}\right)}\right]^{-3} \times \left[\sum \dfrac{\Delta(\Delta g_i)(d_i^g - d_i^d) d_i^g d_i^d \ln\left(\dfrac{d_i^g}{d_i^d}\right) - \Delta g_i \Delta d_i (d_i^g - d_i^d)\left[d_i^d\left(\ln\left(\dfrac{d_i^g}{d_i^d}\right)+1\right) + d_i^g\left(\ln\left(\dfrac{d_i^g}{d_i^d}\right)-1\right)\right]}{\left(d_i^g d_i^d \ln\left(\dfrac{d_i^g}{d_i^d}\right)\right)^2}\right]$
USBR	$\log \Delta K_{USBR} = \dfrac{0.36\left(2.3 \times d_{20}^{1.23} \Delta d_{20}\right)}{K_{USBR}}$	

Appendix C

MATLAB Scripts

```
%{
Spring 2013
Boston College
Fernando Alvarado Blohm

dX calc. Results in the same units as c.

for thesis, C is in mm

if 10% is not recorded in GSD then assumes 0.06 mm (Line 40)

%}


function [d10] = dx(gracabe,C,dx)

%Vectors d,c must be of the same length
%for these calculations:
    %d= %finer. matrix of #samples by %finer
    %c= sieve#. VECTOR containing the sieve #s that were used (in mm)
    %dx= value for interpolation (i.e dx=0.1 will find d10. dx=0.6 will fi
    %d60 and so forth.

    C = log10(C);

    a = size(gracabe);
    last = a(1,1);

    lgd10(last)=0;

    for i=1:last

        lgd10(i) = interp1(gracabe(i,:),C,dx);

        %if 10% is not recorded in the interpolation

        if isnan(lgd10(i))

            lgd10(i)=log10(0.02);

        end


    end

    d10 = (10.^lgd10)';

end
```

d_x percentiles calculations

```matlab
%{
Summer 2013
Boston College
Fernando Alvarado Blohm

The following function calculates permeabilities through Beyer's Method.
_______________________________________________________________________+
%}

function [a] =K_Beyer(d10mm,u)

%Variables

g = 9.80; %gravity [m/s^2]

%mu = 1.002*10^-3; %viscosity of the fluid. For this case, water at 20degC [Pa*s].
(Reff: http://www.engineeringtoolbox.com/water-dynamic-kinematic-viscosity-
d_596.html)
%rho = 1000; %density of the fluid. For this case, water [1,000 Kg/m^3].
%nu = mu*(100^2)/rho; %kinematic viscosity [cm^2/s]

nu=1.004e-6;

def2 = d10mm.^2;

x=log10(500./u);

t= g*(6e-4)/nu;

a = ((t*x).*def2)*100/(3600*24); %Permeability in [cm/s]

end
```

Beyer equation

```
%{
Summer 2013
Boston College
Fernando Alvarado Blohm

FAIR AND HATCH [cm/s]
The following function calculates permeabilities through the fair and hatch
Method.df
________________________________________________________________________+
%}

%{
IMPORANT CONSIDERATIONS:

1) The matrix % Finer (gracabe) input should be in hundreths [i.e. 10 instead of
0.1
for 10%, 27 instead of 0.27 for 27% and so on]

2) The sieves used (C)vector should be entered in mm and will be converted
to cm.

3) This script assumes that the total loss of head (h) is equal to the elevation
head (L). Therefore,both parameters cancel each other and are not considered
in this script. Modify accordingly if the loss of head differs from
elevation.
%}

function [a] = K_Fair_Hatch(gracabe,C,s,u)

%Calculate Effective Radius:

deff=Fair_Hatch_Deff(gracabe,C,s);

n = porosity(u);
g = 980; %gravity. cm/s^2;
k = 32;
r = 0.001; %Kg/cc density of the fluid. For this case, water [Kg/m^3].
m = 1.002*10^-5; %Viscosity of the fluid. For this case, water at 20degC [Pa*s or
Kg/(cm*s)]...
...(Reff: http://www.engineeringtoolbox.com/water-dynamic-kinematic-viscosity-
d_596.html)

t = (g/k)*(r/m);

f = (n.^3)./((1-n).^2);

a = (t.*f);
a = a.*deff;


end
```

Fair and Hatch equation

```
%{
The following function calculates the effective radius.

UNITS:
DEFF = m^2
gracabe = percentage finer [pecentages]
c = Size of the sieves [mm]
s = shape factor [unitless]
%}

function [a] = Fair_Hatch_Deff(gracabe,c,s)

sumpd=Fair_Hatch_Sum(gracabe,c);

a = 1./((s*sumpd).^2);

end

%{
The following function calculates the sum(P/Di) required for
calculating the effective radius.

That is, the sum(retained weight/particle size) for a given sieve analysis.

UNITS:
[1/cm]
%}

function [a] = Fair_Hatch_Sum(gracabe,c)

c = c/10;  %[mm to cm]
gracabe=gracabe/100;
l = size(gracabe);
row = l(1,1);
col = l(1,2);
fr(row,col)=0;
sum1(length(c),1)=0;
sumfordeff(row,1)=0;

%Vector of Geometrical Averages for particles in Between sieves:
s(col,1)=0;
s(1,1) = c(1);

for i=1:col-1
    s(i+1,1)=sqrt(c(i)*c(i+1));
end

for i=1:row

    flag = true;

    for j=1:col

        if flag
```

Effective radius for Fair and Hatch

```
                fr(i,j) = 1 - gracabe(i,j);
                sum1(j) = fr(i,j)/s(j);

                flag = false;

            else

                fr(i,j) = gracabe(i,j-1)-gracabe(i,j);
                sum1(j) = fr(i,j)/s(j);

            end

        end

        sumfordeff(i,1)=sum(sum1);

    end

    a = sumfordeff;
```

Effective radius for Fair and Hatch

```matlab
%{
Spring 2013
Boston College
Fernando Alvarado Blohm

The following function calculates permeabilities through the Hazen Method.

ASSUMPTIONS:
Water at 10 degrees celcius
Change in head (h) equals length of the sample (l)
Hazen Constant=100;

K results in cm/s
___________________________________________________________________________+

%}

function [a] = K_Hazen(d10mm)

a = 100*d10mm.^2;
a= a*100/(24*3600); %Unit conversion from m/d to cm/s;

end
```

Hazen Equation

```
%{
Summer 2013
Boston College
Fernando Alvarado Blohm

The following function calculates permeabilities through Kozeny-Carman
CARRIER'S VERSION.
_______________________________________________________________________________+

%}

function [a] = K_Carrier(gracabe,C,u,s)

deffcarriercm=Carrier_Deff(gracabe,C);

n = porosity(u);
e = (n./(1-n));


[a] = 1.99e4.*deffcarriercm.*(1/s^2).*((e.^3)./(1+e));

end




%{
The following function calculates the sum(P/Di) required for
calculating the effective radius for Kozeny-Carman as for (Carrier 2003)

That is, the sum(retained weight/particle size) for a given sieve analysis.

UNITS:
1/CM
%}

function [a] = Carrier_Sum(gracabe,c)

%mat= is the % finer matrix.
%c = vector of meshes used [mm] (must contain the same columns as mat).
gracabe=gracabe/100;
c = c/10;  %[mm to cm]
l = size(gracabe);
row = l(1,1);
col = l(1,2);
fr(row,col)=0;
sum1(length(c),1)=0;
sumfordeff2(row,1)=0;

%Vector of WEIGHTED Geometrical Averages for particles in Between sieves:
s(col,1)=0;

for i=1:length(c)

    if i==1
```

```
        s(i)=c(i);
    else
        s(i) = (c(i-1)^0.404)*c(i)^0.595;
    end
end


for i=1:row

    flag = true;

    for j=1:col

        if flag

            fr(i,j) = 1 - gracabe(i,j);
            sum1(j) = fr(i,j)/s(j);

            flag = false;

        else

            fr(i,j) = gracabe(i,j-1)-gracabe(i,j);
            sum1(j) = fr(i,j)/s(j);

        end

    end

    sumfordeff2(i,1)=sum(sum1);

end

a = sumfordeff2;



%{
The following function calculates the effective radius
sum(retained weight/particle size) for a given sieve analysis in [m].
%}

function [a] = Carrier_Deff(gracabe,c)

sumpd=Carrier_Sum(gracabe,c);
%c is in mm, and sum provides cm.

a = (1./sumpd).^2;

end



%{
```

Kozeny-Carman equation

```
Summer 2013
Boston College
Fernando Alvarado Blohm

The following function calculates permeabilities through Kruger's Method
_________________________________________________________________________+
%}

function [k] = K_Kruger(gracabe,c,n)

deffkrugermm=Kruger_Deff(gracabe,c);

beta = 4.35e-3; %Empirical coefficient for coarse grains. (Vukovic and Soro pg 63)
g = 9.80; %gravity [m/s^2]
nu = 1.004e-6; %kinematic viscosity [m^2/s]
% n = porosity(u);

k = ((g*beta/nu)*(n./((1-n).^2)).*deffkrugermm.^2)*100/(24*3600); %[cm/s]

end

%{
The following function calculates the effective diameter established by the
Kruger's method.
%}


function [a] = Kruger_Deff(gracabe,c)

%mat= is the % finer matrix
      %For "GranulometrÌas" the first column is the mass of the whole sample and
      %the successive columns correspond to the weight of the material entrapped
      %in between sieves.
%c = vector of meshes used [mm] (must contain the same columns as mat).

gracabe=gracabe/100; %converting percentages to fractions
l = size(gracabe);
row = l(1,1);
col = l(1,2);
fr(row,col)=0;
sum1(length(c),1)=0;
sumfordeff(row,1)=0;

%Vector of Geometrical Averages for particles in Between sieves:


for i=1:row

    flag = true;

    for j=1:col

        if flag

            fr(i,j) = 1 - gracabe(i,j);
```

Kruger equation

```
            sum1(j) = 2*fr(i,j)/c(j);

            flag = false;

        else

            fr(i,j) = gracabe(i,j-1)-gracabe(i,j);
            sum1(j) = 2*fr(i,j)/(c(j-1)-c(j));

        end

    end

    sumfordeff(i,1)=sum(sum1);

end

a = 1./sumfordeff;
```

Kruger equation

```matlab
%{
Summer 2013
Boston College
Fernando Alvarado Blohm

The following function calculates permeabilities through Slitcher's Method.
_______________________________________________________________________________+
%}

function [a] = K_Slitcher(d10mm,u)

%Variables

g = 9.80; %gravity [cm/s^2]
%mu = 1.002*10^-3; %viscosity of the fluid. For this case, water at 20degC [Pa*s].
(Reff: http://www.engineeringtoolbox.com/water-dynamic-kinematic-viscosity-
d_596.html)
%rho = 1000; %density of the fluid. For this case, water [1,000 Kg/m^3].
%nu = mu*(100^2)/rho; %kinematic viscosity [cm^2/s]
nu=1.004e-6;

def2 = d10mm.^2;

n = (porosity(u)).^3.287;

t= g/nu*(1*10^-2);

a = (t*n.*def2)*100/(24*3600); %Permeability in [cm/s]

end

%{
```

Slichter equation

```
Summer 2013
Boston College
Fernando Alvarado Blohm

The following function calculates permeabilities through Terzaghi's Method.

K results in cm/s
_____________________________________________________________________________+
%}

function [k] = K_Terzaghi(d10cm,n)

beta = 6.1e-3; %Empirical coefficient for coarse grains. (Vukovic and Soro,1992) pg
63
g = 9.8; %gravity [m/s^2]
%n is porosity

nu = 1.004e-6;

k = (g/nu)*(beta)*(((n-0.13)./((1-n).^(1/3))).^2).*d10cm.^2;

end
```

Terzaghi equation

```
%{
Summer 2013
Boston College
Fernando Alvarado Blohm

The following function calculates permeabilities through USBR's Method.
_________________________________________________________________________+

%}

function [a] = K_USBR2(d20mm)


a = 0.36*d20mm.^2.3; %Permeability in [cm/s]

end
```

USBR equation

```
%{
Summer 2013
Boston College
Fernando Alvarado Blohm

The following function calculates permeabilities through the Zunker's
Method

UNITS:
[cm/s]
__________________________________________________________________________+
%}

function [a] = K_Zunker(gracabe,c,n)

deffzunkermm=Zunker_Deff(gracabe,c);

beta = 1.4e-3; %Empirical coefficient for coarse grains. (Vukovic and Soro)
g = 9.8; %gravity
nu = 1.004e-6; %kinematic viscosity [m^2/s] from (Vukovic and Soro, pg 51 Table)
% n is porosity

deffzunkermm = (1./deffzunkermm);
deffzunkermm = deffzunkermm.^2;

a = (g/nu)*beta*(n./(1-n)).*deffzunkermm;

a= a*100/(24*3600); %Conversion from m/day to cm/s

end


 %{
The following function calculates the sum(dgi/di) required for
calculating the effective radius wthrough ZUNKER's method

That is, the sum(retained weight/geometrical average) for a given sieve analysis.
%}

function [a] = Zunker_Deff(gracabe,c)

%mat= is the % finer matrix. (It was 1,672 x 9 for "GranulometrÌas", and
      %672 x 8 for "IMH").
      %For "GranulometrÌas" the first column is the mass of the whole sample and
      %the successive columns correspond to the weight of the material entramped
      %in between sieves.
%s = vector of meshes used [mm] (must contain the same columns as mat).

gracabe=gracabe/100;

upper = 50; %5cm chosen to be the upper threshold
l = size(gracabe);
row = l(1,1);
col = l(1,2);
fr(row,col)=0;
```

Zunker equation

```
sum1(length(c),1)=0;
sumfordeff(row,1)=0;

%Vector of Geometrical Averages for particles in Between sieves:


for i=1:row

    flag = true;

    for j=1:col

        if flag

            fr(i,j) = 1 - gracabe(i,j);
            sum1(j) = fr(i,j)*(upper-c(j))/(upper*c(j)*log(upper/c(j)));

            flag = false;

        else

            fr(i,j) = gracabe(i,j-1)-gracabe(i,j);
            sum1(j) = fr(i,j)*(c(j-1)-c(j))/(c(j-1)*c(j)*log(c(j-1)/c(j)));

        end

    end

    sumfordeff(i,1)=sum(sum1);

end

a = sumfordeff;

end
```

Zunker equation

```
%{
Summer 2013
Boston College
Fernando Alvarado Blohm

The following function calculates probability density function (PDF)
________________________________________________________________________+
%}


function a = MakeP(K)

a = pdf('normal',K,mean(K),std(K));

end
```

Probability Density Function

```
%{
Summer 2013
Boston College
Fernando Alvarado Blohm

The following function creates the plots of a histogram with an imposed PDF.
Done once, autogenerated by MATLAB, and edited afterwards.
_____________________________________________________________________________+
%}

function histonormcurv2(xvector1, yvector1, histcolor, X1,
Y1,curvecolor,titlestring)
%CREATEFIGURE1(XVECTOR1, YVECTOR1, X1, Y1)
%  XVECTOR1:  bar xvector
%  YVECTOR1:  bar yvector
%  X1:  vector of x data
%  Y1:  vector of y data

%  Auto-generated by MATLAB on 20-Jun-2013 16:50:43

% Create figure
figure1 = figure;

% Create axes
axes1 = axes('Parent',figure1,'YTick',[0 20 40 60 80],'YMinorTick','on',...
    'YGrid','on',...
    'XMinorTick','on');
%% Uncomment the following line to preserve the X-limits of the axes
% xlim(axes1,[-3 -1.2]);
%% Uncomment the following line to preserve the Y-limits of the axes
% ylim(axes1,[0 80]);
box(axes1,'on');
hold(axes1,'all');

% Create bar
bar(xvector1,yvector1,'FaceColor',histcolor,'Parent',axes1,...
    'DisplayName','data1');

% Create plot
plot(xvector1,yvector1,'Parent',axes1,'LineStyle','none',...
    'DisplayName','data2');

% Create ylabel
ylabel('# Events','FontSize',14);

% Create xlabel
xlabel('Log10(K)   [cm/s]','FontSize',14);

% Create title
title(['Histogram and Probability Distribution',sprintf('\n'),titlestring],...
    'FontSize',16);

% Create axes
axes2 = axes('Parent',figure1,'YTick',[0 0.5 1 1.5 2],...
    'YAxisLocation','right',...
    'ColorOrder',[0 0.5 0;1 0 0;0 0.75 0.75;0.75 0 0.75;0.75 0.75 0;0.25 0.25
```

```
0.25;0 0 1],...
    'Color','none');

hold(axes2,'all');

% Create plot
plot1 = plot(X1,Y1,'Parent',axes2,'MarkerSize',5,'Marker','o','LineWidth',2,...
    'LineStyle','none',...
    'Color',curvecolor,...
    'DisplayName','Probability');

% Create ylabel
ylabel('Probability','VerticalAlignment','cap','FontSize',14);

% Get xdata from plot for data statistics
xdata1 = get(plot1, 'xdata');
% Get ydata from plot for data statistics
ydata1 = get(plot1, 'ydata');
% Make sure data are column vectors
xdata1 = xdata1(:);
ydata1 = ydata1(:);


% Get axes ylim
axYLim1 = get(axes2, 'ylim');

% Find the min
xmin1 = min(xdata1);

minValue1 = [xmin1 xmin1];
% Create plot
statLine1 = plot(minValue1,axYLim1,'DisplayName','   x min','Parent',axes2,...
    'Tag','min x',...
    'LineStyle','--',...
    'Color',[0 0.75 0.75]);

% Find the max
xmax1 = max(xdata1);

maxValue1 = [xmax1 xmax1];
% Create plot
statLine2 = plot(maxValue1,axYLim1,'DisplayName','   x max','Parent',axes2,...
    'Tag','max x',...
    'LineStyle','--',...
    'Color',[0 0 1]);

% Find the mean
xmean1 = mean(xdata1);

meanValue1 = [xmean1 xmean1];
% Create plot
statLine3 = plot(meanValue1,axYLim1,'DisplayName','   x mean',...
    'Parent',axes2,...
    'Tag','mean x',...
    'LineStyle','--',...
    'Color',[0 0.5 0]);
```

```
% Create legend
legend(axes1,'show');

% Create legend
legend1 = legend(axes2,'show');
set(legend1,'Color',[1 1 1]);
```

Graphs of Histograms with an imposed PDF

Appendix D

Hydraulic Conductivities For Eight Equations

In this Appendix the reader is presented with the distribution of hydraulic conductivities estimated by the Beyer, Fair and Hatch, Hazen, Kozeny-Carman, Kruger, Slicther, Terzaghi, and Zunker equations.

Histogram and probability density function for the mine samples using Beyer's equation

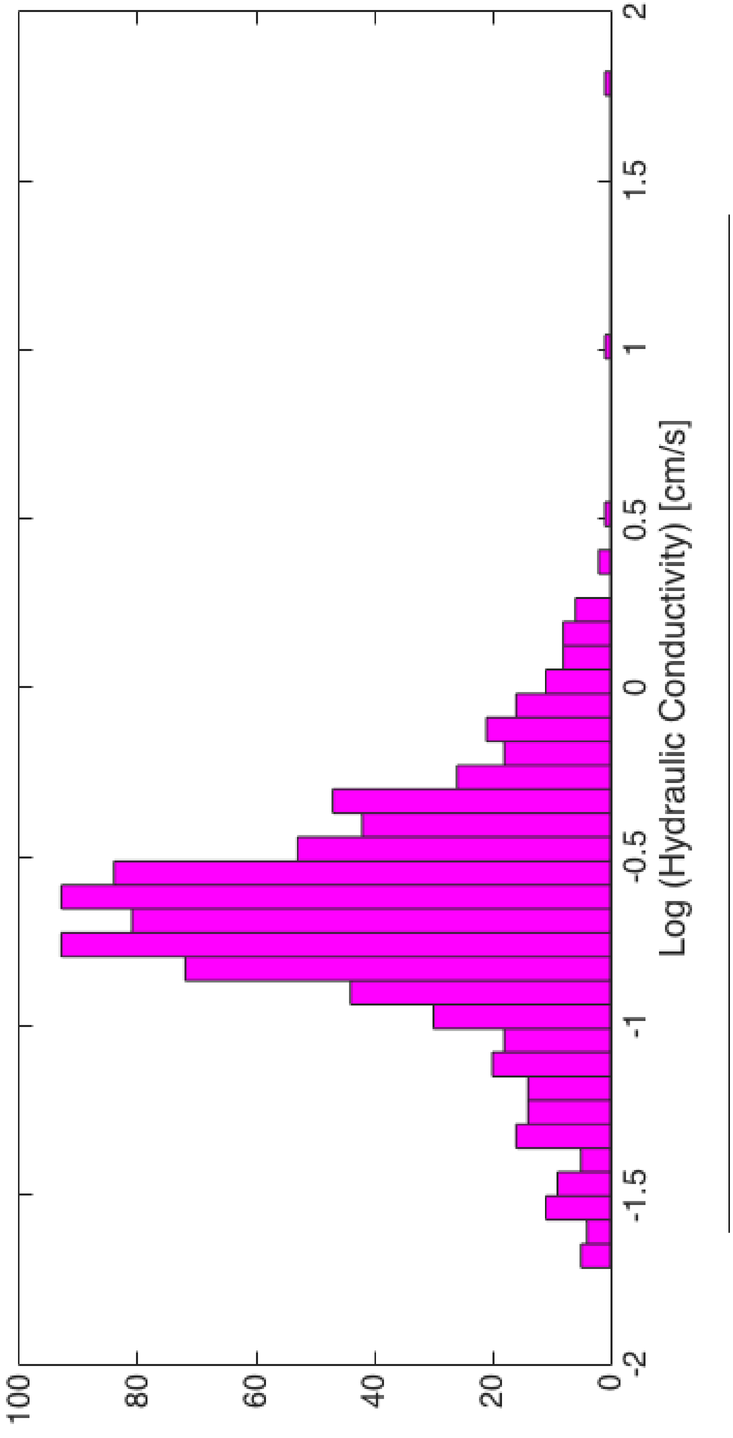

Histogram and probability density function for the mine samples using Fair and Hatch's equation

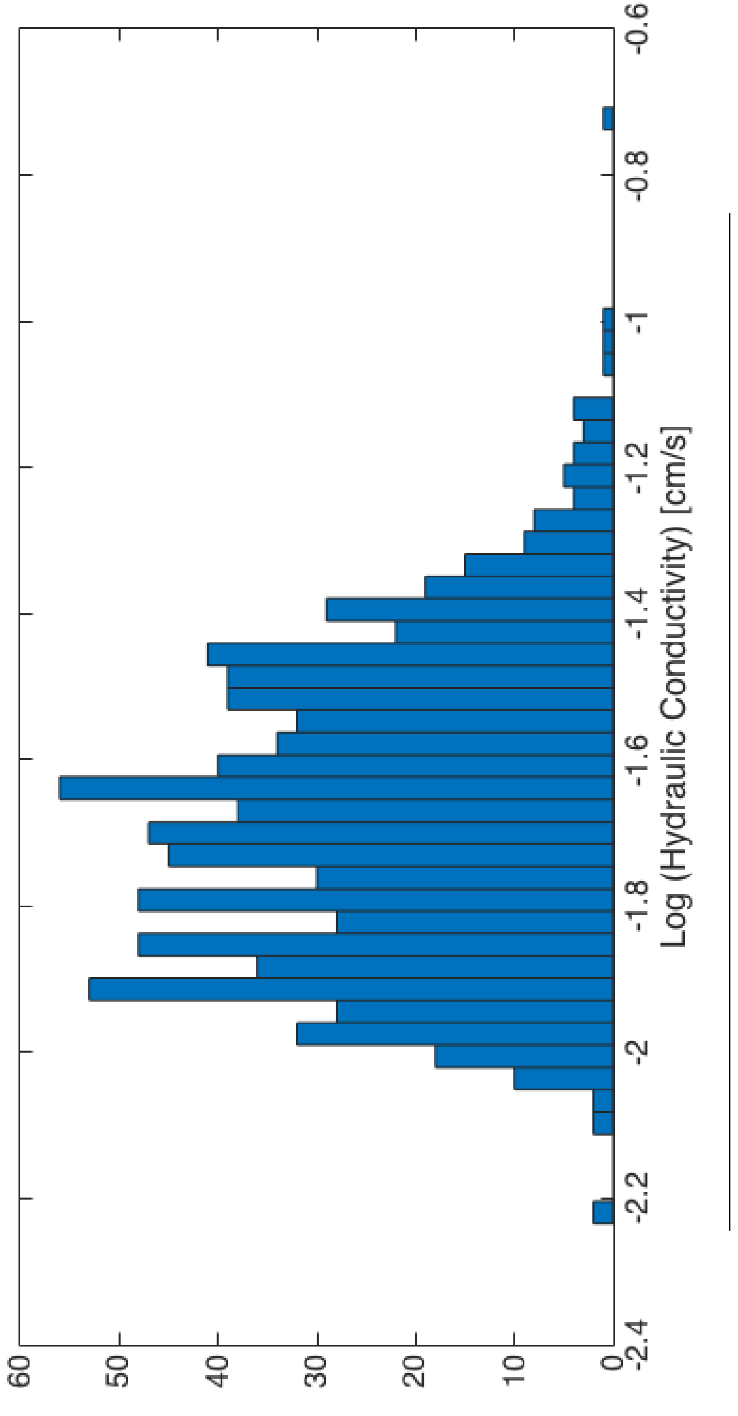

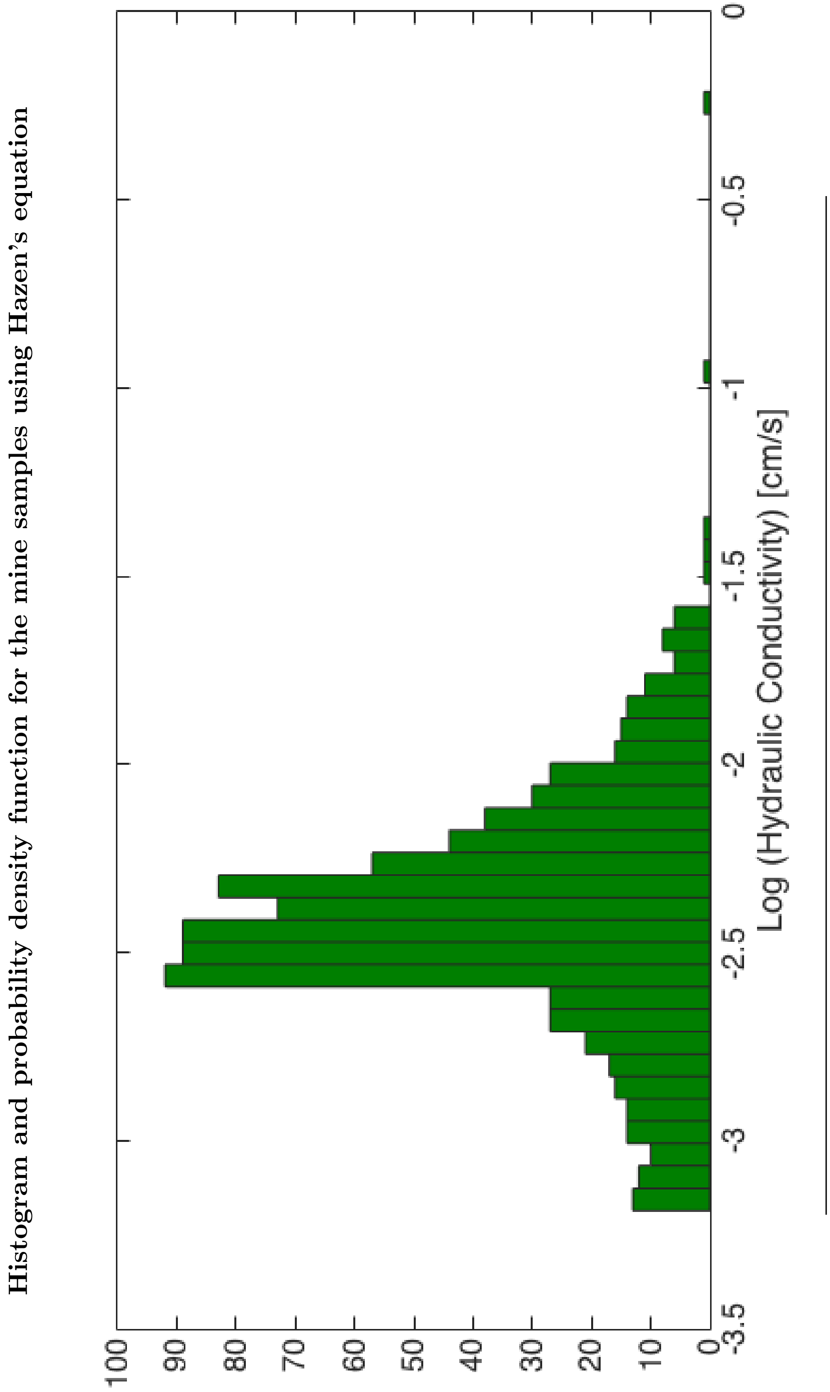
Histogram and probability density function for the mine samples using Hazen's equation
Log (Hydraulic Conductivity) [cm/s]
100
90
80
70
60
50
40
30
20
10
0
-3.5
-3
-2.5
-2
-1.5
-1
-0.5
0

Histogram and probability density function for the mine samples using Kozeny-Carman's equation

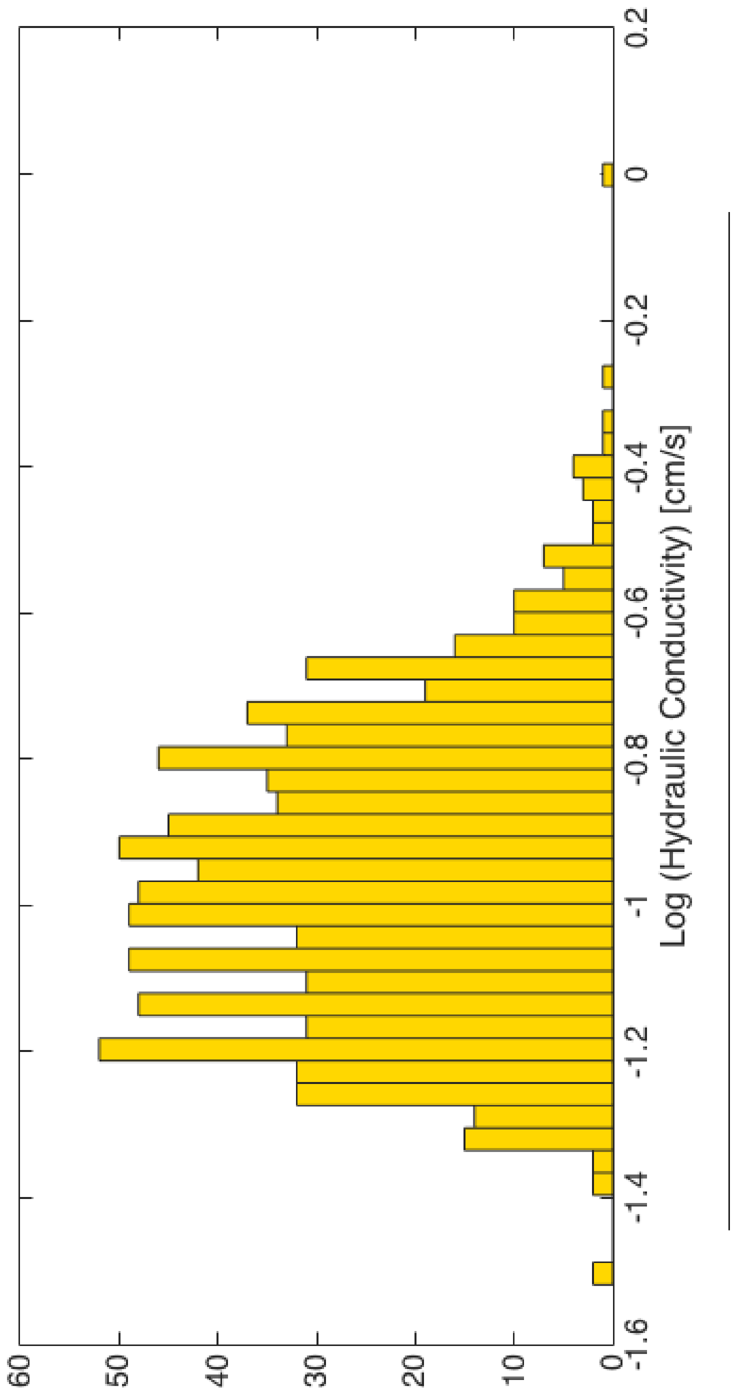

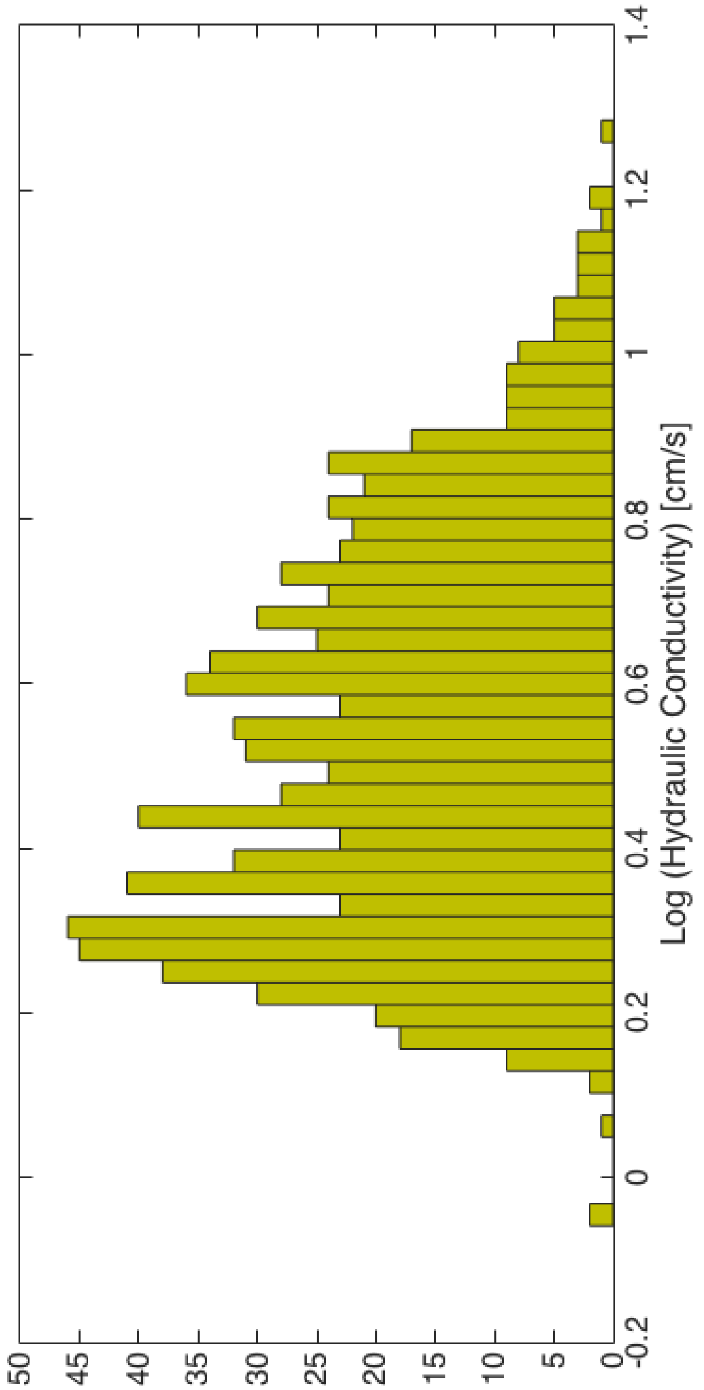

Histogram and probability density function for the mine samples using Kruger's equation

Histogram and probability density function for the mine samples using Slichter's equation

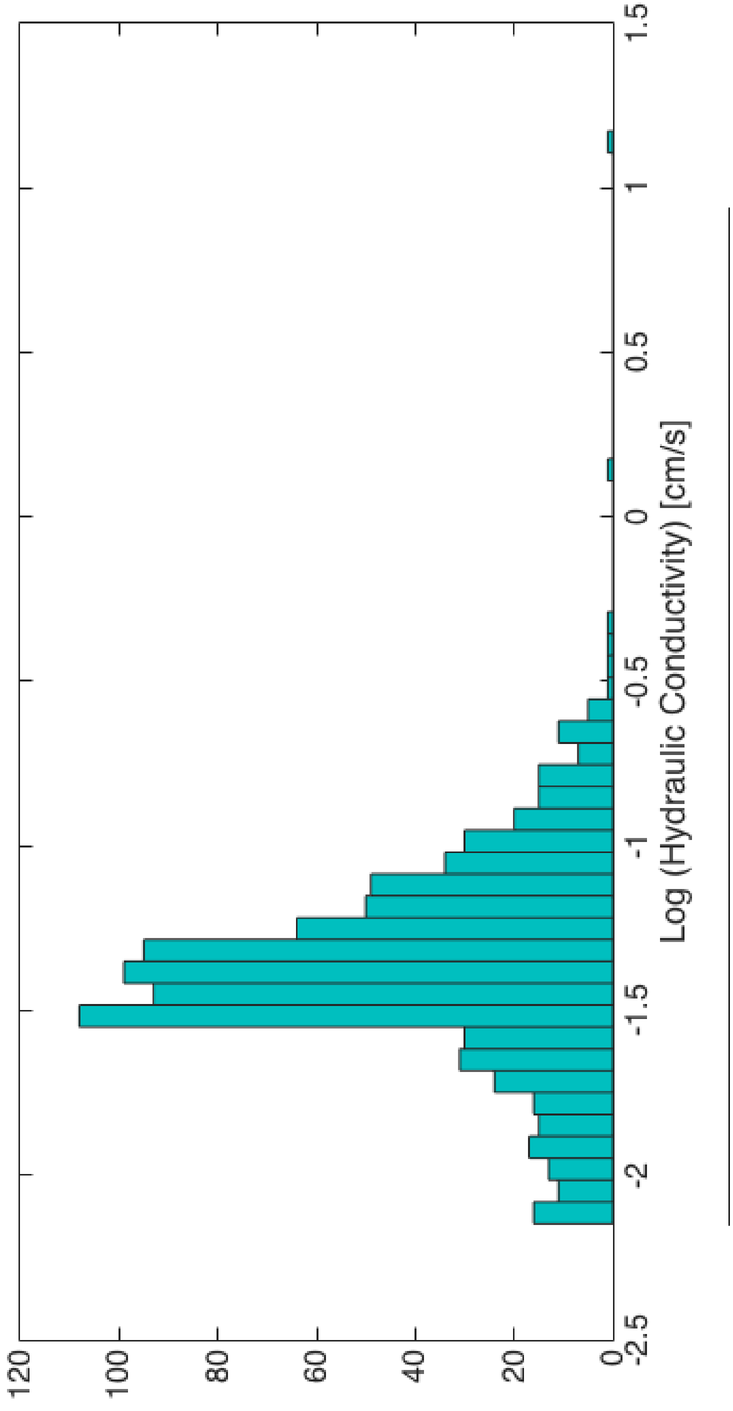

Histogram and probability density function for the mine samples using Terzaghi's equation

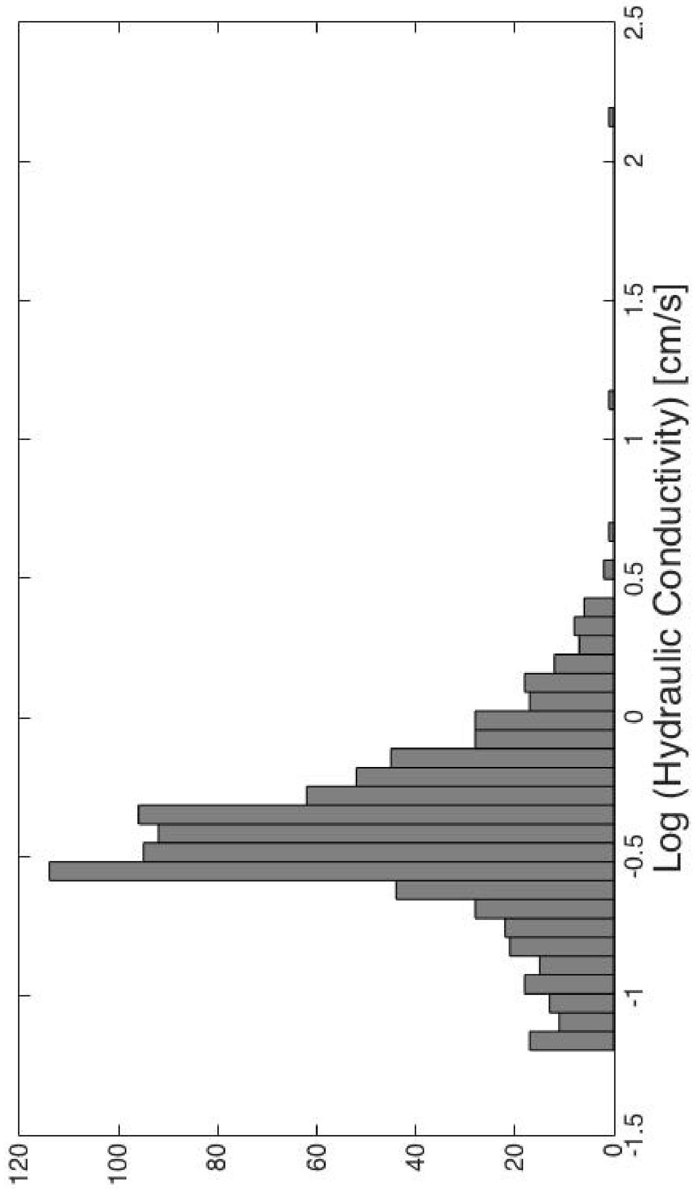

Histogram and probability density function for the mine samples using Zunker's equation

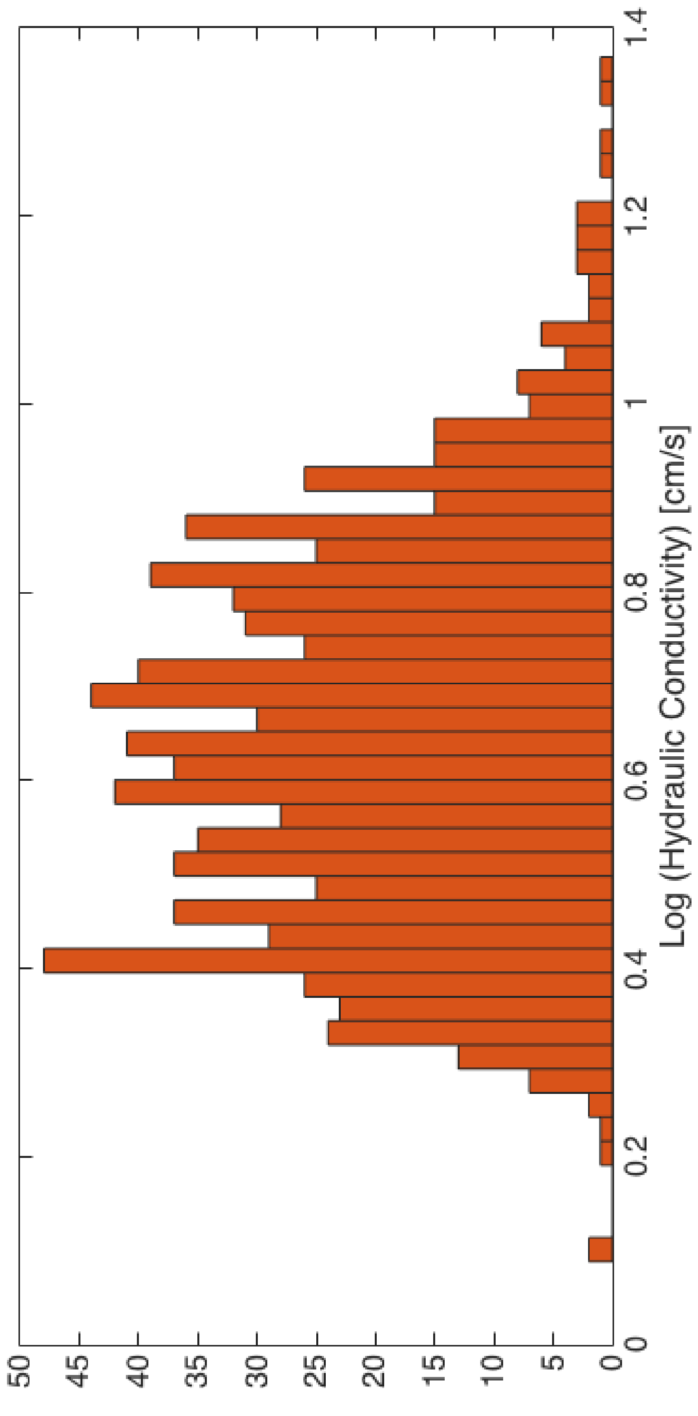

Bibliography

M. Vukovic and A Soro. *Determination of Hydraulic Conductivity of Porous Media From Grain-Size Composition*. 1992.

USBR. *Drainage Manual: A Water Resources Technical Publication*. 1978. URL `http://www.usbr.gov/pmts/wquality_land/DrainMan.pdf`.

A. Hazen. Some physical properties of sands and gravels. *Massachusetts State Board of Health, Annual Report*, pages 539–556, 1892.

C.S. Slichter. Theoretical investigations of the motions of groundwater. *USGS*, pages 295–384, 1898. URL `http://pubs.er.usgs.gov/publication/ar19_2`.

D. Carrier. Goodbye, hazen; hello, kozeny-carman. *Journal of Geotechnical and Geoenvironmental Engineering*, ASCE, 2003. URL `http://www.engr.uconn.edu/~lanbo/Carrier2003.pdf`.

G. Fair and L. Hatch. Fundamental factors governing the streamline flow of water through sand. *American Water Works Association*, 25.11:1557 –1565, 1933.

W. Beyer. Hydrogeological investigations in the deposition of water pollutants. *Journal of Applied Geology*, 12.1:599–606, 1966.

F. Zunker. Fertilization and soil science. *journal for plant nutrition*, A25, 1932.

V.S. Istomina. Filtration stability of soils. 1957.

M. Strobel. The ely times. let?s talk water-hydraulic conductivityr. *USGS*, pages 295–384, 2005. URL `http://nevada.usgs.gov/barcass/strobel_articles.htm`.

A.F. Salarashayeri and M. Siosemarde. Prediction of soil hydraulic conductivity from particle-size distribution. *World Academy of Science, Engineering and Technology*, 2012. URL `http://www.waset.org/journals/waset/v61/v61-81.pdf`.

C. Petalas and F. Pilakas. Determination of hydraulic conductivity of unconsolidated river alluvium from permeameter tests, empirical formulas, and statistical parameters effect analysis. *Water Resource Management*, pages 2877–2899, 2011.

W. Lambe and R. Whitman. *Soil Mechanics*. 1969. URL http://www.agu.org/pubs/crossref/1966/WR002i004p00665.shtml.

F. A. Dullien. Porous media: Fluid transport and pore structure. *Hydrogeology Journal*, Academic Press, 1979.

G. Binkhorst and G. Robbins. A review of factors affecting hydraulic conductivity values determined from slug tests. *U.S. Environmental Protection Agency. Environmental Monitoring Systems Laboratory, Office of Research and Development*, 1994.

M.F. et al. Ahlinhan. Stability of non-cohesive soils with respect to internal erosion. *ICE6*, 2012.

D. et al McCarthy. *Essentials of Soil Mechanics and Foundations*. 6 edition, 2001.

R. Zimmerman and B. Gudmundur. *Transport in Porous Media*. 1996. URL http://www.springerlink.com/content/u4vgqh4208117170/.

Kappes Cassiday. Precious metal heap leach design and practice. *Kappes Cassiday & Associates*, page 25, 2012. URL http://www.kcareno.com/pdfs/mpd_heap_leach_desn_and_practice_07apr02.pdf.

A. Breitenbach. Heap leach pad design and construction practices in the 21st century. *Vector Colorado LLC*, 2000. URL http://www.ausenco.com/uploads/papers/64041_Heap_Leach_Pad_Design_and_Construction_Practices_in_the_21st_Century.pdf.

D.I. Bleiwas. Estimated water requirements for gold heap-leach operation. *USGS*, 1.1: 2012–1085, 1994. URL http://pubs.usgs.gov/of/2012/1085/pdf/ofr2012-1085_v1-1.pdf.

G. Mishra and L. Grayson. Mine modifications for economic survival, a case study. 1987.

Office of Technology Assessment USA Congress. *Copper: Technology and Competititveness*. 2 edition, 1988. URL http://www.princeton.edu/~ota/disk2/1988/8808/8808.PDF.

Dave. et al. Williams. Importance of geomechanics to latheritic nickel heap leaching. *Heap Leaching Conference. Vancouver, Canada*, 2013.

M. et al. Milczarek. Ore permeability methods of evaluation and application to heap leach optimization. *Geosystems analysis, Inc.*, 2013. URL http://www.gsanalysis.com/heap_leach/Milczarek_et_al_Heap_Leach_2013_Ore_Permeability.pdf.

J. Lupo and A. Dolezal. Ore geotechnical testing for heap leach pad design. *AMEC Earth & Environmenta*, pages 3127–3131, 2010. URL `http://www.infomine.com/library/publications/docs/Lupo2010b.pdf`.

J. et al. Hopmans. Introductory soil physics. *University of California Davis*, 2002.

J Odong. Evaluation of empirical formulae for determination of hydraulic conductivity based on grain size analysis. *Journal of American Science*, 2007. URL `http://www.sciencepub.net/american/0303/10-0284-Odong-Evaluation-am.pdf`.

E. Ishaku, J. Gadzama and U. Kaigama. Evaluation of empirical formulae for the determination of hydraulic conductivity based on grain-size analysis. *Journal of Geology and Mining Research*, 34:105 –113, 2011.

D. Detner. Permeability, porosity, and grain-size distribution of selected pliocene and quaternary sediments in the albuquerque basin, central new mexico. *New Mexico Geology*, 1995.

S. Alyamani and S. Mahmoud. Determination of hydraulic conductivity from complete grain-size distribution curves. *National Ground Water Research and Educational Foundation*, 1993.

R. Shepherd. Correlations of permeability and grain-size. *Ground Water*, 27(5), 1989.

C. Cheng and X Chen. Evaluation of methods for determination of hydraulic conductivity properties in an aquifer-aquitard system hydrologically connected to river. *Hydrogeology Journal*, 15, 2007.

J. K. Dimkic. Groundwater management in large river basins. *Hydrogeology Journal*, page 14, 2008.

W. et al Mendenhall. *Introduction to Probability and Statistics*. Brooks Cole, 13 edition, 2009.

D. Kieber. Grain size distribution and its effect on the permeability of unconsolidated sands. *Brown and Root Construction Company*, 1966. URL `http://www.agu.org/pubs/crossref/1966/WR002i004p00665.shtml`.

Harvard Physics Lab. Summary of rules for error propagation. *Harvard University*, 2008. URL `http://www.fas.harvard.edu/~scphys/nsta/error_propagation.pdf`.

W. Chester. A scale of grade and class terms for clastic sediments. *The Journal of Geology*, 1922.

T. Yao, J. Keller, and M. Milczarek. Ore permeability methods of evaluation and application to heap leach optimization. *Heap Leach Conference*, 2013. URL `http://www.heapleachconference.com/wp-content/uploads/2013/10/Michael-Milczarek-Ore-Permeability-Testing.pdf`.

R. Chapuis and M. Aubertin. Predicting the coefficient of permeability of soils using the kozeny-carman equation. *Ecole Polytechnique de Montreal*, ASCE, 2003. URL `http://www.polymtl.ca/biblio/epmrt/rapports/rt2003-03.pdf`.

S.P. Sutera. The histroy of poiseuille's law. *Annual Review of Fluid Mechanics*, pages 1–19, 1993. URL `http://www.annualreviews.org/doi/pdf/10.1146/annurev.fl.25.010193.000245`.

H Darcy. Les fountaines publiques de la ville de dijon (the public fountains of the city of dijon). 1856.

R. Di Francesco. Exact solution of terzaghi's consolidation equation and extension to two/three-dimensional cases. *Scientific Research*, 2013. URL `http://www.scirp.org/journal/PaperInformation.aspx?PaperID=30767#.VN8M1Frw98Z`.

U. Olsson. Confidence intervals for the mean of a log-normal distribution. *Journal of Statistics Education*, 2007. URL `http://www.sciencepub.net/american/0303/10-0284-Odong-Evaluation-am.pdf`.

L. et al Brown. Efficient estimation of log-normal means with application to pharmacokinetic data. *Statistics in Medicine*, 25:3023–3028, 2006.

Mike Yao. *Hydrology Test Report: Pampa Norte*. Geosystems Analysis Inc., 2011.